

**RECOMBINANT ANTIBODIES AGAINST VIRAL  
INTERLEUKIN 6**

**Dissertation**

**zur Erlangung des Doktorgrades  
der Mathematisch-Naturwissenschaftlichen Fakultät  
der Christian-Albrechts-Universität  
zu Kiel  
Fachbereich Biochemie**

**vorgelegt von  
Marina Kovaleva**

**Kiel  
Dezember 2004**

Erster Gutachter: Prof. Dr. Stefan Rose-John  
Zweiter Gutachter: Prof. Dr. Matthias Leippe

*meiner Mutter Galina*

## **Table of contents**

<b>1 INTRODUCTION.....</b>	<b>1</b>
1.1 IL-6 family of cytokines.....	1
1.2 Signaling via IL-6/IL-6R.....	2
1.3 Soluble IL-6R and the phenomenon of transsignaling.....	3
1.4 The sIL-6R in diseases.....	5
1.5 Kaposi's sarcoma associated herpesvirus.....	6
1.6 Structural and receptor-binding properties of viral IL-6.....	6
1.7 Biological activity of viral IL-6 compared to human IL-6.....	8
1.8 Hyper IL-6 and viral IL-6 mimicry of transsignaling.....	9
1.9 Natural neutralisation of IL-6/sIL-6R.....	10
1.10 Recombinant antibodies and strategies of vIL-6 neutralisation.....	11
1.11 Aim of the study.....	15
<b>2 MATERIALS AND METHODS.....</b>	<b>17</b>
2.1 Materials.....	17
2.2 Methods.....	22
2.2.1 Cloning.....	22
2.2.2 Polymerase Chain Reaction (PCR) and Splicing by Overlap Extension- PCR (SOE-PCR).....	22
2.2.3 Transformation of bacteria by heat-shock.....	23
2.2.4 Preparation of recombinant vIL-6 in the bacterial expression system.....	23
2.2.5 Preparation of recombinant vIL-6 in the eukaryotic expression system .....	24
2.2.6 Transient transfection of COS-7 cells using DEAE-dextran.....	24
2.2.7 SDS-PAGE and gel staining.....	24
2.2.8 Proliferation assay.....	25
2.2.9 Selection of vIL-6 specific phages from the phage display libraries.....	25
2.2.9.1 Production of helper phage.....	25
2.2.9.2 Selection on immunotubes.....	26

2.2.9.3 Preparation of soluble scFvs.....	27
2.2.10 Soluble scFv ELISA.....	27
2.2.11 Expression of scFv in bacterial cells <i>E.coli BL21</i> .....	28
2.2.12 Western Blot.....	28
2.2.13 Immunoprecipitation of vIL-6 with MAV.....	28
2.2.14 Proliferation assay.....	29
2.2.15 Stimulation of HepG2 cells.....	29
2.2.16 Analysis of STAT3 phosphorylation in human hepatoma cell line.....	30
2.2.17 Surface Plasmon Resonance (SPR).....	30
2.2.17.1 Immobilisation of vIL-6 to the SPR sensorchip.....	30
2.2.17.2 Interaction analysis.....	30
2.2.18 Immunostaining of transfected COS-7 cells.....	30
<b>3 RESULTS.....</b>	<b>32</b>
3.1 Expression of recombinant vIL-6.....	32
3.1.1 Expression of recombinant vIL-6 in bacteria.....	32
3.1.2 Eukaryotic expression of vIL-6.....	35
3.2 Production of recombinant antibodies against vIL-6.....	40
3.2.1 Phage library screening.....	40
3.2.2 Western blot and sequence analysis of screened scFvs.....	46
3.2.3 Production and purification of large amounts of MAV.....	47
3.2.4 Properties of MAV.....	49
3.2.4.1 MAV recognition of vIL-6 in ELISA and Western blot.....	49
3.2.4.2 Binding of MAV to vIL-6 in solution: immunoprecipitation of vIL-6 with MAV.....	51
3.2.4.3 Epitope mapping: binding site of vIL-6 to MAV.....	52
3.2.4.4 “Sandwich” ELISA.....	53
3.2.4.5 Neutralising properties of MAV.....	54
3.2.4.6 Binding kinetics of MAV to recombinant vIL-6.....	56
3.2.5 Model system for the intracellular retention of vIL-6.....	61
3.2.5.1 Cloning and expression of the recombinant antibody carrying the retention sequence KDEL.....	61
3.2.5.2 Cloning and expression of vIL-6 fused to GFP.....	64

3.2.5.3 Retention of vIL-6 in the ER due to binding to MAV-KDEL.....	66
----------------------------------------------------------------------	----

<b>4 DISCUSSION.....</b>	<b>68</b>
4.1 Expression, purification and biological activity of viral interleukin-6.....	68
4.2 Phage display: human antibody library.....	69
4.3 Properties of the selected scFv against vIL-6.....	70
4.4 Elimination of vIL-6 secretion.....	72
4.5 HHV-8 associated diseases and potential therapeutic application of anti-vIL-6 antibodies.....	73
<b>5 SUMMARY.....</b>	<b>78</b>
<b>6 ZUSAMMENFASSUNG.....</b>	<b>80</b>
<b>7 REFERENCES.....</b>	<b>82</b>
<b>8 APPENDIX.....</b>	<b>98</b>
8.1 Abbreviations.....	98
8.2 Sequences.....	101
8.3 Curriculum Vitae.....	104
8.4 Publications.....	105
<b>9 ACKNOWLEDGEMENTS.....</b>	<b>106</b>

# 1 Introduction

## 1.1 IL-6 family of cytokines

Cytokines are a group of low molecular weight regulatory peptides or proteins produced by multiple cell types such as lymphocytes, monocytes/macrophages, mast cells, eosinophils, and endothelial cells lining blood vessels. Each individual cytokine can have multiple functions depending on the cell that produces it and the target cell(s) on which it acts. Also, several different cytokines can have the same biological function. Cytokines can exert their effect through the bloodstream on distant target cells (endocrine), on target cells adjacent to those that produce them (paracrine) or on the same cell that produces the cytokine (autocrine). To express a certain cytokine the cell has to be exposed to a stimulus. For example, monocytes/macrophages secrete IL-1, IL-6 and TNF- $\alpha$  after contact with bacterial lipopolysaccharides [1]. IFN- $\beta$ , TNF- $\alpha$  and viral infections stimulate the synthesis of IL-6 in fibroblasts [2, 3]. Cytokines act on target cells via binding to cell-surface receptors which leads to the activation of specific transcription genes resulting in the control of cell growth, differentiation or apoptosis.

All members of the haematopoietic IL-6 cytokine family, also called gp130 cytokine family, exert their biological effects via binding to a receptor homodimer of gp130 or a heterodimer of gp130/LIFR (gp130/OSMR, gp130/WSX-1). Gp130 as well as LIFR or OSMR are the signal transduction receptors ( $\beta$ -receptors) activated by binding of the cytokine. Some cytokines (IL-6, IL-11, CNTF) can not bind to  $\beta$ -receptors unless they first form a complex with a specific ligand binding receptor ( $\alpha$ -receptor) (Tab1.1).  $\alpha$ -receptors are not involved in signaling.

**Tab.1.1** IL-6 cytokine family and their receptors [7-9]

cytokine	$\beta$ -receptor	$\alpha$ -receptor
IL-6	gp130, gp130	IL-6R
IL-11	gp130, gp130	IL-11R
CNTF	gp130, LIFR	CNTFR
CLC	gp130, LIFR	CNTFR
neuropoietin	gp130, LIFR	CNTFR
LIF	gp130, LIFR	-
OSM	gp130, LIFR	-
OSM	gp130, OSMR	-
IL-27(p28/EBI3)	gp130, WSX-1	EBI3
CT-1	gp130, LIFR	unknown

## 1.2 Signaling via IL-6/IL-6R

As shown in Fig.1.1, IL-6 first binds to the membrane-bound non-signaling IL-6 receptor (IL-6R) before the IL-6/IL-6R complex activates gp130 [4-6]. Homodimerisation of two gp130 molecules causes phosphorylation of receptor tyrosines by Janus-kinases (JAK1, JAK2, TYK2), which are constitutively associated with gp130 [7]. These phosphotyrosin motifs are docking sites for the signal transducers and activators of transcription STAT1/STAT3 factors which also become phosphorylated by the JAKs activity. Phosphorylation of the STAT factors leads to their dimerisation and localisation to the nucleus where they induce the transcription of target genes. STAT3-dependent gene expression causes upregulation of inhibitory proteins of the suppressor of cytokine signaling (SOCS) family that interfere with JAK activity [10-12]. Phosphorylation of gp130 also triggers the Ras/Raf/MAP-kinase pathway via adaptor proteins such as SHP-2, Grb2 and SOS, leading to activation of the transcription factors NF-IL-6 and AP-1 [7].



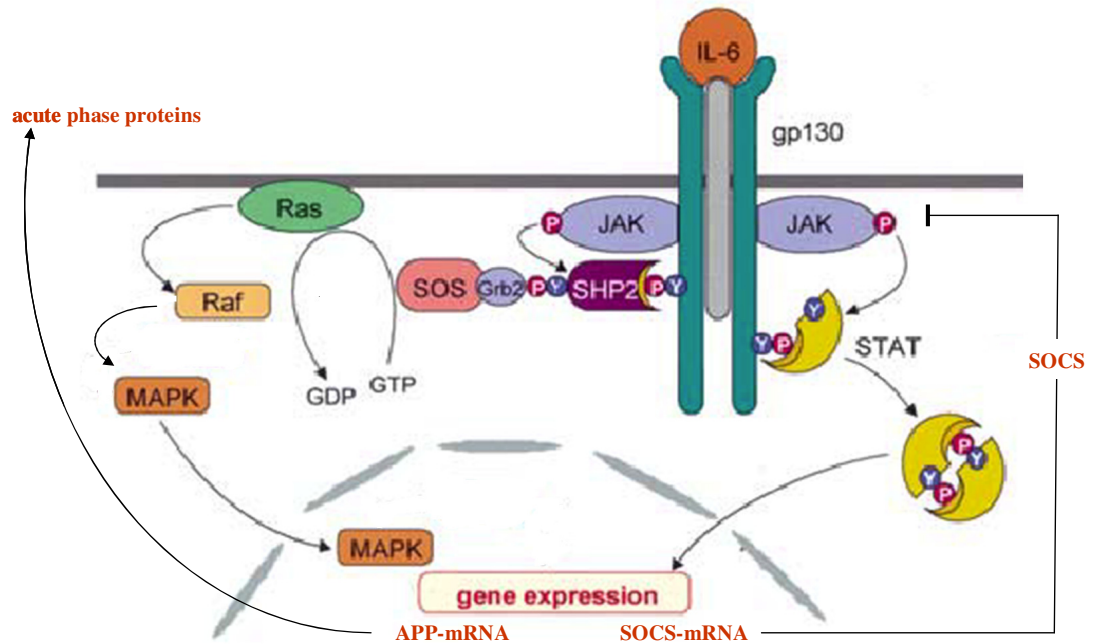


**Fig. 1.1 Signaling pathways induced by IL-6.** IL-6 first binds to the membrane-bound IL-6R and then to the gp130-homodimer to form the active cytokine complex. The signal transduction receptor gp130 is activated via phosphorylation by JAK. JAK phosphorylates also STAT molecules leading to their dimerisation and relocalisation to the nucleus where they induce the expression of target genes like the acute phase proteins or adaptorproteins (SHP-2, Grb2, SOS) to turn on the Ras/Raf/MAPK pathway. SOCS expression causes downregulation of the cytokine signaling [7, 10-12].

### 1.3 Soluble IL-6R and the phenomenon of transsignaling

The IL-6R protein has been shown to exist in soluble as well as in membrane-bound form. The release of sIL-6R is regulated via two mechanisms. First, the soluble receptor that lacks cytoplasmic and membrane-spanning domains can be synthesised from an alternatively spliced mRNA [13-16]. The second mechanism is the proteolytic cleavage of the membrane-bound IL-6R from the cell surface [17-19]. The soluble form of the receptor can control the bioactivity and the pathophysiological effect of IL-6.

Soluble IL-6R is still able to bind to IL-6 and the complex of IL-6/sIL-6R can stimulate target cells that do not express the IL-6R and are nonresponsive to IL-6 alone [5, 8]. Interestingly, membrane-bound IL-6R is present on only a small number of cells, i. e.

hepatocytes, monocytes/macrophages and some lymphocytes, whereas gp130 is expressed by all cells in the body [21]. Therefore, cells which release sIL-6R render cells which only express gp130 responsive towards IL-6 [22-24]. This process has been termed “transsignaling” (Fig. 1.2) [21, 25-27]. Transsignaling cell types that are exclusively responsive to IL-6/sIL-6R but not to IL-6 alone include haematopoietic progenitor cells [21, 22], endothelial cells [28], osteoclasts [23], smooth muscle cells [29], and neuronal cells [24, 30].

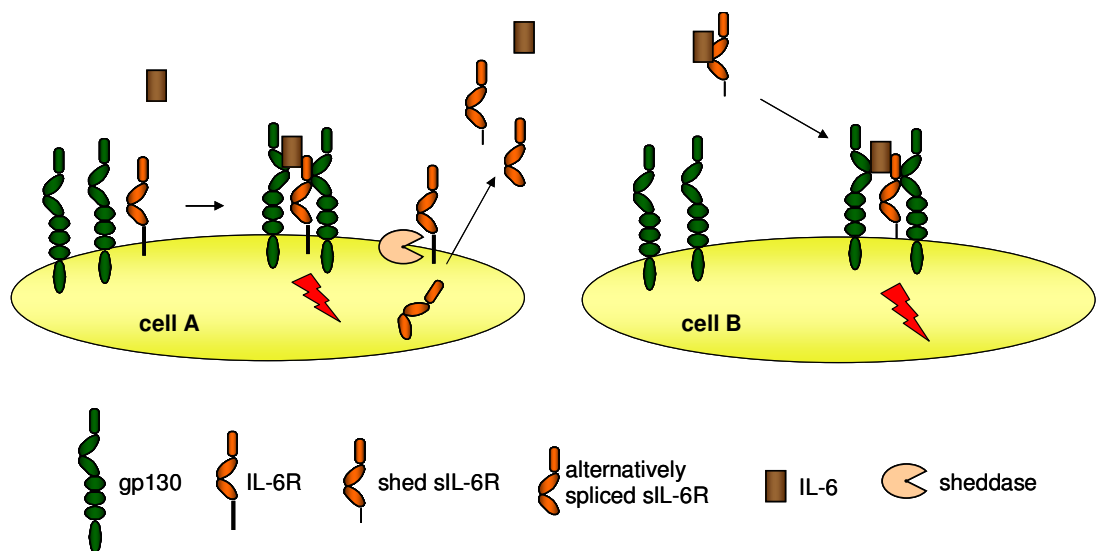


**Fig. 1.2 Transsignaling of the soluble IL-6R.** IL-6 classically activates cells by binding to the membrane-bound IL-6R followed by recruitment of two gp130 molecules which activates downstream signal cascades. A soluble IL-6R can be generated by proteolytic cleavage or by alternative splicing. IL-6/IL-6R complex associates with gp130 expressed on a cell which does not express the IL-6R and initiates signalling [21, 25-27].

Transsignaling is regulated via the release of soluble IL-6 receptor and the presence of soluble gp130 (sgp130) in the serum [31]. Importantly, sgp130 inhibits only IL-6 effects that are mediated by the sIL-6R, but not those transmitted via the membrane-bound receptor [32].

The agonistic properties of the soluble receptor/cytokine complex and the transsignaling phenomenon were also described for other cytokines of the IL-6 cytokine family such as IL-11 and CNTF [33, 34].

## 1.4 The sIL-6R in diseases

Transsignaling may be a pathogenetic factor in human diseases as diverse as multiple myeloma (MM), Castleman's disease, prostate carcinoma, Crohn's disease, systemic sclerosis, Still's disease, osteoporosis and cardiovascular disease [27].

In most autoimmune disorders the affected organ displays an infiltrate of mononuclear cells and very often vasculitic syndromes. The role of IL-6 and sIL-6R in the pathogenesis of such diseases is the regulation of leukocyte infiltration via activation of a positive autocrine feedback loop. Endothelial cells are unresponsive to IL-6, but can be stimulated by the IL-6/sIL-6R complex. Activated endothelial cells upregulate gp130 and LIFR and secrete monocyte attractant protein (MCP)-1, MCP-3, IL-8, IL-6, vascular cell adhesion molecule (VCAM)-1, intracellular adhesion molecule (ICAM)-1 and protein S, which provides the basis for leukocyte recruitment and adhesion [28, 35]. Leukocyte recruitment during acute inflammation is characterised by an initial infiltration of neutrophils [36], which are later replaced by mononuclear cells. The secreted IL-8 activates CXCR1 and induces shedding of the IL-6R from infiltrating neutrophils [37] that leads to activation of endothelial cells [38]. In this way, IL-6 and sIL-6R induce the expression of inflammatory molecules required for the recruitment of inflammatory cells found in vasculitis.

A key factor in the pathogenesis of autoimmune diseases is the resistance of autoreactive cytotoxic CD8<sup>+</sup>-T-cells against apoptotic cell death. This can be a consequence of activation of STAT3 by the IL-6/sIL-6R complex and STAT3-dependent upregulation of anti-apoptotic genes [39]. Autoimmune reactions can arise in all tissues where uncontrolled/unlimited release of IL-6/sIL-6R occurs.

Many neural cells only react to IL-6 in the presence of sIL-6R suggesting that transsignaling is an important event in neuronal differentiation and survival responses [30, 40-43].

The IL-6/sIL-6R complex plays a role in the pathogenesis of neoplastic diseases, for example multiple myeloma. Multiple myeloma cells do not express IL-6 but stimulate bone marrow stromal cells to produce high levels of IL-6 [44, 45]. IL-6 inhibits apoptosis of myeloma cells due to activation of STAT3 and upregulation of bcl-x<sub>L</sub> and mcl-1. In addition, shedding or secretion of the sIL-6R is induced [46]. Soluble IL-6R produced by

myeloma cells enhances IL-6 synthesis by bone marrow stromal cells (positive feedback loop). The IL-6/sIL-6R complex stimulates expression of metalloproteinases and VEGF [47] by bone marrow stromal cells and may activate osteoclasts [48]. These effects could be involved in angiogenesis, osteolytic lesions and chemoresistance frequently observed in patients with multiple myeloma [49-50].

## **1.5 Kaposi's sarcoma associated herpesvirus**

Human herpesvirus type 8 (HHV-8) or Kaposi's sarcoma associated herpesvirus was first identified by Chang et al [52] in Kaposi's sarcoma tissues of acquired immunodeficiency syndrome patients and appears to be the first member of the human  $\gamma$ -herpesviruses (rhadinoviruses). HHV-8 is linked to the development of Kaposi's sarcoma (KS) as well as primary effusion lymphoma (PEL) [53, 54] and multicentric Castelman's disease (MCD) [55]. It has also been associated with multiple myeloma [56, 57]. Similar to other human herpesviruses, HHV-8 has a particular cell tropism, infecting predominantly endothelial and other mesenchymal cells, as well as B-lymphocytes. Like other rhadinoviruses, the viral genome consists of linear double-stranded DNA of about 165 kb and contains numerous open reading frames encoding cellular homologues, including a G-protein-coupled receptor, macrophage inhibitory factors, cyclin D, bcl-2 and chemokine genes [58-61]. However, several of the homologous genes encoded by HHV-8 are not shared by other rhadinoviruses or any other known viruses. One of these genes encodes a structural equivalent of interleukin-6 with high similarity to cellular IL-6 and was therefore named viral interleukin 6 (vIL-6) [56, 62, 63].

## **1.6 Structural and receptor-binding properties of viral IL-6**

Although cellular and viral IL-6 proteins show only ~25% sequence homology (human: 24,7%, murine: 24,2%), the crystal structures of a receptor complexes demonstrated a strong relationship of the binding epitops to their receptors [64].

Viral interleukin-6 (vIL-6) has a protein fold typical for most cytokines, the so-called four-helical bundle [65]. This consists of four antiparallel  $\alpha$ -helices with up-up-

down-down topology which are connected by three loops (Fig. 1.3). The receptor binding epitops have been identified for cellular IL-6 as well as for viral IL-6. Human IL-6 (huIL-6) binds to its receptors via three distinct sites [65, 66]. Site I is formed by the C-terminal part of helix D and the C-terminal region of the AB-loop and interacts with the IL-6R. Site II on helix A and C, and site III on the initial part of the AB-loop and helix D bind to gp130

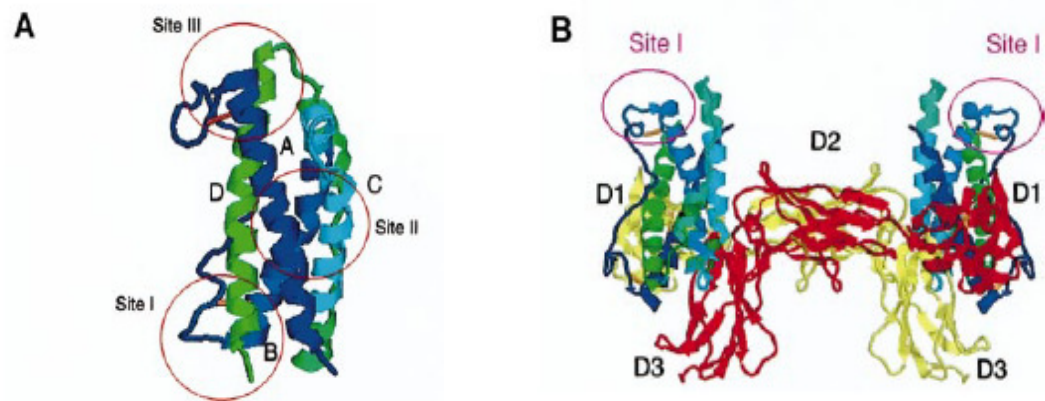


**Fig. 1.3 Schematic cartoon representation of vIL-6 structure.** **A** vIL-6 ABCD 4-helix bundle connected by peptide loops is displayed in different colours. Site I, composed of the N-terminal region of the AB-loop and the C-terminal region of helix D, corresponds to the presumed site where huIL-6 would interact with IL-6R. Site II on helix A and C, and site III on the initial part of the AB-loop and helix D represent binding surfaces to gp130. **B** vIL-6 is juxtaposed to gp130 in a tetrameric (2:2) signaling model. Site II of vIL-6 is occupied by the D2D3 sites of one gp130 chain (yellow), and site III is occupied by the D1 site of another gp130 chain (red). Site I of vIL-6 is not occupied by gp130 and is sterically accessible for engagement by other molecules [68].

[67, 70]. As with cellular IL-6, the structure of vIL-6 has identified site II and site III as directly binding to gp130, the common signal transducer for the IL-6 family of cytokines [68,70]. Site I corresponds to the presumed site where human IL-6 would interact with the IL-6R.

Despite similarities in their global structures, huIL-6 and vIL-6 differ in their mode of receptor usage [67, 70]. Viral IL-6 and huIL-6, like other cytokines of the IL-6 family, such as CNTF, LIF, OSM, CLC, CT-1, and IL-11, use the gp130 receptor for signal transduction [71]. In contrast to cellular IL-6, vIL-6 does not need to interact with the ligand-binding  $\alpha$ -receptor IL-6R to induce signaling [72]. Viral IL-6 shows activity on cells

expressing only gp130, but not IL-6R. This suggests that vIL-6 directly binds to and activates gp130 [69, 70, 72, 73], which seems to play a decisive role in the manifestation of the vIL-6 activity and pathogenesis of diseases induced by vIL-6.

Interestingly, G. Miller et al. [74] reason that N-glycosylation of vIL-6 is required for its binding and function. vIL-6 has an unused site I not occupied by gp130. The equivalent site in huIL-6 interacts with the IL-6R. N-glycosylation sites at N78 and N89 of the viral cytokine are located in the vicinity of site I (Fig. 1.4) and their use markedly enhanced binding to gp130. Although huIL-6 is N- and O-glycosylated, neither N-linked nor O-linked glycosylation is necessary for IL-6 receptor dependent binding to gp130 or signaling through JAK/STAT [75].

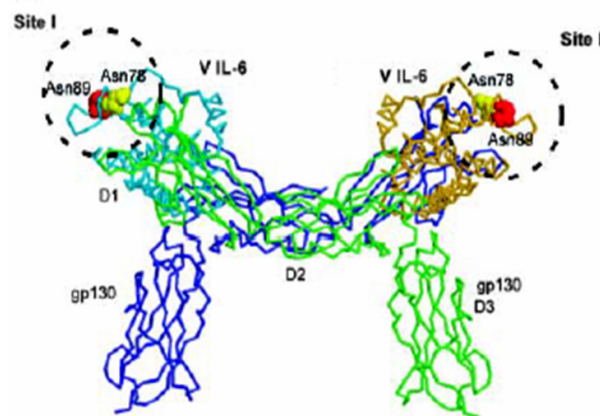


**Fig. 1.4 Localisation of the N-glycosylation sites of vIL-6 in a schematic representation of the crystal structure of the vIL-6/gp130 complex.** Site I of vIL-6 is not a contact site with gp130, but corresponds to a site where huIL-6 interacts with IL-6R. N78 (yellow) and N89 (red) are highlighted as spacefilling residues and are shown to occupy site I, but not sites II or III.

## 1.7 Biological activity of viral IL-6 compared to human IL-6

Viral IL-6 has been shown to mimic a number of huIL-6 activities such as stimulating IL-6-dependent B-cell line growth [76] and activating the JAK/STAT-signal transduction pathway in HepG2 cells [77] as well as the Ras/Raf/MAPK pathway in MH60 and B9 cell lines [78]. Human IL-6 is expressed by a number of cell types including B and T lymphocytes, monocytes, fibroblasts, keratinocytes, bone marrow stromal cells, endothelial cells, and astrocytes. The wide range of biological activities attributed to huIL-

IL-6 includes proliferation of lymphocytes and stem cells, differentiation of B cells and osteoclasts, induction of acute phase proteins in hepatocytes, and promotion of neuronal regeneration [79]. huIL-6 serves as a growth factor for multiple myeloma and plasmacytoma cells [80]. vIL-6 is expressed in HHV-8-infected B cells and endothelial cells and induces proliferation, angiogenesis, and hematopoiesis in IL-6-dependent cell lineages [60, 69]. Viral IL-6 can serve as an autocrine growth factor for PEL cell lines [81]. Expression of vIL-6 accelerates hematopoiesis and induces vascular endothelial growth factor (VEGF), a factor implicated in PEL and Kaposi's sarcoma pathogenesis [82]. However, the precise role of vIL-6 in HHV-8 pathogenesis is not well understood. Viral IL-6 may act as an antiapoptotic factor for survival of HHV-8-infected cells and/or promote the proliferation of HHV-8-infected cells or potential host cells. In lymphoma cells infected with HHV-8 the viral cytokine protects cells against innate immune defenses triggered by viral infection [83, 84] via blocking of interferon signaling [85].

Alongside huIL-6 being the central regulator of the hepatic acute-phase response [86, 87], vIL-6 elicits a local acute-phase response in human primary Kaposi's sarcoma cell cultures. The induction of the acute-phase protein pentraxin-3 may contribute to local tissue damage and the attraction of an inflammatory phenotype [88].

## **1.8 Hyper IL-6 and viral IL-6 mimicry of transsignaling**

To exert their function cytokines have to bind to the receptor complex on the membrane. After binding to the receptor complex, signaling occurs within the cell eventually leading to transcriptional induction of target genes. The receptor complex of the IL-6 family of cytokines includes two or three receptor subunits (Tab. 1.1). The composition of the signal competent receptor complex is crucial for cytokine function. For example, LIF can stimulate cells expressing gp130 and LIFR, such as hematopoietic and epithelial cells, hepatoma and breast cancer cells [89-92]. CNTF stimulates cells expressing gp130, LIFR and CNTFR like neuronal cells, skeletal muscle cells, bone marrow stromal cells, hepatocytes and adipocytes [93-95]. IL-6 acts on hepatocytes, monocytes/macrophages and some lymphocytes expressing IL-6R and gp130 [26, 27]. Viral IL-6 seems to be the only cytokine which only requires gp130 to transduce the signal

and is able to affect all cells in the body, including normal human vascular smooth muscle cells, hematopoietic progenitor cells and Kaposi's sarcoma cells [63].

Some years ago, a recombinant cytokine with the property to induce signal transduction only via gp130 was designed and named Hyper-IL-6 (HIL-6) [96]. Hyper IL-6 is a fusion protein of huIL-6 and its soluble receptor sIL-6R connected by a flexible polypeptide linker. It has been shown that Hyper-IL-6 is able to stimulate the proliferation of cells only expressing gp130 [72]. Interestingly, the fusion protein exhibits a markedly increased bioactivity as compared to IL-6 and sIL-6R. The concentration of Hyper-IL-6 needed for full stimulation of murine Baf/3-cells stably transfected with gp130, is 2-3 orders lower than that needed of the two separate components IL-6 and IL-6R. Also, the expression of the acute-phase protein haptoglobin can be induced by much lower concentrations of Hyper-IL-6 compared to the combination of IL-6 and IL-6R. Such potential applications make Hyper-IL-6 a promising *ex vivo* or even *in vivo* therapeutical agent [97, 98].

The mode of action of viral IL-6 and Hyper-IL-6 can be compared with the IL-6/sIL-6R complex and seems to mimic transsignaling. Although the vIL-6 activity is lower than the one of Hyper-IL-6 or the combination huIL-6/sIL-6R, vIL-6 is unique in that it is a natural cytokine capable to induce signal transduction directly via gp130 without the interaction with the soluble form of the  $\alpha$ -receptor. Hence, vIL-6 can stimulate a broader spectrum of target cells than huIL-6. Like the combination of huIL-6 and sIL-6R, but not huIL-6 alone, vIL-6 can stimulate the expansion of hematopoietic progenitor cells and affect different neuronal cells [42, 69, 72, 99, 100].

## 1.9 Natural neutralisation of IL-6/sIL-6R

Because gp130 is ubiquitously expressed, the complex of sIL-6R and IL-6 could theoretically stimulate all cells of the body. In several cell culture and animal models soluble gp130 (sgp130), generated by translation from differentially spliced mRNA [101], specifically blocked IL-6 responses dependent on sIL-6R. In contrast, responses via the membrane-bound IL-6R remained unaffected [32]. It has been shown that sgp130 can not block IL-6-induced activation of IL-6R expressing cells, but abrogates activation of transsignaling cells (Fig. 1.5). In this way, sgp130 acts as a regulator of transsignaling and



could be the natural neutralisation agent of the IL-6/sIL-6R complex [32]. Sgp130 concentrations have been shown to be increased in patients with systematic sclerosis [102], multiple sclerosis [103] and melanoma cells [104].

Recombinant sgp130Fc, which is the extracellular domain of human or murine gp130 fused to the constant region of a human IgG1 heavy chain [32], is expected to be a valuable therapeutic tool to specifically block disease states in which sIL-6R transsignaling responses exist [36, 39, 105, 106].

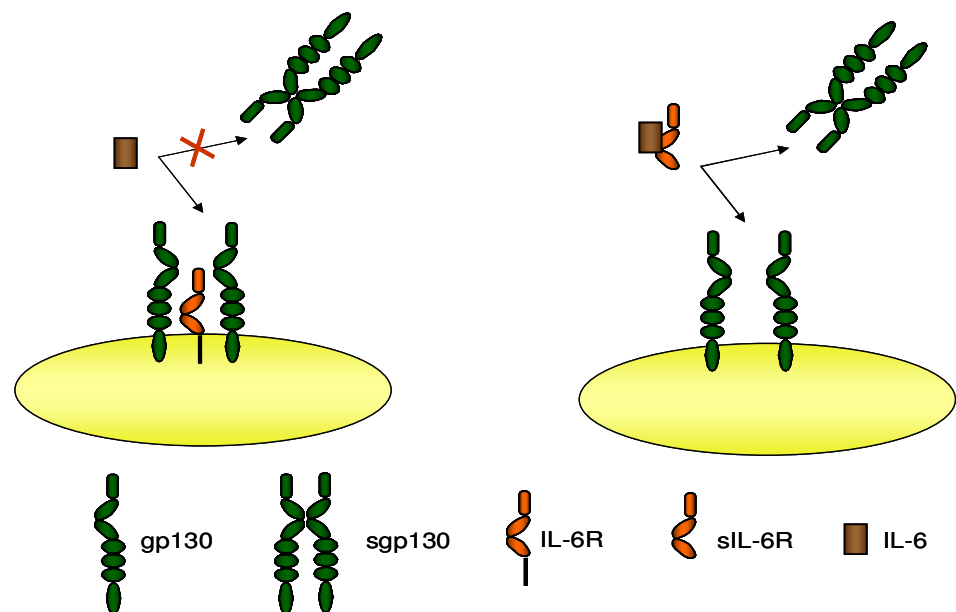


**Fig. 1.5 Soluble gp130 is the natural inhibitor of IL-6/sIL-6R responses.** **A** IL-6 can not bind to sgp130. Soluble gp130 has no access to IL-6 complexed by IL-6R and two molecules of membrane-bound gp130 and exhibits no inhibitory activity. **B** The IL-6/sIL-6R complex can equally bind to both membrane-bound and soluble gp130. IL-6/sIL-6R binding to sgp130 leads to competitive inhibition of its response [32].

## 1.10 Recombinant antibodies and strategies of vIL-6 neutralisation

Because vIL-6 binds directly to gp130, an Fc fusion protein of gp130 can be an inhibitor of vIL-6. Proliferation of Baf/3-gp130 cells upon stimulation with vIL-6 is blocked after adding 1µg/ml of recombinant sgp130Fc [72]. The prospects of neutralisation

of viral IL-6 hold great promise for therapy in vIL-6 associated diseases. sgp130Fc can be helpful for the suppression of transsignaling via IL-6/sIL-6R and via vIL-6 in various disease states. Molecular strategies for inhibition of signaling induced by vIL-6, but not by IL-6/sIL-6R can be based on the production of an antibody against viral IL-6 capable of neutralising the vIL-6 effect or destroying the HHV-8-infected cells.

Antibodies constitute a modular defence system of our body created by evolution to identify and mark any foreign intruder. By combination of a set of variant gene cassettes with additional mutation mechanisms, more than a billion different antibody-sequences can be generated. The genetic material for this huge “library” of different antibodies is stored in the B-cell pool of our lymphatic tissue.

Naturally occurring antibodies produced by B-cells consist of four polypeptide chains (Fig. 1.6 A). Two heavy chains (composed of one variable and three constant domains) and two light chains (composed of one variable and one constant domain) are held together by disulphide bonds. Antigen recognition by the antibody occurs via the

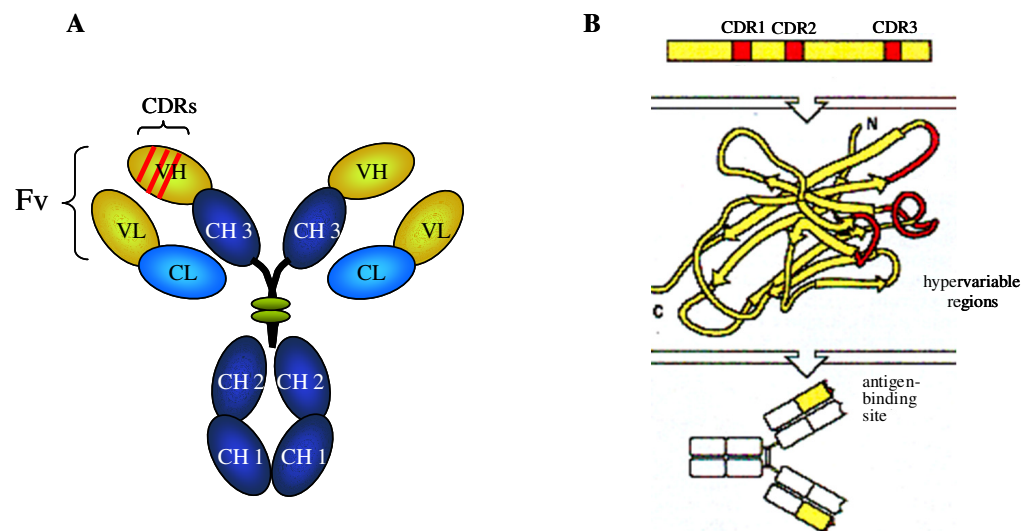


**Fig. 1.6 Structure of an antibody molecule.** **A** Schematic representation of the structure illustrating the four-chain composition and the separate domains comprising each chain: VL- variable domain of light chain; CL- constant domain of light chain; VH- variable domain of heavy chain; CH- constant domain of heavy chain; variable domains of both, light and heavy chain, form the variable fragment (Fv) of the antibody; CDR- complementarity-determining region. **B** The hypervariable regions (CDRs) lie in discrete loops of the folded structure and form the antigen-binding site [115].

variable regions (VH and VL). Each variable domain contains three hypervariable regions known as complementarity-determining regions, or CDRs. The CDRs together form the antigen binding paratope (Fig. 1.6 B).

Monoclonal antibodies are clonal populations of antibodies with the same specificity. They are very important research tools and find increasing use in various therapies [107-110]. Such antibodies are generated by fusing B-cells from immunised animals with myeloma cells. This generates a population of immortal hybridomas, from which the required clones can be selected. However, the therapeutic application of such antibodies produced by animal cells is limited by reactions of the human immune system leading to rejection of the animal proteins [111]. This can be reduced in part by humanizing the antibody by grafting the CDRs from the parent monoclonal into the backbone of a human IgG antibody [112].

New fascinating perspectives have been revealed by development of recombinant antibody libraries which can be screened for specific monoclonal antibodies outside the human body without the need of animal immunisation [113]. For this purpose, huge antibody gene libraries have been created. This is usually achieved by PCR-amplification from B-lymphocyte cDNA. Alternatively, antibody genes can be constructed *in vitro* by gene synthesis using “randomised wobble”-primers and inclusion of these foreign random sequences into the CDR regions. A combination of both methods also has been published [113-116]. The antibody library does not consist of native antibodies, but of single polypeptides retaining the antigen binding properties of the monoclonal antibody (Fv-variable fragment or Fab-antigen-binding fragment). Such polypeptides are called recombinant antibodies (Fig. 1.7A). To screen a library that contains many millions of different clones, a selection system is required with an efficiency comparable to that of the immune system. This can be achieved by displaying the antibodies on the surface of bacteriophages containing the antibody’s gene, in analogy to the expression of the IgM antibodies on the surface of unactivated B-lymphocytes. One example is the filamentous bacteriophage M13 [116]. A phage display library is a heterogeneous mixture of phage clones, each displaying a different single-chain Fv peptide (scFv) on its surface. Clones specific for the antigen can be isolated by affinity selection and used for production of the antibody fragment in *E.coli* or other suitable host organisms.

The screening procedures provide the power to select one from over a billion different expression clones in solution. The screened libraries can contain synthetic sequences, e. g. randomised antigen binding regions, or new combinations of light/heavy chains, thus creating the potential for generating human antibodies which could never be found in the blood stream. By random or designed mutations, the affinity or specificity of the antigen binding can be improved, reaching affinities observed with natural antibodies. These methods opened the way to use recombinant antibodies in research, diagnosis and therapy. For example, human anti mouse immune response, a major obstacle in patient treatment or in vivo diagnosis with conventional mouse monoclonal antibodies, can be avoided using recombinant human antibody fragments [111, 117].

Furthermore, genetic coupling of the antibody to a heterologous protein by fusion of gene fragments generates possibilities for immunotargeting. Immunotargeting employs the affinity of the antibody part to direct the activity of the heterologous protein towards the antigen.

To target vIL-6-secreting cells, a bispecific antibody (diabody) could be produced. This diabody is a recombinant antibody against vIL-6 conjugated with a T-cell receptor activating antibody (Fig. 1.7B). Cells secreting vIL-6 can be specifically killed by human T-cells when treated with bispecific antibodies binding to viral IL-6 and the T-cell receptor complex. Cells that do not express vIL-6 are unaffected. Such a strategy has been successfully employed for scFv antibodies specific for human IL-6 [118, 119].

A completely different strategy would exploit the intracellular recognition of vIL-6. Using this strategy, cells which synthesise the viral cytokine could be phenotypically changed not to secrete vIL-6. By using the ER targeting KDEL protein sequence (Lys-Asp-Glu-Leu) [118, 120] that can be added to an antibody at cDNA level (Fig. 1.7C), it should be possible to anchor such a fusion-antibody in the endoplasmic reticulum of an HHV-8 infected cell. Viral IL-6 on the way to the cell membrane would bind to this antibody and be retained within the cell. Thus, it could be possible to suppress the cellular secretion of the viral cytokine.

Potent cell killing agents are immunotoxins [121] that are emerging as therapeutic agents for the treatment of cancer and some immunological disorders [122-126]. They are constructed by attaching antibodies to cellular toxins, such as *Pseudomonas* exotoxin A

(PE). An antibody against vIL-6 fused to PE38 (Fig. 1.7D) could specifically kill the cells binding vIL-6.

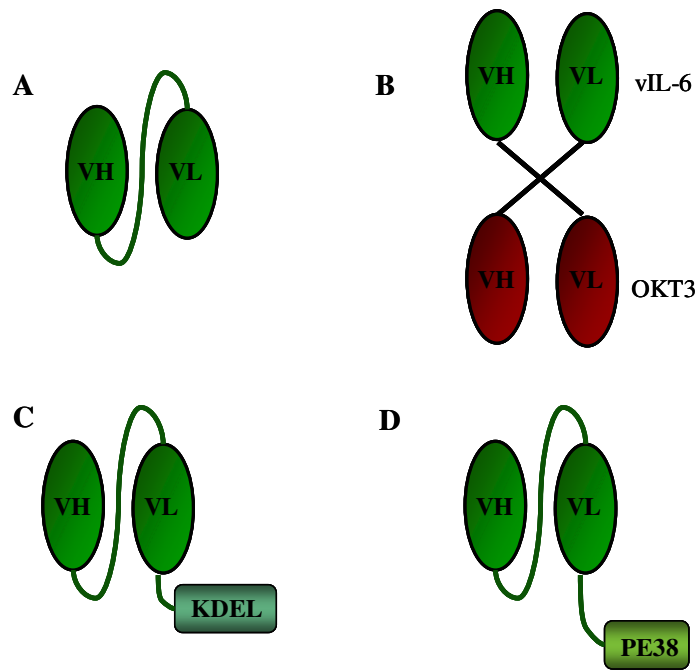


**Fig. 1.7 Recombinant antibody fragments.** **A** scFv- single-chain Fv fragment; **B** bispecific diabody, which is the scFv against vIL-6 conjugated with the OKT3 antibody; **C** scFv fused with the endoplasmic retention sequence KDEL; **D** scFv fused with the cellular toxin PE38.

## 1.11 Aim of the study

Viral IL-6 (vIL-6) encoded by human herpesvirus 8 (HHV-8) is a structural homologue of human and murine IL-6 and affects the cells via binding to the signal transducer gp130. vIL-6 is believed to be important in the pathogenesis of HHV-8 caused diseases including Kaposi's sarcoma as well as primary effusion lymphoma, multicentric Castelman's disease and perhaps multiple myeloma [56, 57]. The neutralisation of vIL-6 biological activity is thought to be helpful to combat these diseases. Therefore, the aim of this study was to generate recombinant antibodies against vIL-6 and to develop strategies for the targeting or elimination of cells expressing vIL-6.

In this study the recombinant vIL-6 had to be expressed, purified and tested for biological activity. Active purified vIL-6 could be used as antigen for phage display to isolate and later on to characterise the recombinant anti-vIL-6 antibodies.

The human recombinant antibodies against vIL-6 had to be screened using phage display technology. Selected antibodies had to be expressed, purified and characterised. The specificity and affinity of the antibodies to vIL-6 needed to be analysed and their ability to neutralise vIL-6 had to be tested.

The last objective of the study was to eliminate vIL-6 secretion using an antibody fused to the endoplasmic retention sequence KDEL. It was to be shown that vIL-6 can intracellularly bind to such an antibody and be retained in the endoplasmic reticulum.

## 2 Materials and methods

### 2.1 Materials

#### **Bacterial strains:**

BL21 (Novagen) *F<sup>-</sup> ompT hsdS<sub>B</sub> (r<sub>B</sub><sup>-</sup>m<sub>B</sub><sup>-</sup>)gal dcm (DE3)*

BL21pLysS (Novagen) *F<sup>-</sup> ompT hsdS<sub>B</sub> (r<sub>B</sub><sup>-</sup>m<sub>B</sub><sup>-</sup>)gal dcm (DE3)pLysS (Cam<sup>R</sup>)*

DH5α (MBI Fermentas) *F<sup>-</sup> gyrA96(Nal<sup>r</sup>) recA1 relA1 endA1 thri-1 hsdR17 (r<sub>k</sub><sup>-</sup>m<sub>k</sub><sup>+</sup>) glnV44 deoR Δ(lacZYA-argF) U169[φ80d Δ(lacZ)M15]*

TG1 (Amersham) *SupE hsdΔ5 thi Δ(lac-proAB) F'[traD36 proAB<sup>+</sup> lacI<sup>q</sup>lacZΔM15]*

HB2151 (Amersham) *K12 ara Δ(lac-pro) thi/F' pro A<sup>+</sup>B<sup>+</sup> lacI<sup>q</sup>lacZΔM15*

#### **Cell lines:**

COS-7 (african green monkey kidney fibroblast cell line)

HepG2 (human hepatocarcinoma cell line)

Baf/3-gp130 (murine IL-3 dependent pro-B-cells, stably transfected with gp130 [127])

Baf/3-gp130, IL-6R (murine IL-3 dependent pro-B-cells, stably transfected with gp130 and IL-6R [128])

EBNA-293 (human embryonic kidney cell line, stably expressed EBNA-1 gene of Epstein Barr virus, Invitrogen)

#### **Phage library:**

Human Single Framework scFv Libraries, Tomlinson A+B (Tomlinson, T., MRC, Centre for Protein Engineering, Cambridge, UK)

#### **Phagemids and vectors:**

pIT1 (Invitrogen)                      amp<sup>r</sup>

pET16b (Novagen)	amp <sup>r</sup>
pET22b (Novagen)	amp <sup>r</sup>
pET23a (Novagen)	amp <sup>r</sup>
p409B (modified in our lab)	amp <sup>r</sup>
pcDNA3.1 (Invitrogen)	amp <sup>r</sup>
pESL (modified in our lab)	kan <sup>r</sup>

**Antibiotics:**

Ampicillin to 50µg/ml

Kanamycin to 50µg/ml

**Media:****LB medium:**

5g/l yeast extract, 10g/l tryptone, 10g/l NaCl

**LB-agar:**

5g/l yeast extract, 10g/l tryptone, 10g/l NaCl, 15g/l agar

**TYE medium:**

5g/l yeast extract, 10g/l tryptone, 8g/l NaCl, 15g/l agar

**2xTY medium:**

10g/l yeast extract, 16g/l tryptone, 5g/l NaCl

**cell growth medium:**

DMEM (PAA), 10%FCS, 60mg/l penicillin, 100mg/l streptomycin

**Enzymes:**

All used restriction endonucleases, T4 polynucleotide kinase, T4 DNA ligase, *Pfu* DNA polymerase, calf intestine alkaline phosphatase were from MBI Fermentas.

**Enzyme substrates:**

p-nitrophenyl phosphate tablets (Sigma) – alkaline phosphatase substrat for ELISA (1 tablet : 15ml diethanolamine buffer)



ECL plus Western blotting detection system (Amersham)

**Antibodies and antisera:**

Anti-vIL-6 rabbit serum [69], 1:10.000

Anti-flag M2 monoclonal antibody (Sigma), 1:1000

Anti-myc monoclonal antibody 9E10 (research group Phytoantibodies, IPK, Gatersleben), 1:50

Anti-mouse alkaline phosphatase conjugate (Sigma), 1:2000

Anti-rabbit IgG goat peroxidase conjugate (Pierce), 1:10.000

Anti-mouse IgG goat peroxidase conjugate (Pierce), 1:10.000

Anti-STAT3-antibody (Biolabs), 1:1000

Anti-phospho-STAT3-antibody (Biolabs), 1:1000

Anti-mouse Alexa Fluor 594 goat antibody (Molecular Probes), 1:500-1:1500

**Recombinant cytokines:**

Hyper-IL-6 (5ng/ml for cell cultivation)

Human-IL-6 (5ng/ml for cell cultivation)

**Molecular markers:**

DNA molecular weight marker X (Roche)

Protein molecular weight marker #SM0431 (Fermentas)

Prestained protein molecular weight marker #SM0441 (Fermentas)

Full range protein molecular weight Rainbow marker RPN800 (Amersham)

**Chemicals:**

All used chemicals were from ROTH or MERCK.

**Kits:**

CONCERT Rapid Gel Extraction System (Gibco BRL)

NucleoSpin Plasmid DNA Purification Kit (Macherey-Nagel)

Gateway LR-clonase Enzyme Mix (Gibco BRL)

SlowFade Light Antifade Kit (Molecular Probes)

**Reagents for protein purification:**

Ni-NTA spin column (Amersham)

Ni-NTA agarose (Qiagen)

Dynabeads TALON (Dyna)

**Buffers:**

**TBS:**

50mM Tris pH=7.6, 200mM NaCl

**TBS-T:**

50mM Tris pH=7.6, 200mM NaCl, 0.05% Tween-20

**PBS:**

250mM NaCl, 20mM KCl, 48mM Na<sub>2</sub>HPO<sub>4</sub>, 1.5mM KH<sub>2</sub>PO<sub>4</sub>

**PBS-T:**

250mM NaCl, 20mM KCl, 48mM Na<sub>2</sub>HPO<sub>4</sub>, 1.5mM KH<sub>2</sub>PO<sub>4</sub>, 0.05% Tween-20

**Diethanolamine buffer:**

97ml diethanolamine, 0.1g MgCl<sub>2</sub>, 0.2g NaN<sub>3</sub>, add 1l H<sub>2</sub>O, pH=9.8

**12,5% -SDS-electrophoresis gel:**

3.75ml H<sub>2</sub>O, 3ml 1.5M Tris pH=8.8, 120μl 10% SDS, 5ml 30% acrylamid/0.8% bisacrylamid, 120μl 10% APS, 6μl TEMED

**7,5% -SDS-electrophoresis gel:**

4.9ml H<sub>2</sub>O, 2.5ml 1.5M Tris pH=8.8, 100μl 10% SDS, 2.5ml 30% acrylamid/0.8% bisacrylamid, 100μl 10% APS, 10 μl TEMED

**4% -SDS-electrophoresis stacking gel:**

6.1ml H<sub>2</sub>O, 2.5ml 0.5M Tris pH=6.8, 100μl 10% SDS, 1.33ml 30% acrylamid/0.8% bisacrylamid, 50μl 10% APS, 10μl TEMED

2 x SDS gel-loading buffer (Laemmli [129]):

100mM Tris pH=6.8, 4% SDS, 0.2% bromphenol blue, 20% glycerol

Tris-glycine electrophoresis buffer:

25mM Tris, 250mM glycine pH=8.3, 0.1% SDS

Solutions for silverstaining:

Fixate I: 40% methanol, 10% acetic acid

Fixate II: 10% ethanol, 15% acetic acid

Reducer: 0.2g reducer after Farmer (TETENAL) in 50ml H<sub>2</sub>O

Silversolution: 0.1g AgNO<sub>3</sub> in 50ml H<sub>2</sub>O

Developer: 2,9g Na<sub>2</sub>CO<sub>3</sub>, 40µl formaldehyde

Coomassie solution:

1g/l Coomassie R250, 40% methanol, 10% acetic acid

Destaining solution:

40% Methanol, 10% acetic acid

Transfer buffer:

39mM glycine, 48mM Tris base, 20% methanol

Stripping buffer:

2% SDS, 62.5mM Tris, 100mM β-mercaptoethanol

Software:

Prism (PPC) Alias, DNA Strider 1.3f12 Alias, EditView 1.0.1, Image reader LAS-1000, TECAN 5.0a, Quantity One, Fastfit 2.01, IAsys 2.

## 2.2 Methods

### 2.2.1 Cloning

Plasmid DNAs were isolated using the NucleoSpin Plasmid DNA Purification Kit (Macherey-Nagel), restriction digests and ligations were prepared using enzymes from Fermentas according to the manufacturer's instructions. The LR-clonase reaction was done as described in the application guide for the Gateway Cloning Technology (Gibco BRL).

### 2.2.2 Polymerase Chain Reaction (PCR) and Splicing by Overlap Extension - PCR (SOE-PCR)

The following PCR protocol was employed: 1-5ng of template, 0.2 $\mu$ M dNTPs, 5 $\mu$ M primers, 1U *Pfu*-Polymerase and 1x reaction buffer were mixed and the volume made up to 50  $\mu$ l with sterile water. For the reaction, the Robocycler Gradient 96 (STRATAGENE) was used and programmed as follows:

95°C – 5min  
95°C – 45sec  
55°C – 90sec  
72°C – 120sec  
72°C – 3min

} 27 cycles

SOE-PCR was used for amplification of SP-MAV (signal peptide of huIL-6 with MAV sequence) to clone a construct for eukaryotic expression of MAV. The signal peptide of huIL-6 (SP) was amplified by PCR using the primers MK104 and MK704 (Fig. 3.2.28 A). The reverse primer MK704 included the N-terminal sequence of MAV (7 a.a. = 21 bp). Thus, the PCR product of the signal peptide contained the N-terminal part of the MAV sequence at its C-terminal. The MAV sequence was amplified from pIT1-MAV employing the primers MK304 and MK404. The reverse primer MK404 included 12 nucleotides encoding the KDEL and the translational stop-codon TAG. The PCR-products of SP and MAV were applied to an agarose gel, extracted by CONCERT Rapid Gel Extraction

System (GibcoBRL) and used for Splicing by Overlap Extension (SOE)-PCR [156-159]. The PCR-products of MAV and SP were mixed and denaturised. The ssDNA of MAV annealed to the complementary ssDNA of the signal peptide. SOE-PCR was done under same conditions as PCR in 50µl reaction volume containing 5µl of amplified and extracted SP, 5µl of amplified and extracted MAV, 5µM terminal primers (MK104 and MK404), 0.2µM dNTPs, 1U Pfu-Polymerase and 1x reaction buffer.

### **2.2.3 Transformation of bacteria by heat-shock**

Stored chemically competent bacterial cells DH5α were refrozen on ice. DNA samples or aliquots of a ligation mixture (5µl), chilled on ice, were added to 100µl competent cells, mixed and incubated on ice for 20min. The transformation was achieved by heat-shock at 42°C for 90sec and subsequent incubation on ice for 3min. 350µl of LB medium were added to each sample and incubated at 37°C for 45min to allow the bacterial cells to recover. Transformed cells were plated onto LB agar containing the selective antibiotic and grown overnight at 37°C.

### **2.2.4 Preparation of recombinant vIL-6 in the bacterial expression system**

A bacterial culture of *E. coli BL21plysS* transformed with the plasmid pET16b-vIL-6-his was grown under shaking at 37°C to OD<sub>600</sub>=0.5. The expression of vIL-6-his was induced by adding 0.4mM IPTG for 4h. Afterwards, the bacterial culture was centrifuged at 6000g for 20 min, the supernatant was discarded and the bacterial cells were lysed using the French Press (FRENCH PRESSURE CELL PRESS, ThermoSpectronic) [130]. Inclusion bodies were separated from soluble proteins by centrifugation at 13000g for 1h. After three times washing with PBS, the inclusion bodies were dissolved in 6M guanidine hydrochloride and applied to a 1ml Ni-NTA column (Amersham Pharmacia). Before that, the column was equilibrated with 50mM phosphate-buffer pH=7.4 containing 500mM NaCl and 6M guanidine hydrochloride. After application of the proteins, the column was washed again, first with the same buffer, then with 50mM Tris-buffer pH=7.4. Recombinant vIL-6-his was eluted with

0.5M imidazole in 50mM Tris-buffer pH=7.4 and dialysed to 50mM Tris-buffer pH=7.4 without imidazole.

### **2.2.5 Preparation of recombinant vIL-6 in the eukaryotic expression system**

Stably transfected EBNA cells were grown in culture medium containing 10% FCS to 80-100% confluency. Then, the medium was changed to FCS-free medium and expressed vIL-6 protein was collected in the supernatant for 7 days. vIL-6 expressed in transiently transfected COS-7 cells (2.2.4) was also collected in FCS-free medium for about 5-7 days up to the point where the medium turned yellow. Cell supernatants were centrifuged to clean them from cell debris and incubated at RT with 300 µl/50 ml Ni-NTA agarose (Qiagen) for 2h. The agarose was washed with phosphate buffer containing 500 mM NaCl at pH=7.4, and recombinant vIL-6 was eluted with 1 ml of the same buffer containing 0.5 M imidazole.

### **2.2.6 Transient transfection of COS-7 cells using DEAE-dextran**

COS-7 cells were splitted to be 70-80% confluent the next day. Before transfection, the culture medium was changed to medium containing 75 µM chloroquine. For one 10 cm Petri dish, 5µg plasmid DNA was added to 435µl chloroquine-containing medium and 65µl DEAE-dextran (4mg/ml). This mixture was dropwise added to the cells followed by 4h incubation at 37°C and 5% CO<sub>2</sub>. Subsequently, the medium was removed and the cells were treated with 10% DMSO containing DMEM at RT for 7min. Afterwards, the cells were washed with PBS and new DMEM was added.

### **2.2.7 SDS-PAGE and gel staining**

SDS-polyacrylamide gel electrophoresis was carried out at 150 V for about 1h using the BIO-RAD system. Separated proteins were stained with Coomassie-solution at RT for 2h or silver. For silverstaining, the gel was incubated in fixate I and fixate II for 5 min

each. After 5 times washing for 1 min with 60°C warm H<sub>2</sub>O, the gel was incubated in reducer for 30sec. After another washing step, the gel was stained with silver solution for 12min. Then, the gel was washed with RT- H<sub>2</sub>O for 90sec and developed (see 2.1). The reaction was stopped with 10% acetic acid.

## 2.2.8 Proliferation assay

For the proliferation assay, the Baf/3 transfectants Baf/3-gp130 and Baf/3-gp130, IL-6R were used. Cultured cells were washed three times with PBS to remove the cytokine used to sustain proliferation. Afterwards, the cells ( $5 \times 10^3$ /well of 96-well microtiter plate) were incubated in the presence of different cytokine concentrations for 68h and subsequently puls-labeled with 0.25μCi [<sup>3</sup>H]thymidine for 4h. Proliferation rates were measured by harvesting the cells on glass filters, and the incorporated radioactivity was determined by scintillation counting. For each cytokine concentration, the proliferation assay was performed at least three times in triplicates.

## 2.2.9 Selection of vIL-6 specific phages from the phage display libraries

### 2.2.9.1 Production of helper phage

200 μl of the *E. coli TGI* culture (OD<sub>600</sub>=0.2) were infected with 10μl of 1:10<sup>2</sup>, 1:10<sup>4</sup>, 1:10<sup>6</sup> dilutions of helper phage M13KO7, incubated at 37°C for 30 min and plated on TYE medium for overnight growth at 37°C. Individual clones were picked into 5 ml of exponentially growing *E. coli TGI* cultures and incubated with shaking at 37°C for 2h. Phage-infected *TGI* culture was diluted with 500 ml of 2xTY and grown with shaking at 37°C for 1h. Thereafter, kanamycin was added to a final concentration of 50 μg/ml and the culture was incubated with shaking at 30°C overnight. The cells were spun down at 10000g for 15min, and the phage particles were precipitated from the supernatant by adding 100ml of PEG/NaCl solution and incubation on ice for 1h. Precipitated phage particles were collected by centrifugation at 10000g for 30min and then resuspended in 8ml TE buffer. Phage precipitation was repeated by supplementation with 2ml PEG/NaCl solution to the phage suspension on ice for 20min

before the phages were collected by centrifugation at 3000g for 30min. The phage pellet was resuspended in PBS and spun again at 10000g for 10min to clean the phage particles from bacterial cell debris. The helper phage particles were resuspended in PBS with 15% glycerol for storage at -70°C.

Titration of the phage stock was done by infection of 1ml *E. coli* TG1 culture (OD<sub>600</sub>=0.4) with 1µl of 1:1000 phage stock dilution in PBS. 50µl of the infected culture and 50µl of its dilutions 1:10<sup>2</sup>, 1:10<sup>4</sup>, 1:10<sup>6</sup> with 2xTY were plated on TYE medium containing 50µg/ml kanamycin and 1% glucose. Phage plaques were counted after overnight incubation at 37°C.

### **2.2.9.2 Selection on immunotubes**

Immunotubes (3 or more per library) were coated with 100µl 10µg/ml flag-vIL-6-his solution in PBS and incubated at room temperature overnight. To block the free binding sites of the tubes, they were treated with 200µl 2% BSA in PBS for 2h. After blocking, the tubes were loaded with 10<sup>12-13</sup> phage particles diluted in 100µl 2%BSA and incubated 30 min with shaking and 60 min without. The tubes were washed 20 times with PBS containing 0.1% Tween-20. The phage particles were eluted by adding 90µl 100mM triethylamine per tube and shaking for 10min. The solution containing the eluted phages was neutralised by supplementation with 0.5 volume 1M Tris pH=7.4. The phage particles were amplified by infection of *E. coli* TG1 for the next round of phage selection. 9ml of TG1 fresh culture at OD<sub>600</sub>=0.4 were infected with the phage particles by incubation at 37°C for 30 min. To determine the phage titre, 50µl of the stock culture and its dilution (10<sup>-2</sup>, 10<sup>-4</sup>, 10<sup>-6</sup>) were plated on TYE medium containing 100µl/ml ampicillin and 1% glucose. The infected culture was centrifuged at 3000g for 10 min. The cell pellet was resuspended in 1 ml 2xTY medium and plated on a Bio-Assay dish containing TYE with 100µl/ml ampicillin and 1% glucose for overnight growth at 37°C with shaking. Colonies were scraped with a glass spreader from the agar using 5ml 2xTY supplemented with 15% glycerol. 50µl of this suspension were inoculated to 50 ml of 2xTY containing 100µl/ml ampicillin and 1% glucose and grown with shaking at 37°C to OD<sub>600</sub>=0.4. 5x10<sup>10</sup> helper phage particles were added to 10ml of the bacterial culture and incubated without shaking in a 37°C water bath for 30 min. Subsequently, the cells were centrifuged at 3000g for 15 min, resuspended in 50ml 2xTY containing 100µl/ml ampicillin and 50µl/ml kanamycin and incubated with



shaking at 30°C overnight. The cells were again centrifuged at 3000g for 15 min, and the phages were precipitated from 40 ml of supernatant by adding 10ml PEG/NaCl and incubation on ice for 1h. After centrifugation at 3000g for 30 min, the pellet containing the phage particles was resuspended in 1ml PBS and centrifuged at 11000g for 10 min to remove bacterial debris. The supernatant, i.e. the phage solution, was used for the next round of selection.

### **2.2.9.3 Preparation of soluble scFvs**

For the preparation of soluble scFvs, 200µl of the non-suppressor bacterial strain *E. coli* HB2152 were infected with 10µl of the eluted phages and incubated at 37°C for 30 min without shaking. 2µl of bacterial culture were inoculated into 175µl 2xTY medium containing 100µl/ml ampicillin and 0.1% glucose and grown for 3h at 37°C with shaking. The expression of soluble scFvs was induced by adding 1mM IPTG and overnight shaking at 30°C. The bacterial culture was centrifuged at 1800g for 10 min and 50µl supernatant was used as primary antibody solution for the scFv ELISA.

### **2.2.10 Soluble scFv ELISA**

A 96 well microtiter plate was coated with 100µl of 10µg/ml recombinant vIL-6 (or other antigens for cross-reactivity ELISA) and incubated at RT overnight. For blocking, 200µl 3% BSA/PBS were loaded per well and incubated for 2 h. Then, 100µl of cell supernatant containing soluble scFv (2.2.11.3) diluted 1:2 with 2% BSA/PBS-T were applied per well and incubated at 25°C for 1h. The plate was washed 5 times with PBS-T to remove unbound scFv. 100µl of monoclonal anti-myc antibody 9E10 diluted 1:50 in 1% BSA/PBS-T were loaded per well and incubated for 1h. After 5 times washing with PBS-T, 100µl/well of anti-mouse IgG conjugated with alkaline phosphatase (1:2000 in 1% BSA/ PBS-T) were added and the plate incubated at RT for 1h. 5 times washing was followed by adding 100µl/well substrate for alkaline phosphatase (1mg/ml p-nitrophenylphosphate in diethanolamine buffer) and 15 min incubation at 37°C. The colour intensity was measured as extinction at 405nm using an ELISA reader. The results were analysed by Microsoft Excel.

### **2.2.11 Expression of scFv in bacterial cells *E.coli BL21***

*E. coli BL21* bacteria were transformed with the plasmid pET23a-MAV encoding the scFv. 1 litre LB medium containing 50µl/ml ampicillin was inoculated with 2ml overnight culture of transformed *E. coli BL21* and grown with shaking at 37°C to OD<sub>600</sub>=0.5. The periplasmic expression of MAV was induced by adding 0.4mM IPTG and overnight shaking at 30°C. The bacterial culture was centrifuged at 6000g for 20 min. The supernatant containing the soluble scFv was purified by Ni-NTA agarose. 100ml of the bacterial supernatant were incubated with 0.5ml Ni-NTA agarose (QUIAGEN, Hilden) at RT for 2h. The matrix was then washed with 50mM phosphate-buffer pH=7.4 containing 500mM NaCl and bound MAV was eluted with 1ml 0.5M imidazole in the same buffer.

### **2.2.12 Western Blot**

For Western Blot analysis of the cell lysates, the cells from a 10 cm dish were lysed with 1 ml 2x Laemmli buffer [129], 10 µl of which were applied to SDS-PAGE. To analyse the proteins of the cell supernatant, 15 µl out of 5 ml were used. The samples were separated on 12.5% polyacrylamide gels for vIL-6, huIL-6 and MAV, and on 7.5% gels for STAT3 at 160 V. The protein transfer onto a PVDF membrane (Hybond-P, Amersham Biosciences) was performed at 10 V for 1 h. The membrane was blocked in 6% BSA/TBS at room temperature for 2 h followed by overnight incubation with the primary antibody diluted in 1% BSA/TBS-T at 4°C. After washing with TBS-T buffer, the membrane was incubated with the secondary POD conjugated antibody (Pierce) at room temperature for 1 h. After repeated washing with TBS-T and finally TBS the peroxidase substrate ECL(+) was applied (Amersham Biosciences). The enzymatic reaction caused chemiluminescence, so that the protein-antibody complex could be visualised on X-ray film.

### **2.2.13 Immunoprecipitation of vIL-6 with MAV**

COS-7 cells were transiently transfected with p409-vIL-6. The next day, the DMEM medium containing 10%FCS was changed to 5 ml FCS-free DMEM. After 24h the

supernatant was removed and centrifuged at 10000g for 2min to remove cell debris. 1ml supernatant containing vIL-6 was incubated with 15µg of MAV at 4°C overnight under continuous rolling. Immunocomplexes were collected with 25µl Talon beads (Dyna) during incubation at 4°C for 2h. Unspecifically bound proteins were washed away with PBST and PBS buffers, before the MAV/vIL-6 complexes were eluted with 20µl 0.5M imidazole in PBS. The eluates were separated by SDS-polyacrylamide-gel-electrophoresis and Western blot analysis was done using anti-vIL-6 serum as described.

### **2.2.14 Proliferation assay**

The neutralising assay was carried out with Baf/3-gp130 and Baf/3-gp130-IL-6R cells. Cultured cells ( $5 \times 10^3$ /well of a 96-well microtiter plate) were washed three times with PBS. Thereafter, the cells were incubated in the presence of different concentrations of MAV (or without MAV as control) and a constant concentration of one of the following cytokines: vIL-6 (500 ng/ml), HIL-6 (1 ng/ml) or huIL-6 (1 ng/ml). After incubation for 68h the cells were puls-labeled with 0.25 µCi [<sup>3</sup>H]thymidine for 4 h. Proliferation rates were measured by harvesting the cells on glass filters and determination of the incorporated radioactivity by scintillation counting. For each cytokine concentration the proliferation assay was performed at least three times in triplicates.

### **2.2.15 Stimulation of HepG2 cells**

HepG2 cells were seeded out on 10 cm dishes to reach 70-80% confluency the next day. The cell growth medium containing 10%FCS was changed to FCS-free medium for 18 h. Subsequently, the cells were stimulated with 150 ng/ml recombinant vIL-6 alone or with MAV (150 ng/ml, 1.5 µg/ml, and 15 µg/ml) at 37°C and 5% CO<sub>2</sub> for 10 min. After washing with PBS the cells were lysed in 1 ml 2xLaemmli and frozen down.

## **2.2.16 Analysis of STAT3 phosphorylation in human hepatoma cell line**

The lysates of the stimulated cells were subjected to 7.5% SDS-PAGE and the proteins transferred onto Hybond-P PVDF membrane (Amersham). Phosphorylated STAT3 was detected in the Western blot (2.2.12) by an anti-phospho-STAT3 antibody (Biolabs). After 30 min incubation of the membrane in stripping buffer at 60°C, the total amount of STAT3 was analysed by Western blotting using an anti-STAT3 antibody (Biolabs).

## **2.2.17 Surface Plasmon Resonance (SPR)**

### **2.2.17.1 Immobilisation of vIL-6 to the SPR sensorchip**

The SPR sensorchip (IASys) was placed in the instrument and left with PBS-T for 45 min to equilibrate. The cuvette was then washed with PBS-T three times for 5 min, before 0.2 M EDC/0.05 M NHS was added for 10 min to activate the chip. After another washing step with PBS-T to remove excess EDC/NHS, the buffer was changed to 10 mM Na-acetat pH=5.5 immobilisation buffer. Having recorded a stable baseline, 40 µg recombinant vIL-6 were applied to the sensorchip. Non-coupled vIL-6 was removed by washing with PBS-T for 10 min and 1 M ethanolamine pH=8.5 was added for 2-3 min to block the free carboxyl groups of the dextran. The chip was washed again and could be used for the interaction analysis.

### **2.2.17.2 Interaction analysis**

The binding experiment was performed at room temperature with different concentrations of MAV using the IAsys™ optical biosensor. Affinograms were analysed by nonlinear regression with the FASTfit software, which uses the Marguard-Levenburg algorithm for iterative data fitting [131].

## **2.2.18 Immunostaining of transfected COS-7 cells**

Approximately 40.000 COS-7 cells grown on cover glasses for 24h were washed with PBS containing 0.1% acid and fixed with cold methanol at -20°C for 10min. The cells

were then washed two times with TBS and incubated with blocking buffer (1%BSA, 0.2% glycerine, TBS) at room temperature for 2h. A 1:100 dilution of the anti-myc antibody was applied at 4°C overnight. The cells were washed with TBS-T and TBS and incubated with the Alexa Fluor 594 anti-mouse antibody at 37°C for 1h. The washing was repeated as before and the cover glasses were mounted on slides with SlowFade Light (Molecular Probes, USA) and analysed using fluorescence microscopy. A 543-fold magnification was used to photograph the cells.

## 3 Results

### 3.1 Expression of recombinant vIL-6

#### 3.1.1 Expression of recombinant vIL-6 in bacteria

About 7 mg of recombinant viral IL-6 were required as antigen for phage panning and immunological characterisation of selected antibodies. Viral IL-6 was first expressed as a fusion protein containing 6xhis residues as a C-terminal tag in the *E. coli* pET-expression system (Novagen). pET vectors are one of the the most powerful systems for high bacterial expression of recombinant proteins [132, 133].

The vIL-6 cDNA sequence was amplified by PCR using the primers KJ1601 and KJ1701, before cloning into the his-tag containing vector pET16b opened by *Bam*HI and *Nde*I (Fig. 3.1.1). To verify the vIL-6 sequence (see appendix) and the ORF, the construct

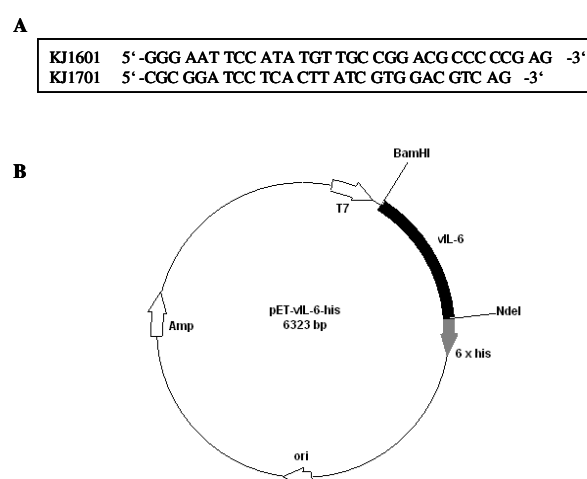


**Fig. 3.1.1 Vector map of pET16b-vIL-6-his:** **A** Sequence of the primers used for vIL-6 amplification; **B** Amplified vIL-6 was cloned into pET16b plasmid vector opened by *Bam*HI and *Nde*I. Amp-ampicillin resistance gene, T7 – T7 promoter, 6xhis- histidin tag sequence.

was sequenced using the same primers as for the amplification. The expression of vIL-6 upon IPTG induction was successful in the bacterial strain *BL21plysS* but not in *E. coli BL21* (Fig. 3.1.2 A). Bacterial cells containing the plasmid pLysS produce T7 lysozyme, which is a natural inhibitor of T7 RNA polymerase and thus reduces the transcription of the target gene in uninduced cells. The expression of the protein prior induction might be harmful for the bacteria. The bacterial culture was grown under inducing conditions for 4h. After collecting the bacteria by centrifugation, they were lysed using the French Press. Subsequently, the bacterial products accumulated in the cytoplasm in soluble form or as insoluble inclusion bodies were separated by high speed centrifugation. The recombinant vIL-6 was located in inclusion bodies (Fig. 3.1.2 B), which were resolved in 6 M guanidine hydrochloride and

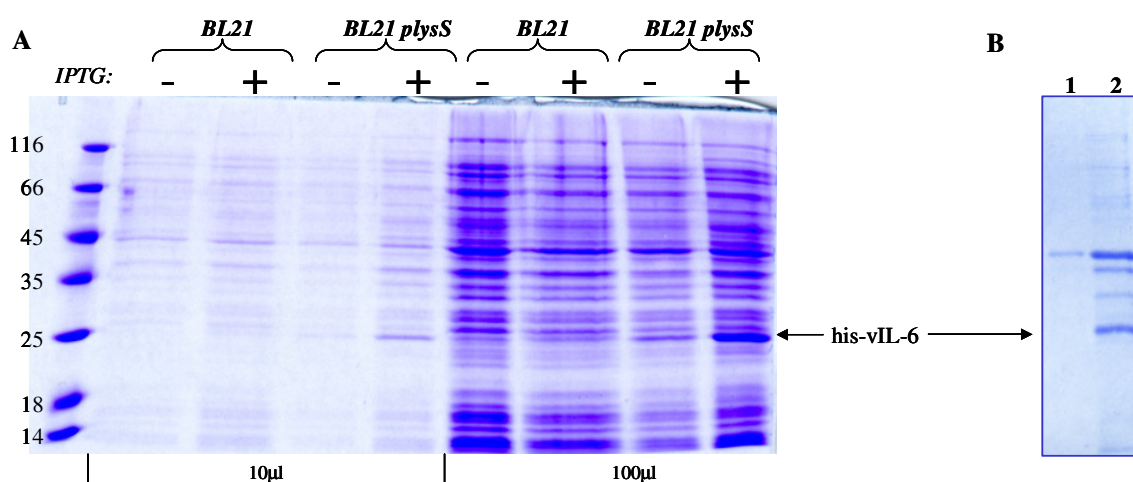


**Fig. 3.1.2 Bacterial expression of recombinant vIL-6:** A SDS-PAGE of *E. coli BL21/BL21plysS* cells from 10 µl and 100 µl bacterial culture. IPTG induced expression of vIL-6 was obtained only with bacterial strain *BL21plysS*. B Coomassie staining of soluble (lane 1) and insoluble (lane 2) proteins expressed in bacteria. Bacterial cells were lysed by sonication. vIL-6 was expressed in inclusion bodies (lane 2).

loaded onto a Ni-NTA spin column (Amersham). The purification was accomplished via binding of the his-tag of vIL-6 to the  $\text{Ni}^{2+}$  of the column's matrix (Fig 3.1.3). Unbound proteins were removed by washing with guanidine hydrochloride-containing buffer. After washing with guanidine hydrochloride-free buffer, the bound recombinant vIL-6 was eluted from the Ni-matrix with 0.5 M imidazole. This way, the vIL-6 was refolded directly on the column. The eluted protein was dialyzed against Tris-buffer. To analyse its molecular mass and purity it was applied to an SDS polyacrylamide gel (Fig. 3.1.4A). The recombinant vIL-6

preparation was additionally checked by Western blot analysis using an anti-vIL-6 serum [69] (Fig. 3.1.4 B).

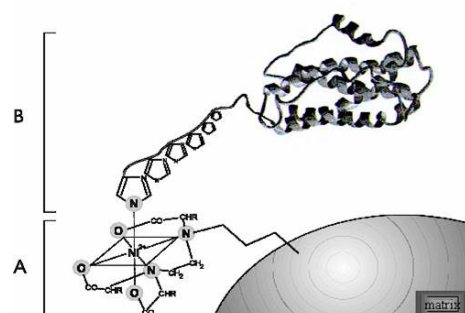


**Fig. 3.1.3 Binding of the polyhistidine-tagged vIL-6 to Ni-NTA-agarose (schematic illustration):** A Ni resin; a matrix bead bearing the pentadentate metal chelator with bound Ni<sup>2+</sup> ion; B One histidine residue of the polyhistidine-tag of the recombinant protein binds to the resin.

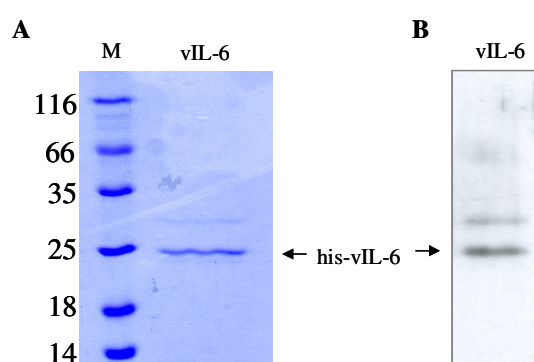


**Fig. 3.1.4 Purification of recombinant vIL-6 protein:** His-vIL-6 was purified from inclusion bodies dissolved in 6 M guanidiniumhydrochloride by Ni-NTA-agarose. A Coomassie staining of purified protein, M- protein marker, vIL-6- purified recombinant viral IL-6; B Western Blot using anti-vIL-6-serum (1:10000).

The bioactivity of the expressed and purified vIL-6 was measured using Baf/3 cells stably transfected with gp130. Baf/3 cells are murine IL-3 dependent pro-B-cells, which do not express receptors of the IL-6 cytokine family [127, 128]. In the absence of IL-3, Baf/3 cells transfected with the gp130 receptor cDNA proliferate after stimulation by vIL-6 as well as Hyper-IL-6 (see introduction) [72, 96]. In proliferation assays performed to test the activity of recombinant vIL-6, Baf/3-gp130 cells were stimulated with different concentrations of the viral cytokine and with Hyper-IL-6 as positive control. Unfortunately, the result was not consistent. In some experiments the vIL-6 seemed to be functional. But in



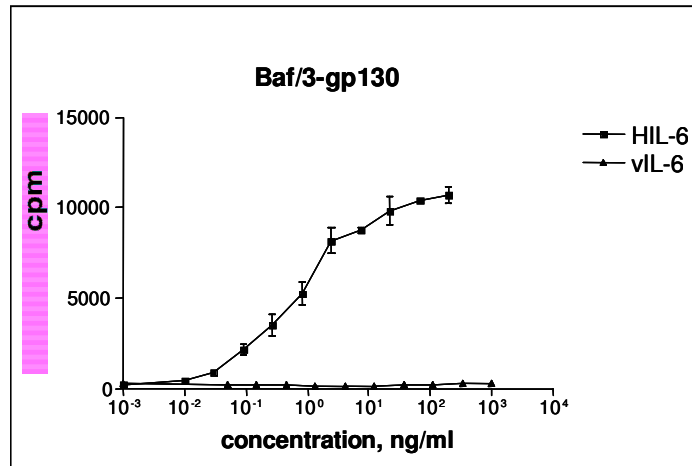


**Fig. 3.1.5. Biological activity of recombinant vIL-6:** Baf/3-gp130 cells were stimulated to grow by increasing amounts of Hyper-IL-6 and purified recombinant vIL-6. Proliferation of cells was assessed by measuring of [3H]thymidine incorporation into DNA.

most experiments it was clearly inactive (Fig. 3.1.5). Therefore, as an alternative, secreted eukaryotic expression of vIL-6 was explored in COS-7 cells. Viral IL-6 carrying the N-terminal signal peptide was synthesised at the ribosomes of the endoplasmic reticulum, transported to the cell membrane and released. The expression in eukaryotic cells supported the folding and posttranslational modification of vIL-6, resulting in secretion of biologically active vIL-6 [72, 135].

### 3.1.2 Eukaryotic expression of vIL-6

The COS-7 cell (African Green Monkey kidney fibroblast cells) expression system achieves high-level, transient expression of proteins. These cells express the SV40 large tumor antigen, which is necessary to initiate DNA replication at the SV40 origin. A high copy number of plasmids containing an SV40-driven origin of replication is present in COS-7 cells 48h post-transfection. If the transfected DNA encodes a secretion protein, up to 10 µg of protein per 10<sup>7</sup> cells can be recovered from the supernatant of the transfected COS-7 cells after one week post-transfection [72, 136].

COS-7 cells were transiently transfected [137] with the expression plasmid p409-vIL-6-his [72]. The recombinant protein was collected in the cell medium containing 0.5% FCS over 7 days and purified by Ni-NTA-agarose. 100 ml medium were incubated with 0.5

ml Ni-NTA-agarose, followed by washing with PBS and elution of vIL-6-his from the matrix with 0.5 M imidazole. The purity of the vIL-6 was analysed by SDS-PAGE and subsequent silverstaining (Fig. 3.1.6).

Also, EBNA-293 cells stably transfected with vIL-6 were obtained in collaboration with Jutta Eichler (GBF, Braunschweig). The modular episomal vector pCEP-Pu [138], based on the Epstein-Barr virus genome, was used as an expression system for vIL-6 (Fig. 3.1.7). Two genetic elements, the viral origin of replication and the gene for nuclear antigen

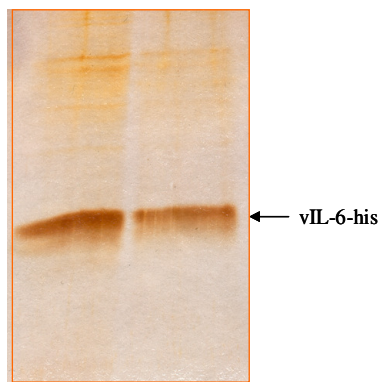


**Fig. 3.1.6 Expression of vIL-6 in eukaryotic cells:** Silverstaining of vIL-6 with C-terminal his-tag expressed in COS-7 cells and purified by affinity chromatography using Ni-NTA-agarose.

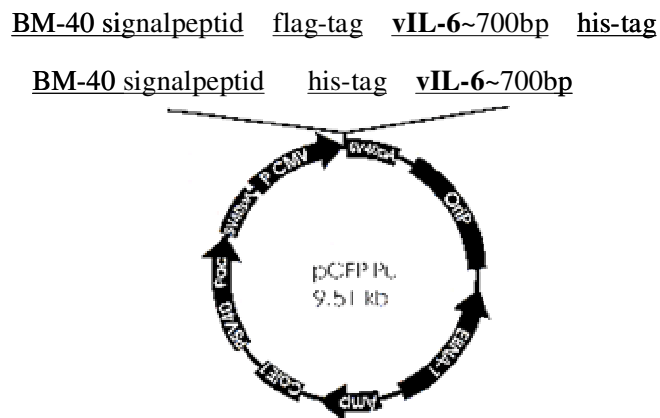


**Fig. 3.1.7 vIL-6 expression cassettes for EBNA-293 expression:** Schematic map of the expression constructs pCEP-Pu-flag-vIL-6-his and pCEP-Pu-his-vIL-6. P CMV- cytomegalovirus promoter; Ori P- EBV (Epstein Barr Virus) origin of replication; EBNA-1- gene 1 of the Epstein Barr Virus; colE1 ori- colE1 origin of replication; PSV40- SV40 promoter; SV40pA- SV40 poly-A.

EBNA-1, are necessary to sustain high-copy-number episomal replication of recombinant vectors in cells [139]. The expression constructs contained the vIL-6 sequence with an N-terminal his-tag and vIL-6 with two affinity tags, an N-terminal flag-tag and a C-terminal his-tag (see appendix).

The EBNA-293 cells were cultured under the same conditions as the COS-7 cells. After 7 days the supernatant of stably transfected cells was analysed for vIL-6 expression. 1  $\mu$ l of the medium from each cell line was applied to a 12.5% SDS-PAGE, blotted onto a PVDF membrane and stained by anti-vIL-6-serum [69]. Interestingly, the expression of flag-vIL-6-his in EBNA-293 cells was much higher than that of his-vIL-6 in COS-7 or EBNA-293 cells (Fig. 3.1.8). Because both recombinant proteins expressed in EBNA-293 cells contained a his-tag, they were purified by Ni-NTA-agarose. The successful purification of the EBNA-293 cell expressed proteins was shown by SDS-PAGE and Western blot using the anti-vIL-6-serum (Fig. 3.1.9 A, B, C).

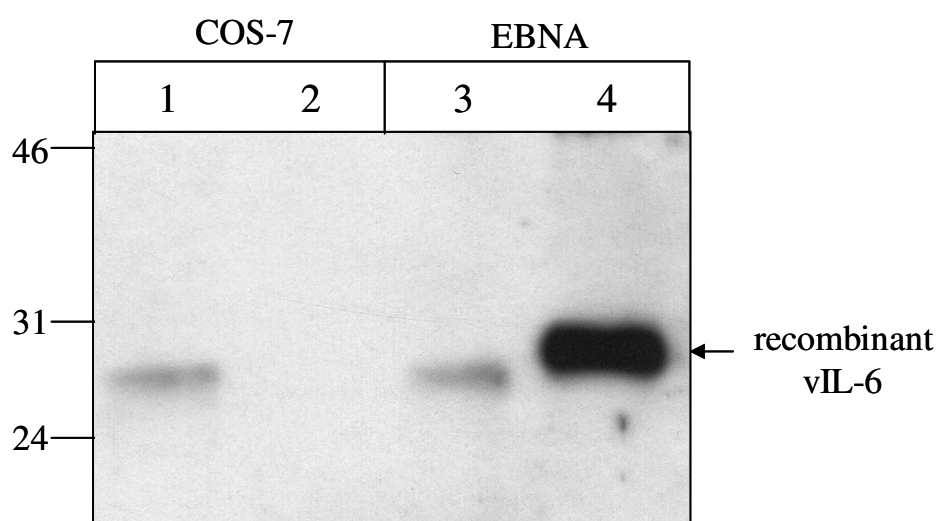


**Fig. 3.1.8 Expression of vIL-6 in eukaryotic cells:** Comparison of vIL-6 expression in COS-7 cells and EBNA-293 cells. 2  $\mu$ l of cell growth medium were applied onto the SDS-polyacrylamide gel. Western blot with anti-vIL-6-serum was done: lane 1- COS-7 cells transiently transfected with vIL-6-his; lane 2- untransfected COS-7; lane 3- EBNA-293 cells stably transfected with vIL-6-his; lane 4- EBNA-293 cells stably transfected with flag-vIL-6-his.

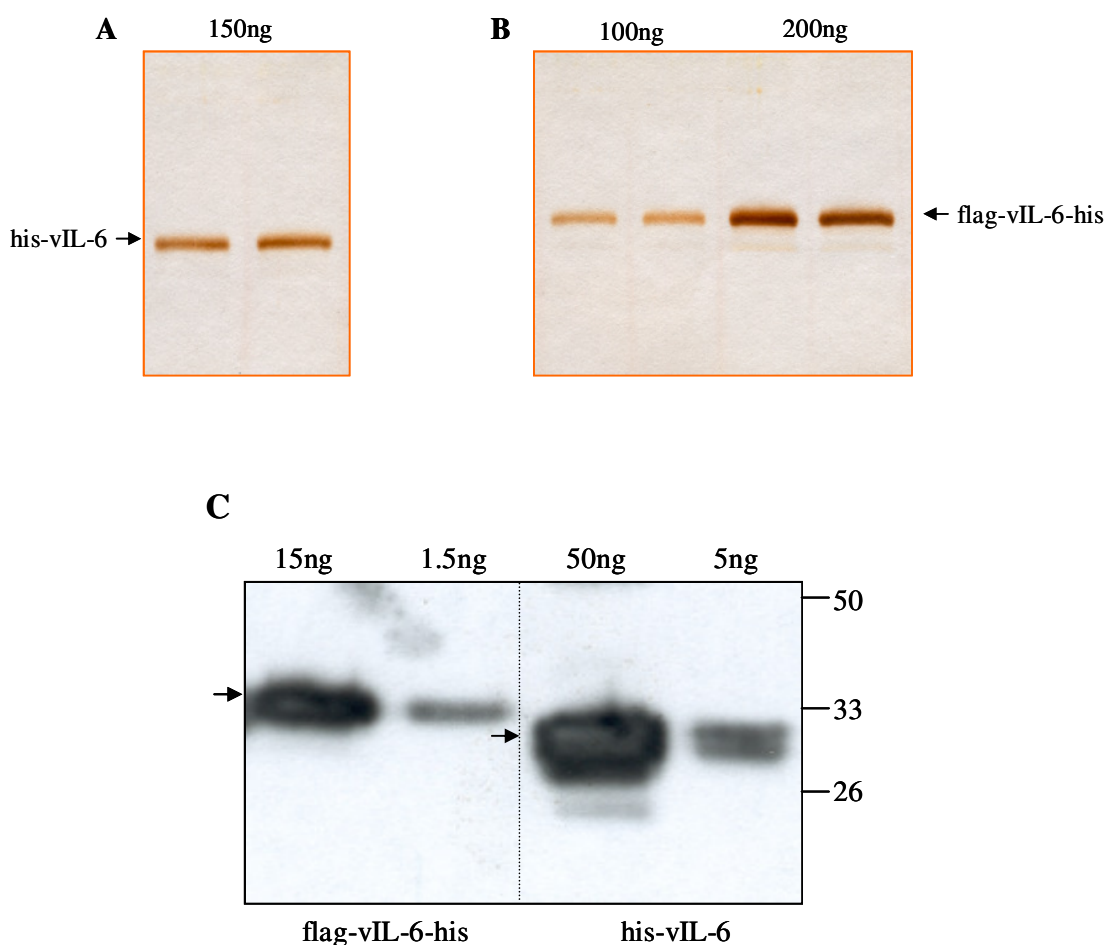


**Fig. 3.1.9 Purification of vIL-6 expressed by EBNA-293 cells:** Silverstaining of his-vIL-6 (A) and flag-vIL-6-his (B) purified by Ni-NTA-agarose. C Western blot of recombinant flag-vIL-6-his (15 ng, 1.5 ng) and his-vIL-6 (50 ng, 5 ng). Viral IL-6 was detected using rabbit anti-vIL-6-serum diluted 1:10000.

To control the correct folding of the recombinant vIL-6 proteins, circular dichroism (CD) spectra were recorded. As other cytokines of the IL-6 cytokine family, correctly folded vIL-6 has a four helical bundle structure [68]. vIL-6 expressed and purified from EBNA-293 cells displayed a typical  $\alpha$ -helical spectrum. His-vIL-6 displayed an even more helical spectrum than the flag-tagged one (Fig. 3.1.10). The CD-spectrum of the bacterial expressed vIL-6 reflects a helical structure of the protein, too, but differences in folding of the eukaryotic and the bacterial expressed proteins are obvious (Fig. 3.1.10). This suggests that high amounts of bacterial expressed vIL-6 were not folded, and that most molecules of the recombinant protein remained unstructured. Such CD-spectra have been observed for higher order structures such as aggregates and oligomers [140].

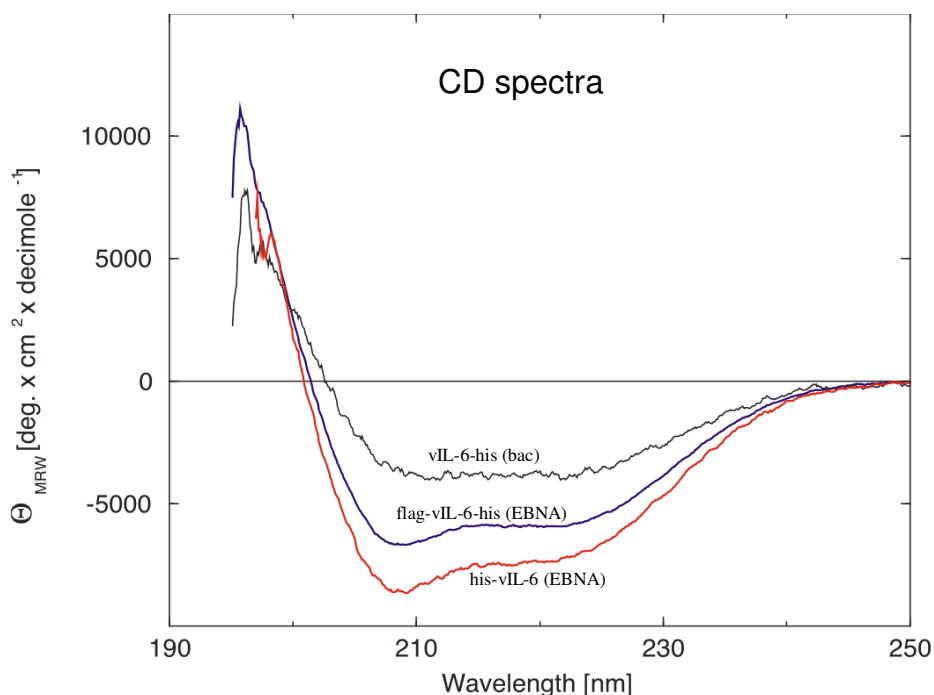


**Fig. 3.1.10 Circular dichroism spectra:**  $\alpha$ -helical fold of flag-vIL-6-his (blue) and vIL-6-his (red) expressed by and purified from EBNA-293 cells and of vIL-6-his expressed in bacterial cells (black).

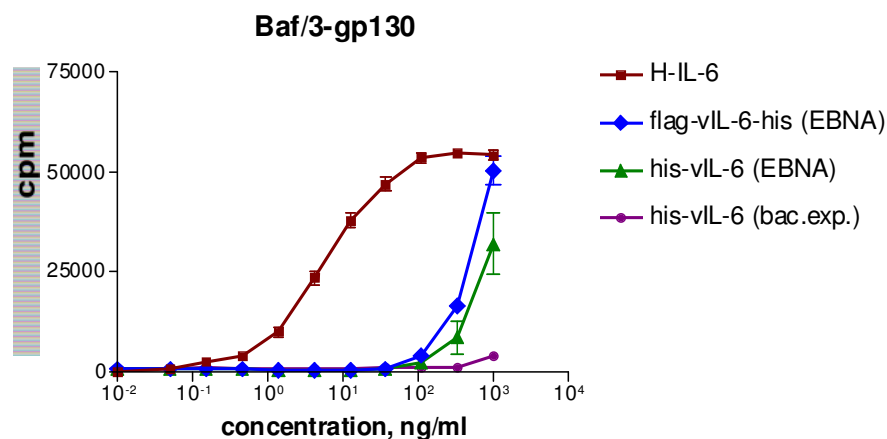


**Fig. 3.1.11 Induction of proliferation of Baf/3-gp130 cells by vIL-6:** Baf/3-gp130 cells were stimulated with increasing amounts of EBNA-293-expressed flag-vIL-6-his or his-vIL-6 or bacterial expressed vIL-6-his or Hyper-IL-6. Proliferation was measured by [<sup>3</sup>H]thymidine incorporation.

To test for biological activity of EBNA-293 expressed vIL-6, the same proliferation assay was used as for recombinant vIL-6 expressed in bacterial cells. Previous studies had shown that Baf/3-gp130 cells are able to proliferate in response to Hyper-IL-6 at a concentration below 1 ng/ml, whereas 100 ng/ml of viral IL-6 were needed to induce Baf/3-

gp130 cell proliferation [69, 72]. The concentration of vIL-6 proteins was determined photometrically at 240-320nm using the method of Waxman [141]. In this study, flag-vIL-6 and his-vIL-6 expressed in EBNA-293 cells induced proliferation of Baf/3-gp130 cells at similar concentrations (Fig. 3.1.11).

Interestingly, in EBNA-293 cells, the expression level of flag-vIL-6-his was three-fold higher than the one of his-vIL-6: About 100 µg were obtained after purification of 100 ml conditioned cell medium (7 days) from flag-vIL-6-his transfected EBNA-293 cells, and only 20-30 µg from 100 ml conditioned medium (7 days) of his-vIL-6 transfected EBNA-293 cells. Thus, flag-vIL-6-his was produced in large enough amounts to be used as coating antigen for the phage display.

## 3.2 Production of recombinant antibodies against vIL-6

### 3.2.1 Phage library screening

For the production of recombinant antibodies against vIL-6 the phage display technology was chosen [142]. The main advantage of this method over the hybridoma technology is the possibility to obtain human antibodies from an antibody library within a few weeks. To isolate gene sequences coding for anti-vIL-6 scFv, the libraries Tomlinson A and B (Tomlinson, T., MRC, Centre for Protein Engineering, Cambridge, UK), each comprising  $10^9$  scFv fragments (IPK Gatersleben, Germany), were screened using

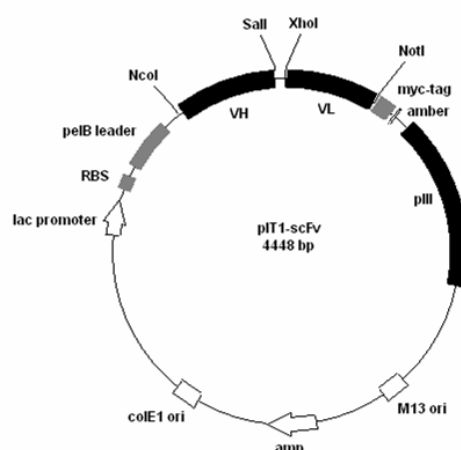


**Fig. 3.2.1 Vector map of pIT-scFv:** VH- variable region of the heavy chain of human IgG; VL- variable region of the light chain of human IgG; myc-tag- myc-tag sequence; amber- stop-codon; pIII- phage coat protein; M13 ori- phage M13 origin of replication; amp- ampicillin resistance gene; colE1 ori- colE1 origin of replication; lac promoter- lacZ promoter; RBS- ribosome binding site; pelB leader – signal peptide for periplasmic expression.

recombinant flag-vIL-6-his as coating antigen for phage panning. Both libraries are based on a single human framework for the variable regions of heavy (VH) and light (VL) human immunoglobulin chains. Artificial scFvs were genetically engineered by random combination of cDNA fragments encoding hypervariable regions (CDRs) of heavy and light variable chains connected by a short glycine-serine linker and cloned into phagemid pIT1 [143, 144]. The phagemid pIT1-scFv encodes the scFv gene fused in-frame with the phage gene coding for the phage surface protein pIII (Fig. 3.2.1). The scFv antibodies were displayed on the phage surface during the phage life cycle, achieved by co-transfection of the bacterial cells *E. coli TGI* with pIT1-scFv and the wild type phage (Fig. 3.2.2).

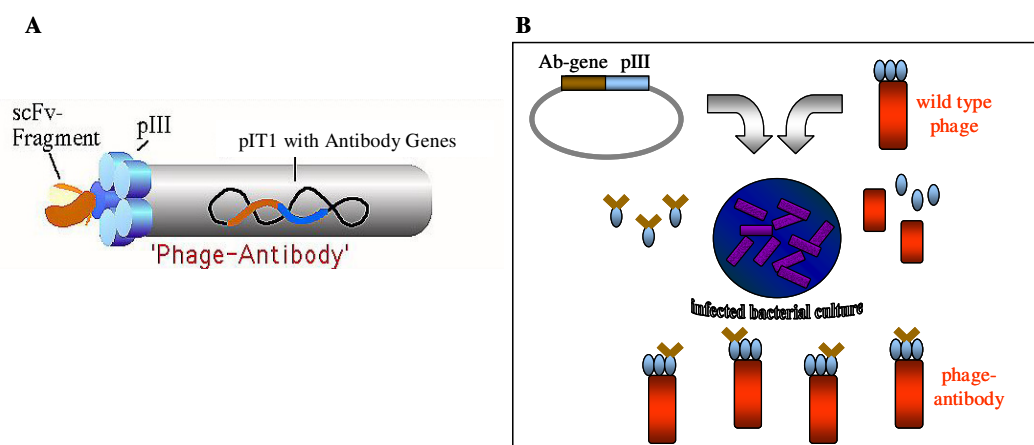


**Fig. 3.2.2 Presentation of antibody fragments on the surface of filamentous phage:** Antibody fragments (brown) are presented on the phage surface as a fusion with phage protein pIII (blue). **A** Scheme of the structure of a “phage-antibody”; **B** Production of phage-antibodies during phage life cycle via co-transfection of bacterial cells with a phagemid.

The antigen-specific phage selection procedure, also called biopanning, relies on the highly specific binding of phage particles from the library to the antigen coated on the solid phase, in this case vIL-6. After panning, non-bound particles were eliminated by washing, and the phages bound to vIL-6 were eluted and amplified by infection of bacterial cells *E. coli TGI* (Fig. 3.2.3). The obtained phage particles were precipitated from the culture supernatant and subjected to the next round of selection. This process had to be repeated three times, because the pool of phages obtained in the first round of selection displayed scFvs with various affinities and specificities to the antigen. The second panning was performed to enrich the phage pool for phages displaying anti-vIL-6 scFvs with high

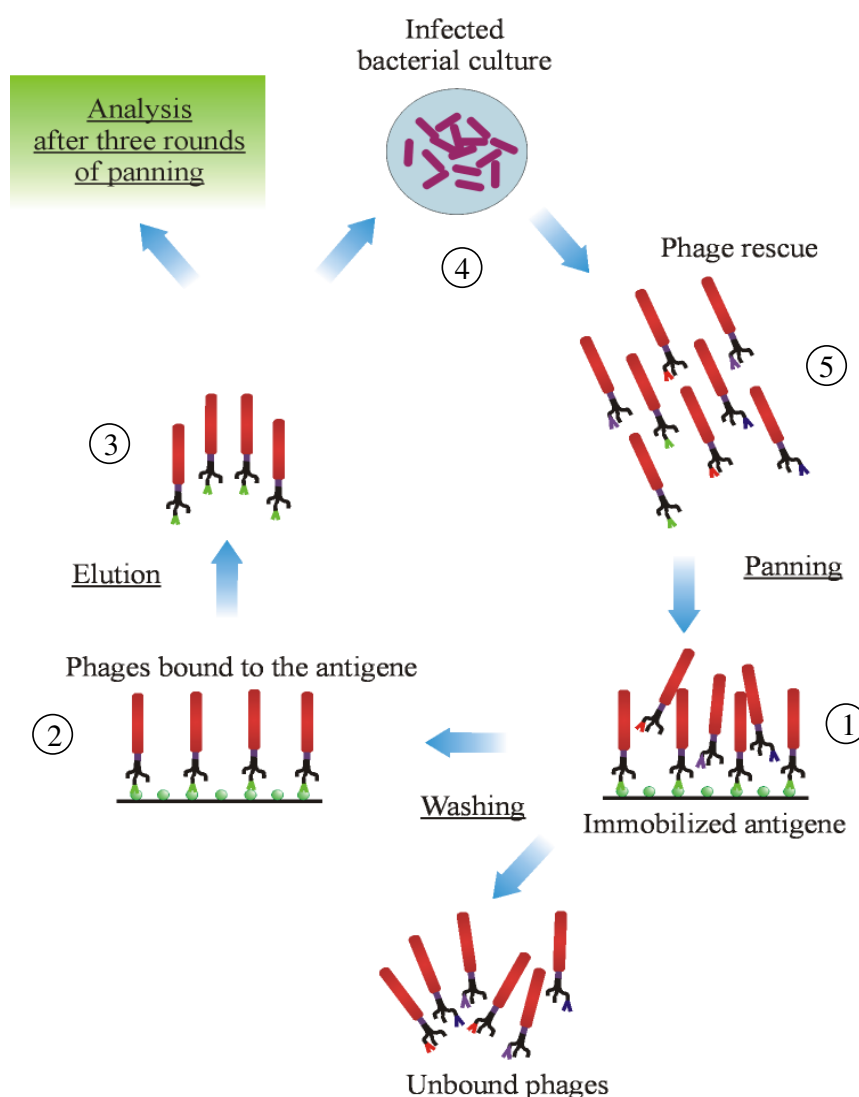


**Fig. 3.2.3 Schematic illustration of one round of biopanning:** Specific phages bind to immobilised antigen and non-specific phages are washed away. Antigen-bound phages can be eluted and amplified by infection of the bacteria.

antigenic specificity and affinity. In the third round, the phage pool was divided into single phage clones. 200 of the phage clones were infected into the bacterial cells *E. coli HB2151* for production of soluble scFvs. The pIT1-scFv phagemid encodes the gene of scFv fused to the gene of the phage surface protein pIII. Between these genes a stop-codon is placed, which in the bacterial suppressor strain *E. coli TG1* is translated into an amino acid. *HB2151* is a non-suppressor strain of the bacteria. In the bacterial cells *E. coli HB2151*, the transcription terminated after the stop-codon, leading to the expression of soluble antibody fragments without the pIII portion (Fig. 3.2.4 A). The expression of the scFvs under the lac-promoter was induced by IPTG. The signal peptide of pectate lyase B (pelB) is responsible



for the secretion of the expressed protein into the periplasmic space (that is the space between the inner and outer membrane) of the gram-negative bacteria. The ability of soluble scFv to recognise recombinant vIL-6 was verified by ELISA. The principle of the scFv ELISA is schematically demonstrated in Fig. 3.2.4 B. Soluble scFvs from individual phage clones were used as primary antibodies to bind to the immobilised recombinant vIL-6. The scFvs bound to the

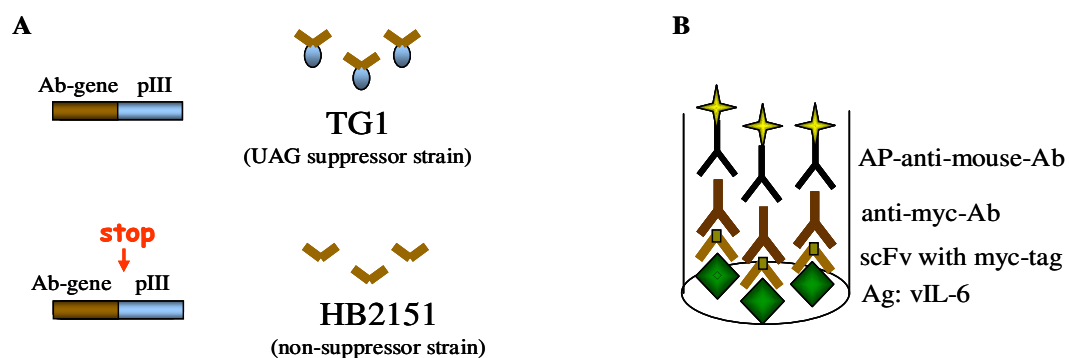


**Fig. 3.2.4 Production and detection of the soluble antibody fragments:** **A** Soluble antibodies were produced by retransfection of the phagemide into the non-suppressor bacterial strain HB2151. **B** Scheme of scFv ELISA: Ag: vIL-6- solid fixed recombinant flag-vIL-6-his as coating antigen; scFv with myc-tag- soluble anti-vIL-6 scFv with myc-tag; anti-myc-Ab- anti-myc antibody 9E10 recognised myc-tag of the scFv; AP-anti-mouse-Ab- anti-mouse-IgG antibody conjugated to alkaline phosphatase to detect bound monoclonal anti-myc antibody.

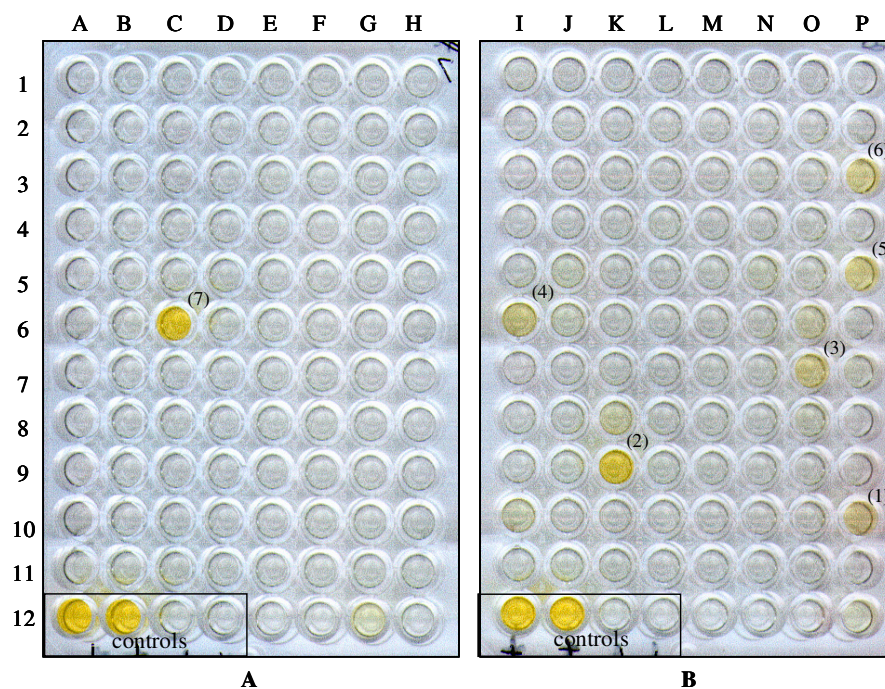


**Fig. 3.2.5 Soluble scFv ELISA:** Detection of the vIL-6 specific scFvs after 3rd round of panning. **A** Library Tomlinson A. **B** Library Tomlinson B. A12, B12 and I12, J12 are positive controls: scFv against plant transcription factor ABI3/7 (IPK Gatersleben) specifically binds to ABI3/7. C12, D12 and K12, L12 are negative controls with BSA.

antigen were specifically recognised by the monoclonal anti-myc-antibody 9E10 followed by an anti-mouse IgG conjugated to alkaline phosphatase (AP). Using the AP-substrate 4-nitrophenyl phosphate, the extinction of the reaction product at 405 nm was a measure for AP activity. As can be seen in Fig. 3.2.5, seven clones seemed to be positive.

The cDNA sequence of each of these seven clones was analysed by PCR using the phagemide primers LMB3 and pHEN. The 908 bp DNA fragment coding for the scFv was obtained for five clones (Fig. 3.2.6). Clones 1 and 4 contained only the variable heavy chain corresponding to the size of about 600 bp. However, such a result was not unexpected, since previous studies had shown that incomplete clones are present in the Tomlinson library [145, 146].

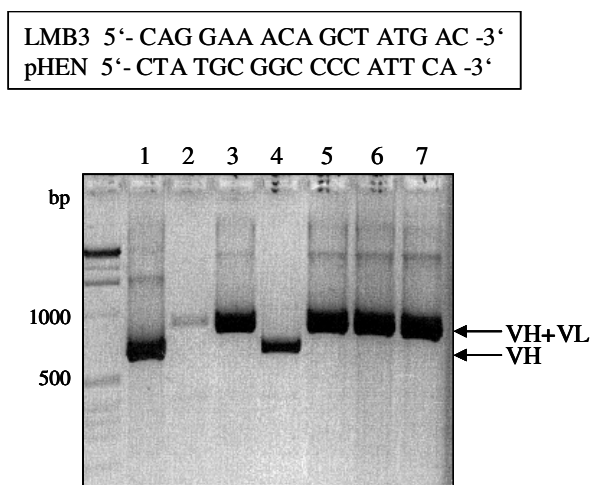


**Fig. 3.2.6 PCR of human recombinant antibodies scFv screened against vIL-6:** PCR of 7 individual phage clones was prepared by phagemid primers LMB3 and pHEN. VH+VL- full sequence of scFv (heavy and light chains); VH- scFv containing only heavy chain.

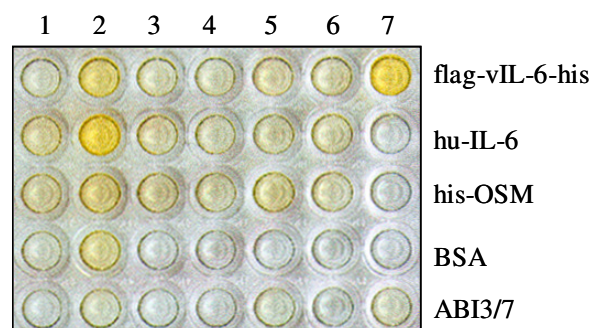


**Fig. 3.2.7 Cross-reactivity of scFv screened against vIL-6:** The specificity of screened recombinant antibodies was analysed by ELISA with different antigens such as human IL-6 (huIL-6), his-OSM (oncostatin M), BSA, ABI3/7 (plant transcription factor). Only one clone of scFv (7, later MAV1) was really specific for vIL-6.

To analyse the specificity of the screened scFvs for vIL-6, they were tested for cross-reactivity with other antigens by ELISA. Unspecific scFvs were those antibody fragments, which did not bind to vIL-6 only, but to other antigens, too. Five clones from seven displayed very little and unspecific binding. Clone 2 exhibited some cross-reactivity with his-OSM and BSA and very strong cross-reactivity with human IL-6. Only clone 7 (later MAV1) was highly specific for vIL-6 (Fig. 3.2.7). Therefore, clones 1-6 were not further analysed.

However, since in previous studies using different antibody libraries and antigens more than one specific antibody could be selected [119, 147], we assumed that we similarly would be able to isolate more scFvs specific for vIL-6. Therefore, further 200 phage clones were analysed for displaying scFvs specific for vIL-6. In the same way as the 200 clones tested before, the 200 new phage clones were retransfected into the non-suppressor bacterial cells *HB2151* to produce soluble scFv. Soluble scFv from individual phage clones were analysed by ELISA for binding to vIL-6 (date not shown). Again, only one recombinant antibody with high specificity to vIL-6 was found (later called MAV2). The cross-reactivity of MAV2 with other antigens was tested by ELISA in comparison to MAV1 (Fig. 3.2.8). MAV2 as well as MAV1 did not display any cross-reactivity and showed specific binding for flag-vIL-6-his and his-vIL-6. The detected weak binding of both antibodies to gp130-Fc was probably unspecific. Most likely, the secondary AP-anti-mouse antibody recognised the Fc part of gp130-Fc (Fig. 3.2.8).

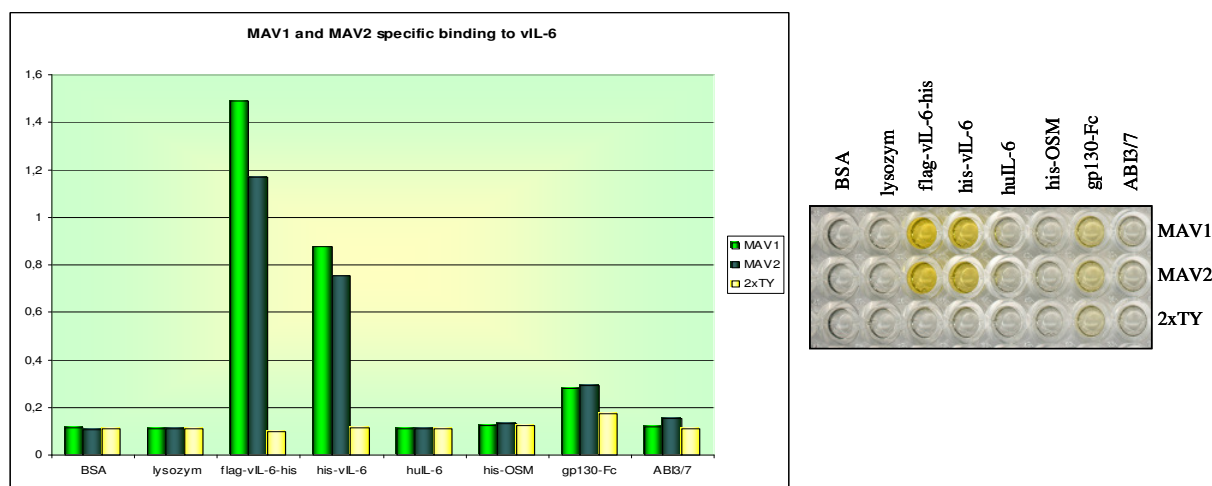


**Fig. 3.2.8 Cross-reactivity of scFv screened against vIL-6:** 200 new clones of scFv were screened and one positive was found (MAV2). Its specificity was analysed by ELISA with different antigens such as BSA, lysozym, human IL-6 (huIL-6), his-OSM (oncostatin M), gp130-Fc, ABI3/7 (plant transcription factor) and compared to MAV1.

### 3.2.2 Western blot and sequence analysis of screened scFvs

The expression of MAV1 and MAV2 in *E. coli HB2151* was analysed by Western blotting using an anti-myc antibody as a secondary antibody that recognised the C-terminal myc-tag of the scFv. Bacterial cells *E. coli HB2151* were infected with the phages containing phagemids pIT1-MAV1 and pIT1-MAV2 or were not infected and grown in medium with low amounts of glucose in order to down-regulate transcription of the phage genes. The glucose was metabolised by the time IPTG was added to induce the expression of scFvs. The secreted recombinant antibody fragments were directly detected in samples of the culture medium. The 30 kDa bands seen in the Western blot of the medium from infected bacteria correspond to MAV1 and MAV2 (Fig. 3.2.9).

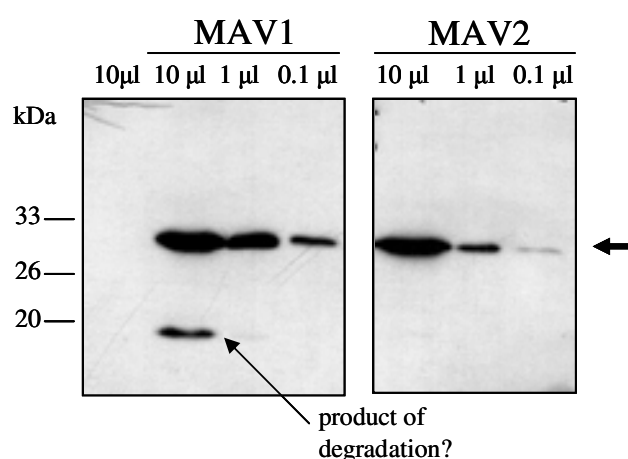


**Fig. 3.2.9 Expression of MAV in HB2151 bacterial cells:** Western blot of medium from HB2151 cells infected with phages and expressing MAV1 or MAV2 (first lane: medium from non-infected cells). 10µl, 1 µl and 0,1 µl of medium were applied to SDS-PAGE, blotted and the scFv expression was detected by anti-myc antibody 9E10 (1:50).

To characterise the cDNA sequence of MAV1 and MAV2, pIT1-MAV1 and pIT1-MAV2 phagemids were isolated from an infected *E. coli HB2151* bacterial cell culture grown in low-glucose-medium. The DNA-sequence encoding the scFv was verified by sequencing (HotShot sequencing, SEQLAB, Goettingen) with the primers LBM3 and pHEN (Fig. 3.2.6). The translated amino acid sequence alignment is shown in Fig. 3.2.10 (for DNA sequence see appendix). Surprisingly, the sequence of MAV1 was identical to the one of MAV2, suggesting that in the course of two different selection procedures the same antibody fragment (MAV) has been isolated. This may indicate that no additional scFvs specific for vIL-6 are present in the library.

```

                VH →
                CDR I           CDR II
1 XASLHANSISRKTVI MKYLLPTAAAGLLLL AAQPAMAEVQLLESG GGLVQPGGSLRLSCA ASGFTFSSYAMSWVR QAPGKGLEWVSDIRG 90
2 XXQLACKFYFKETVI MKYLLPTAAAGLLLL AAQPAMAEVQLLESG GGLVQPGGSLRLSCA ASGFTFSSYAMSWVR QAPGKGLEWVSDIRG 90

                CDR III
1 RGPPTGYADSVKGRF TISRDNKNTLYLQM NSLRAEDTAVYYCAK RMWGFDYWGQGLT VSSGGGSGGGGSGG GGSTDIQMTQSPSSL 180
2 RGPPTGYADSVKGRF TISRDNKNTLYLQM NSLRAEDTAVYYCAK RMWGFDYWGQGLT VSSGGGSGGGGSGG GGSTDIQMTQSPSSL 180
                linker           VL →

                CDR I           CDR II           CDR III
1 SASVGDRVTITCRAS QSISSYLNWYQKPG KAPKLLIYGASRLQS GVPSRFSGSGSGTDF TLTISLQPEDFFATY YCQQAWHLPLTFGQG 270
2 SASVGDRVTITCRAS QSISSYLNWYQKPG KAPKLLIYGASRLQS GVPSRFSGSGSGTDF TLTISLQPEDFFATY YCQQAWHLPLTFGQG 270

1 TKVEIKRAAAEQKLI SEE 288
2 TKVEIKRAAAEQKLI SEE 288

```

**Fig. 3.2.10 Protein Alignment:** MAV1 (1) and MAV2 (2) sequences. VH- variable region of the heavy chain of human IgG; VL- variable region of the light chain of human IgG; CDR- hypervariable region (blue-specific for MAV amino acids compared to other scFv of Tomlinson library); linker (red)- glycin/serin linker.

### 3.2.3 Production and purification of large amounts of MAV

The pET-vector-system (Novagen), which was used for the bacterial expression of vIL-6, was chosen for the expression of the recombinant antibody. The MAV coding sequence was cut out from pIT1 by *NcoI* and *NotI* (Fig. 3.2.1) and inserted into the pET22b vector via *NcoI* and *NotI*. pET22b ensures the expression of the gene of interest in soluble form in the periplasmic space due to the pelB leader sequence, which encodes a signal peptide for periplasmic expression. The antibody sequence together with the pelB leader was recloned into the vector pET23a by *XbaI* and *NotI*, so that MAV obtained a his- and myc-tag, which are missing in pET22b. The tags are helpful for detection and purification of the recombinant scFv. The map of the expression construct pET23a-MAV is depicted in Fig. 3.2.11.

The expression of MAV induced by IPTG was detectable in the supernatant of *E. coli* BL21 as well as BL21plysS transformed with pET23a-MAV cDNA (Fig. 3.2.12 A). 2µl of the supernatant of the bacterial culture, either induced or not induced for expression, were

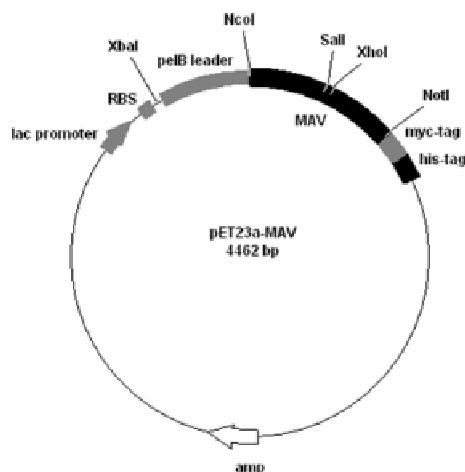


**Fig. 3.2.11 MAV-expression plasmid for bacterial transformation:** MAV- recombinant antibody sequence; amp- ampicillin resistance gene; lac promoter- lacZ promoter; RBS- ribosome binding site; pelB leader- signalpeptide for periplasmic expression.

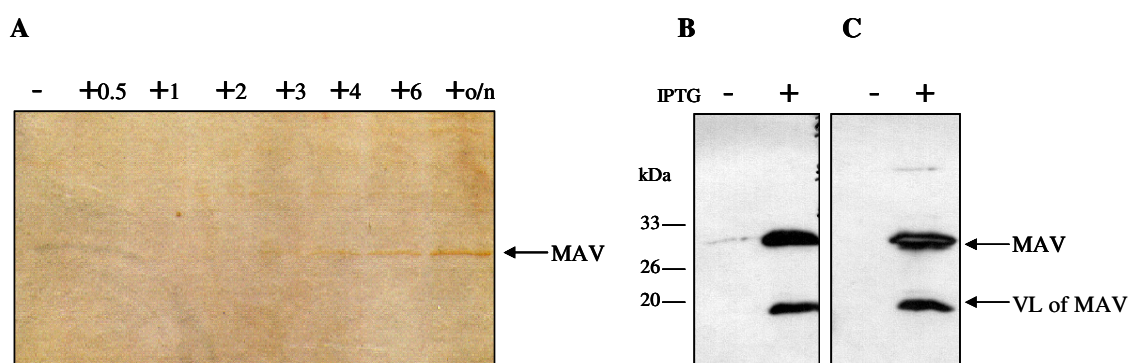


**Fig. 3.2.12 Expression of pET23b-MAV in *E.coli* strains *BL21* and *BL21plysS*:** Periplasmic expression of MAV was induced by IPTG stimulation. After centrifuging, cell medium was electrophoretically separated on a 12.5% polyacrylamide gel. **A** Dependency of MAV expression level in *E. coli BL21* on the expression time, silverstaining of bacterial supernatant (15  $\mu$ l in each lane) before IPTG induction and after 0.5, 1, 2, 3, 4, 6 hours and overnight expression. **B** Western blot analysis of MAV expression in *E. coli BL21*; **C** Western blot of MAV expression in *E. coli BL21plysS* using anti-myc antibody.

applied to a 12.5%polyacrylamide gel and blotted onto a PVDF membrane. An anti-myc antibody recognised expressed MAV (30 kDa) via its C-terminal myc-tag in the Western Blot (Fig. 3.2.12 B and C). The 18 kDa band could be the variable region of the light chain (VL) including the myc- and his-tags generated by limited proteolytical degradation of scFv molecules during expression.

Like the recombinant vIL-6, MAV was purified using Ni-NTA-agarose. The bacterial culture was centrifuged and the supernatant incubated with Ni-agarose beads. MAV bound to the Ni<sup>2+</sup> of the matrix via its his-tag. Unbound proteins were washed away and MAV was

eluted with buffer containing 0.5 M imidazole. The quality of the purification was analysed by SDS-PAGE (Fig. 3.2.13). The VL part of MAV seen in the Western blot (Fig. 3.2.12 B and C) seemed to co-purify via the his-tag.

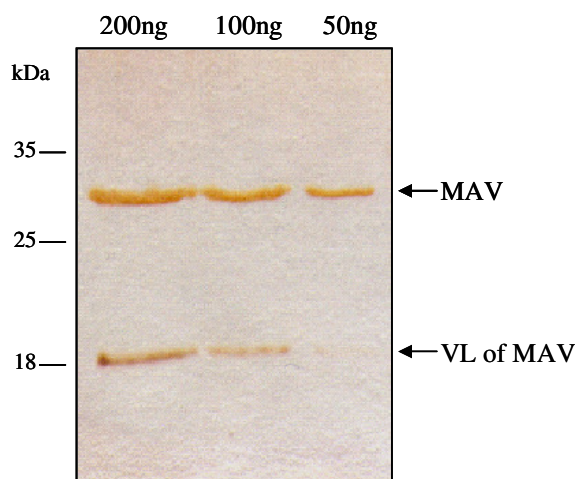


**Fig. 3.2.13 Purification of MAV:** MAV was expressed in the periplasmic space of the bacteria and purified by Ni-NTA-agarose. Pure protein was separated by a 12.5% SDS-PAGE and visualised by silverstaining.

## 3.2.4 Properties of MAV

### 3.2.4.1 MAV recognition of vIL-6 in ELISA and Western blot

The purified recombinant antibody fragment MAV was analysed by ELISA for specific binding to vIL-6. Different antigens were coated at a concentration of 10 µg/ml and 0.5 µg MAV per well were added. Binding of MAV to vIL-6 was detected by an anti-myc antibody. MAV bound to flag-vIL-6-his and his-vIL-6, but did not exhibit any cross-reactivity with other antigens such as huIL-6, his-tagged OSM, BSA, lysozym, ABI 3/7 and gp130-Fc (Fig. 3.2.14). Because flag-vIL-6-his was used as coating antigen for the panning, it was important to test the MAV specificity for the flag- and his-tag. Specific binding of MAV to his-vIL-6 suggested that MAV did not recognise the flag-tag. However, the flag-tag could have an effect on the binding affinity of MAV to vIL-6 (compare flag-vIL-6-his and his-vIL-6 in Fig. 3.2.14). Also, the lack of binding to the his-tagged OSM suggested there was no cross-reactivity with the his-tag.

MAV binding to vIL-6 was also shown by Western blotting. MAV was used as a primary antibody recognising vIL-6, which was applied to a 12.5% SDS-PAGE and transferred onto a PVDF membrane. 100 ng of vIL-6 protein could be detected by MAV under these conditions (Fig. 3.2.15). It is concluded that MAV recognised native and denatured vIL-6 protein.

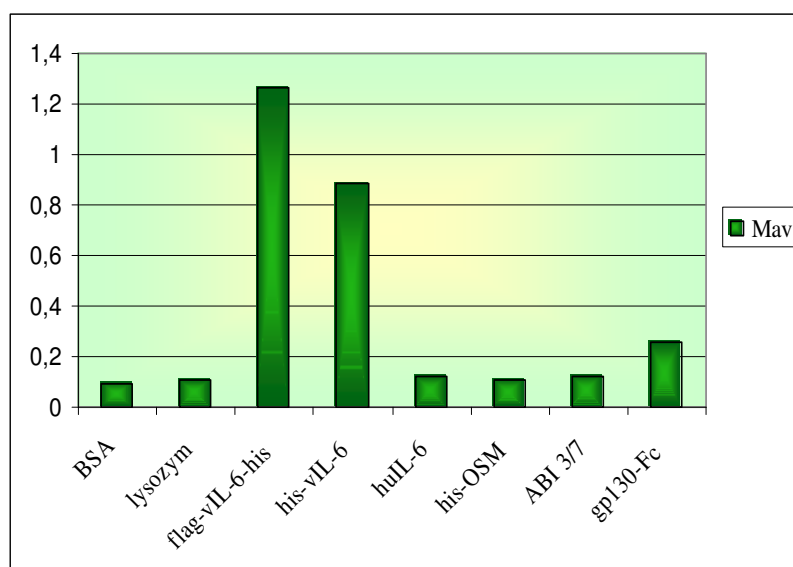


**Fig. 3.2.14 Specific recognition of vIL-6 by MAV:** MAV specific binding to flag-vIL-6-his and his-vIL-6, but not to human IL-6 or other antigens was demonstrated by ELISA.

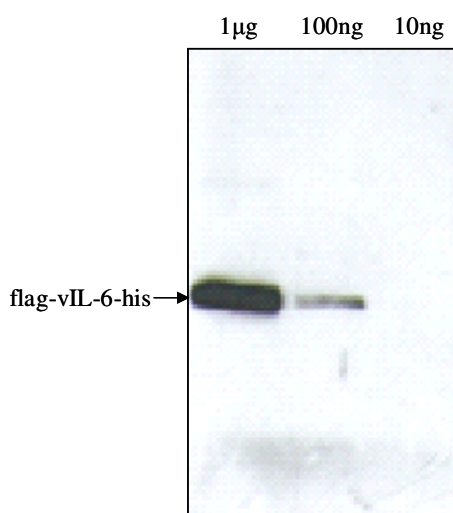


**Fig. 3.2.15 MAV-recognition of vIL-6 by Western Blot:** 1µg, 100ng, 10ng of recombinant vIL-6 was separated on 12.5% SDS-PAGE, blotted and detected by MAV as primary antibody. As secondary antibody anti myc-antibody 9E10 (1:50) was used.



### 3.2.4.2 Binding of MAV to vIL-6 in solution: immunoprecipitation of vIL-6 with MAV

It was shown that MAV recognises vIL-6 in the Western blot and also specifically binds to immobilised vIL-6 in the ELISA. The next step was to investigate whether MAV binds to vIL-6 in solution. Therefore, COS-7 cells were transiently transfected with an expression plasmid encoding vIL-6, and the supernatant of transfected as well as untransfected cells (negative control) was incubated with MAV. Histidine-tagged MAV could then be isolated by cobalt-based metal affinity chromatography using Talon dynabeads (Dyna). vIL-6 bound to MAV was co-precipitated with MAV. Elution of MAV or MAV with bound vIL-6 from the beads was done with 0.5 M imidazole. The presence of vIL-6 in the eluates was monitored by Western blotting using anti-vIL-6-serum. The fact that vIL-6 was precipitated with MAV suggested that vIL-6 can bind to MAV in solution. 15  $\mu$ l supernatant of transfected or untransfected cells were directly applied to SDS-PAGE and blotted as a control for the successful transfection (Fig. 3.2.16).

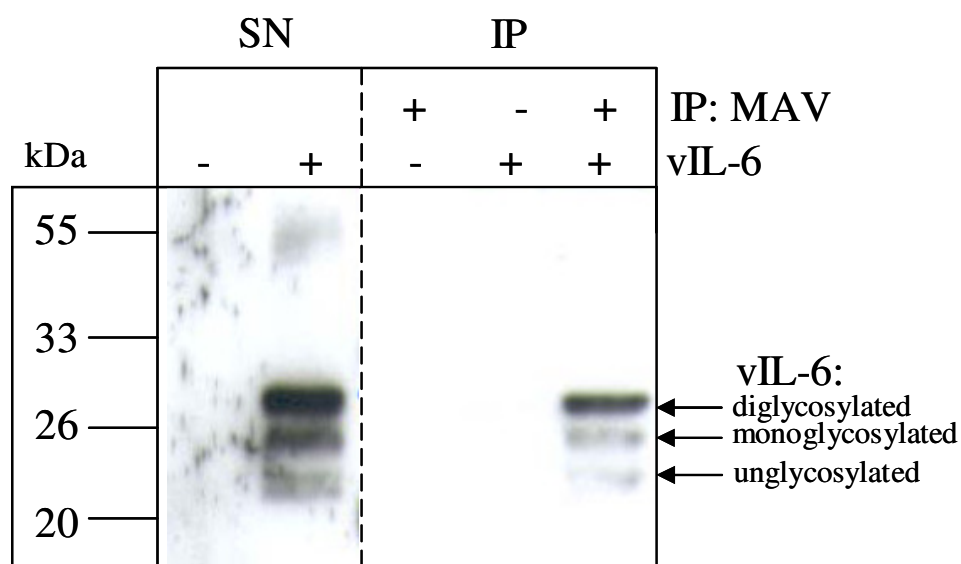


**Fig. 3.2.16 Binding of MAV to recombinant vIL-6 in solution:** supernatants of COS-7 cells transfected with vIL-6 or untransfected were directly applied to SDS-PAGE (first and second lane) or used for immunoprecipitation with MAV. His-tagged MAV and vIL-6 bound to MAV were isolated by Talon and then separated on a 12.5% polyacrylamide gel. Western blot was done using an anti-vIL-6 serum [69]. Detection of unglycosylated as well as glycosylated vIL-6 protein in the supernatant of transfected COS-7 cells was previously described [74, 171].

### 3.2.4.3 Epitope mapping: binding site of vIL-6 to MAV

To identify the epitope of vIL-6 which is recognised by MAV, several chimeras of human and viral IL-6 were produced (Rabe B., unpublished). huIL-6 as well as vIL-6 has a four-helical (ABCD) structure [65]. Gp130 receptor binding sites of these cytokines are defined as sites II, composed of helix A and C, and III, consisting of the initial part of the AB-loop and helix D. The chimeras represent the huIL-6 sequence with the exchange of site II and III of vIL-6 (Fig. 3.2.17 A). Because MAV specifically binds to vIL-6 but not to huIL-6, these chimeras can be used to define which region of vIL-6 is recognised by MAV [148, 149]. The chimeric proteins were separated by SDS-PAGE and blotted onto a membrane which then was incubated with MAV. MAV bound to vIL-6 or the chimera was detected by an anti-myc antibody. As shown in figure 3.2.17 B, MAV bound to vIL-6 and the chimera II+III, which has the complete receptor binding sites II and III of vIL-6. Because MAV did not bind to the chimeras A, C, and A+C, one can conclude that the binding epitope of vIL-6 to MAV is not on site II. MAV binding to chimera II+III suggests that site III of vIL-6 can be the recognition site for MAV. However, the AB-loop of site III does not seem to be involved in the binding of MAV, because MAV does not bind to the AB chimera. Therefore,

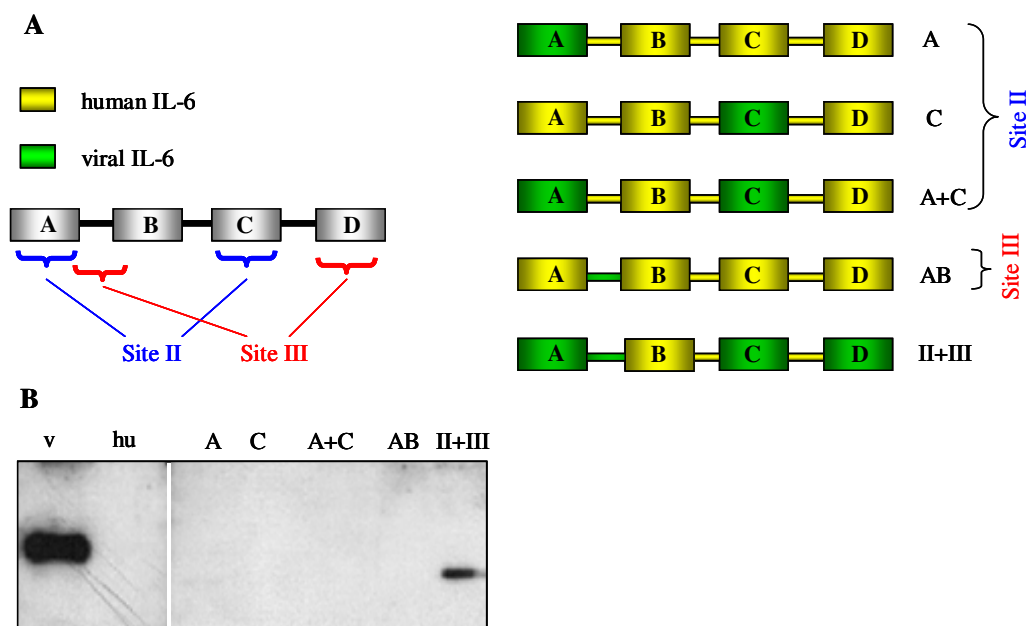


**Fig. 3.2.17 Mapping of the vIL-6 epitopes recognised by MAV:** **A** Schematic illustration of human (yellow)/viral (green) IL-6 chimeras. Chimera A has A-helix of vIL-6, chimera C- C-helix, chimera A+C - both helixes A and C of vIL-6, AB- AB-loop of vIL-6, chimera II+III- complete sites II and III of vIL-6. **B** 1µg vIL-6, huIL-6 or v/huIL-6-chimeras were separated by SDS-PAGE, immunoblotted with MAV and detected with anti-myc antibody 9E10.

we assume that the D-helix of site III of vIL-6 is necessary for recognition by MAV. Unfortunately, it was not possible to confirm this result using a huIL-6 chimera containing the vIL-6 D-helix because this chimera could not be expressed in bacteria so far (Rabe, B., unpublished).

The same results were obtained when the chimeras were analysed by ELISA (Fig. 3.2.18): MAV bound to vIL-6 and to the chimera II+III, which is huIL-6 with the complete exchange of site II and III of vIL-6, but not to the other chimeras.

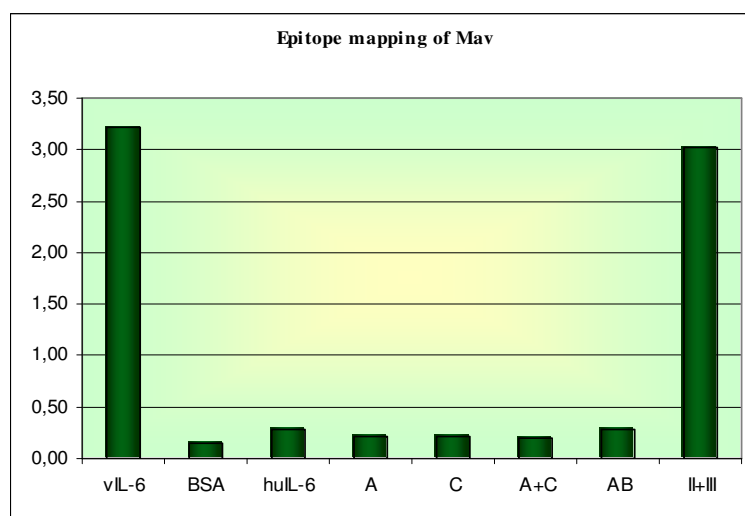


**Fig. 3.2.18 Mapping of the vIL-6 epitopes recognised by MAV:** vIL-6, huIL-6 or v/huIL-6-chimeras (10µg/ml) were coated on the plate and ELISA was performed using MAV (5µg/ml).

#### 3.2.4.4 “Sandwich” ELISA

It is known that vIL-6 binds to sgp130 [72]. In this study, flag-vIL-6-his bound to sgp130-Fc was detected by an anti-flag antibody in the ELISA (Fig.3.2.19 B). To answer the question whether MAV binds to vIL-6 which has already bound to sgp130-Fc, a “sandwich” ELISA was performed (Fig. 3.2.19 A). Sgp130-Fc was the coating antigen; vIL-6 and then MAV were added. vIL-6 bound to sgp130 should bind to MAV, if the MAV binding epitope on vIL-6 is accessible. MAV bound to vIL-6 was detected by a mouse anti-myc antibody followed by an AP-anti-mouse antibody. Figure 3.2.19 C shows the result of the “sandwich” ELISA. Because vIL-6 bound to sgp130-Fc was not detected by MAV any more, sgp130-Fc and MAV seem to have an overlapping binding site on vIL-6, which most likely is the gp130-binding site III.

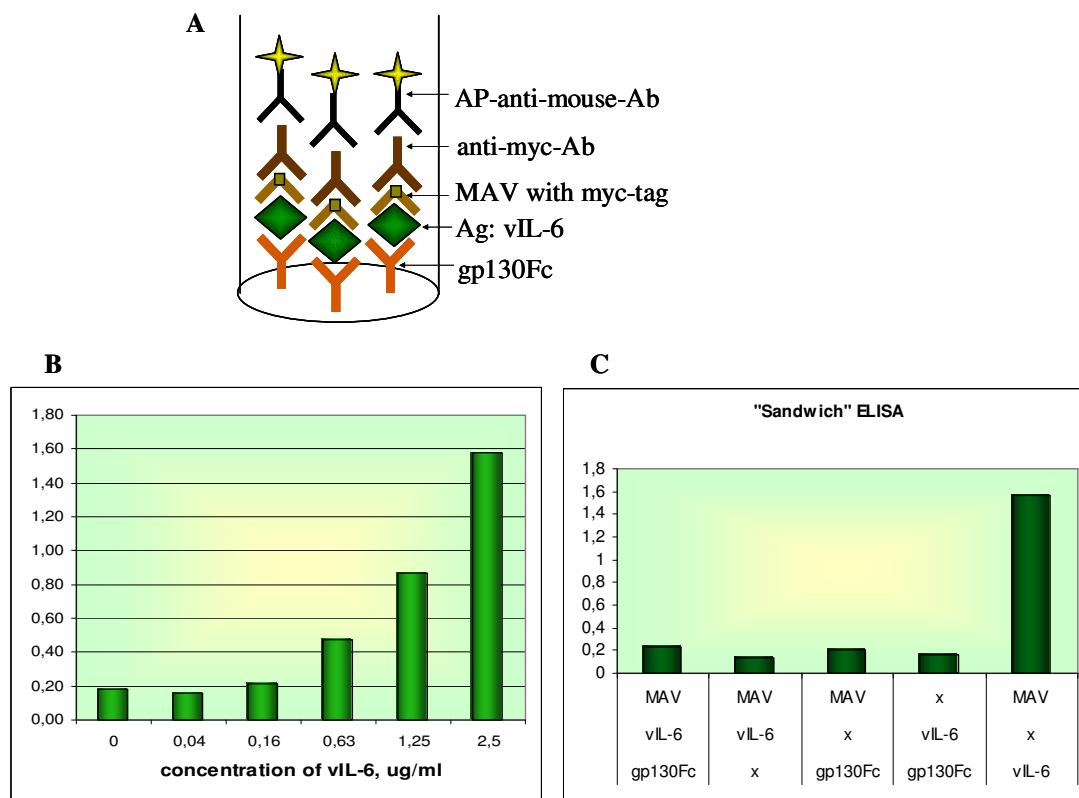


**Fig. 3.2.19 A Scheme of "Sandwich" ELISA:** gp130Fc- solid fixed recombinant gp130Fc; Ag: vIL-6- recombinant flag-vIL-6-his; MAV with myc-tag- soluble anti-vIL-6 scFv MAV with myc-tag; anti-myc-Ab- anti-myc antibody 9E10 recognising myc-tag of MAV; AP-anti-mouse-Ab- anti-mouse-IgG antibody conjugated to alkaline phosphatase to detect bound monoclonal anti-myc antibody. **B vIL-6 binding to gp130 in ELISA:** gp130 was the coating antigen and increased concentrations of vIL-6 were added. Flag-tagged vIL-6 bound to gp130 was detected by an anti-flag antibody. **C "Sandwich" ELISA:** MAV bound to vIL-6 (1  $\mu$ g/ml) could be detected by an anti-myc antibody (last column right). vIL-6 bound to gp130Fc (1  $\mu$ g/ml) could not be detected by MAV any more (first column left).

### 3.2.4.5 Neutralising properties of MAV

Baf/3-gp130 cells can be used to measure the biological activity of vIL-6 [72]. 500 ng/ml of recombinant vIL-6 was sufficient to induce cell proliferation (Fig. 3.1.11). The absence of vIL-6 or blocking its activity led to no cell proliferation and cell death. To analyse whether MAV neutralises the activity of vIL-6, Baf/3-gp130 and Baf/3-gp130, IL-6R cells were stimulated with 500 ng/ml vIL-6 in the presence of increasing amounts of MAV. As a control, the same cells were grown in the presence of Hyper-IL-6 and huIL-6, respectively. MAV did not have an inhibitory effect on the cell proliferation induced by these cytokines. However, adding of MAV to cells stimulated with vIL-6 did not inhibit cell proliferation either (Fig. 3.2.20).

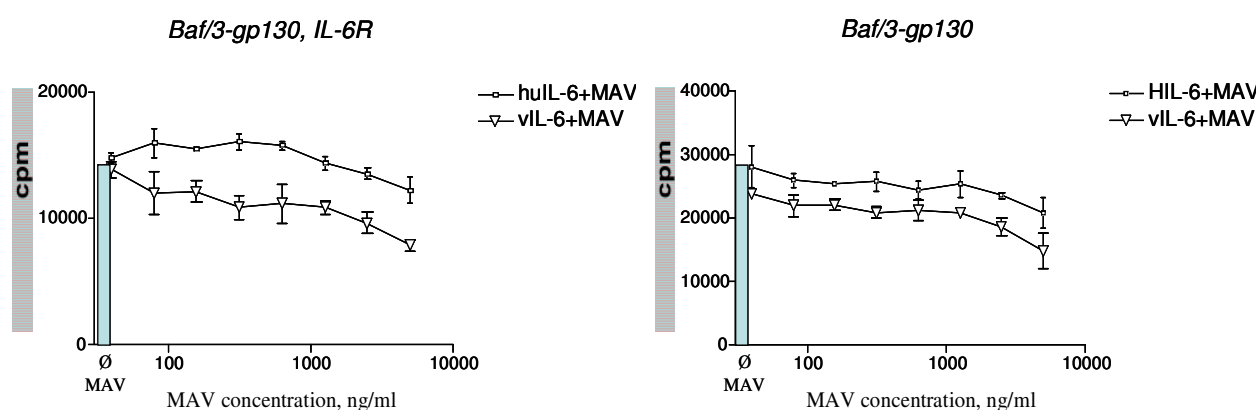


**Fig. 3.2.20 Cytokine-induced cell proliferation in the presence of MAV:** Baf/3-gp130 cells were stimulated with Hyper-IL-6 (1ng/ml) and vIL-6 (500ng/ml). Baf/3-gp130, IL-6R cells were stimulated with huIL-6 (1ng/ml) and vIL-6 (500ng/ml). Simultaneously, cells were treated with increasing amounts of MAV. Proliferation of cells was assessed by measuring of [3H]thymidine incorporation into DNA.

Another possibility to test whether MAV neutralises the vIL-6 effect is to analyse the signal transduction induced by vIL-6 in the presence of MAV. vIL-6 binds to the gp130 receptor, which becomes activated via phosphorylation and induces the JAK/STAT signalling pathway [72]. Active STAT3 can be detected in the cell lysate with an anti-phospho-STAT3 antibody. Inactive vIL-6 would not be able to induce signaling and STAT3 phosphorylation. HepG2 (human hepatocarcinoma cell line) cells were stimulated with 150 ng/ml vIL-6 alone or in the presence of increasing concentrations of MAV. Subsequently, Western blot analysis of the cell lysates was done using an anti-phospho-STAT3 antibody. In fact, MAV reduced STAT3 phosphorylation in a dose-dependent manner indicating some neutralising potential of the MAV protein (Fig.3.2.21).

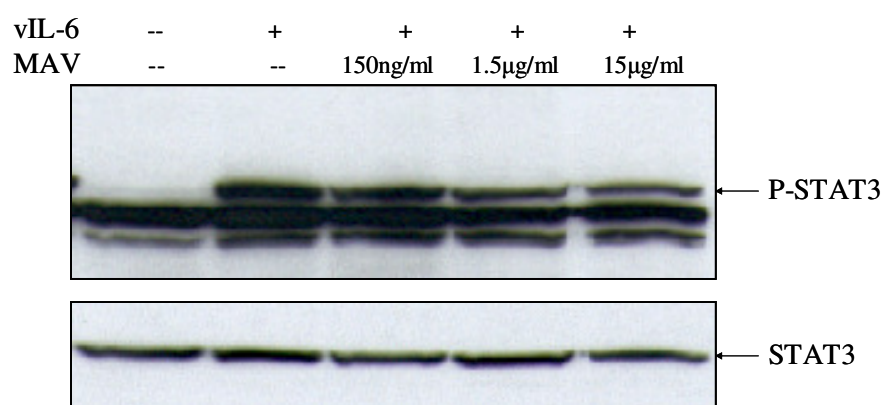


**Fig. 3.2.21 vIL-6-induced STAT3 activation in human hepatoma cells:** HepG2 cells were stimulated with 150ng/ml vIL-6 in the absence or presence of MAV for 10min. Cells were lysed and proteins were separated by SDS-PAGE and blotted onto PVDF membrane. Phosphorylated STAT3 protein was detected by Western blotting using a phospho-STAT3 antibody.

### 3.2.4.6 Binding kinetics of MAV to recombinant vIL-6

The kinetics of MAV binding to vIL-6 immobilised on a solid phase was analysed by surface plasmon resonance (SPR) [150, 151]. SPR arises when light is reflected under specific conditions from a conducting film at the interface between two media of a different refractive index. The media are the sample (immobilised vIL-6) and the glass of the sensor chip, and the conducting film is a thin layer of gold on the chip surface. The resonance is the result of energy transformation from photons into surface plasmons and causes a reduction in the intensity of reflected light at a specific angle of reflection (Fig. 3.2.22). This angle varies

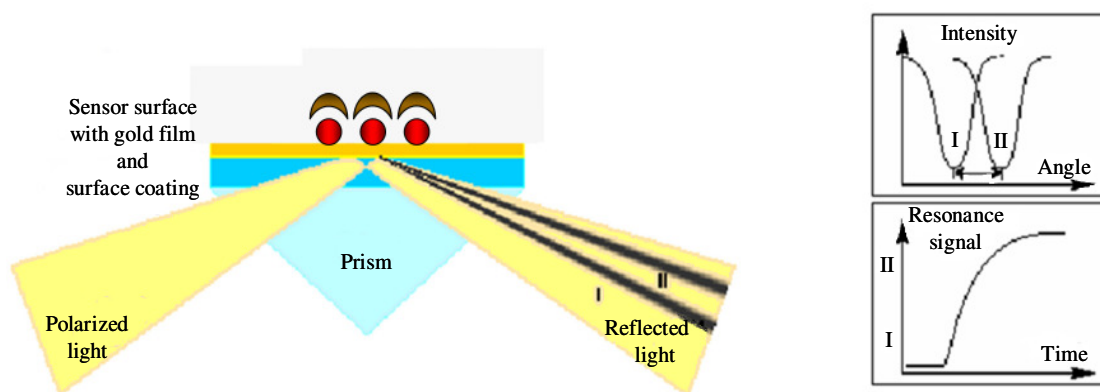


**Fig. 3.2.22 Principle of plasmon resonance:** Schematic illustration of the chip for SPR. Binding of molecules to the sensor surface reduces the intensity of reflected light at a specific angle of reflection.

with the refractive index close to the surface on the opposite side of the film from the reflected light. When molecules in the sample bind to the sensor surface, the concentration and therefore the refractive index at the surface changes and an SPR response is detected. vIL-6 was immobilised to a biosensor surface consisting of an approximately 200 nm thick layer of carboxymethyl dextran (CMD). Dextran, a polymer of glucose residues with a low degree of branching, has a low polydispersity and an approximate molecular weight of 500 kDa. When it is carboxymethylated it has one carboxyl group ( $pK_a=3.5$ ) per two glucose residues. Hence, the CMD surface is negatively charged in buffers with a pH below 5.0. If the buffer pH is lower than the isoelectric point (pI) of a protein, the protein will exhibit a net positive charge and will be bound to the matrix by electrostatic interaction. The immobilisation of vIL-6 to CMD was achieved by coupling the protein's primary amino

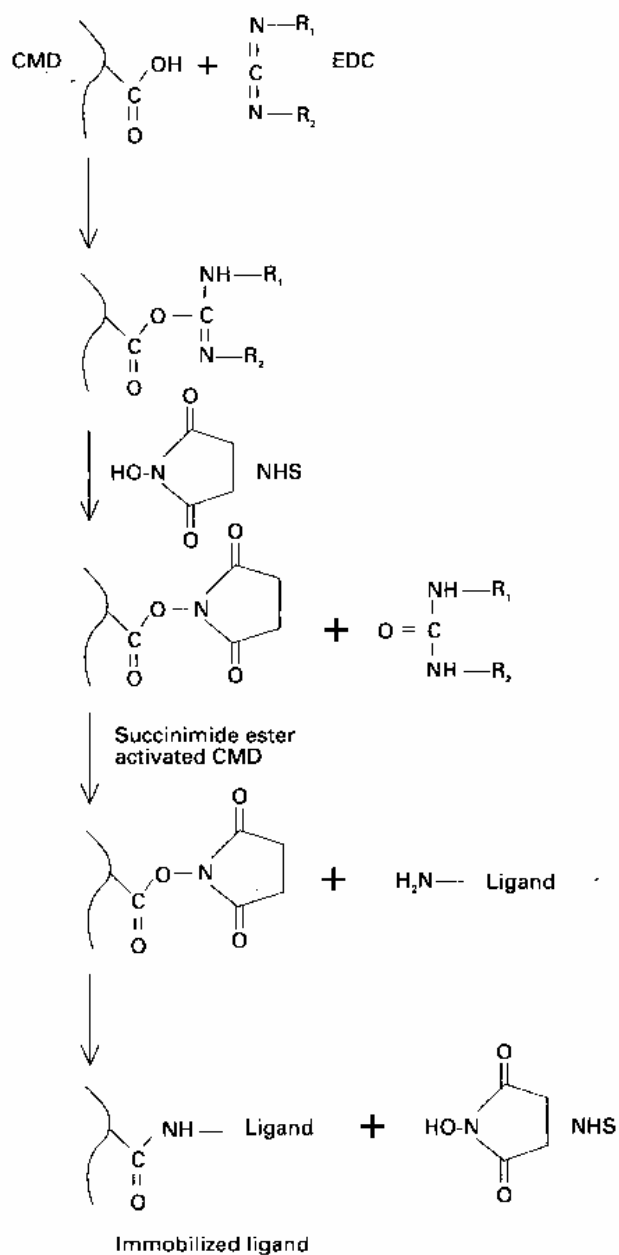


**Fig. 3.2.23 Plasmon resonance: Chemistry for immobilisation of biomolecules to CMD via EDC/NHS chemistry.** CMD- carboxymethyl dextran; EDC- 1-ethyl-3-(3-dimethylaminopropyl) carbodiimide; NHS- N-hydroxysuccinimide; ligand- in this case vIL-6.

groups (N-terminal and lysine residues) to the carboxylate groups of CMD via EDC/NHS chemistry (Fig. 3.2.23 and 3.2.24). Free active carboxy groups were eliminated by ethanolamine.

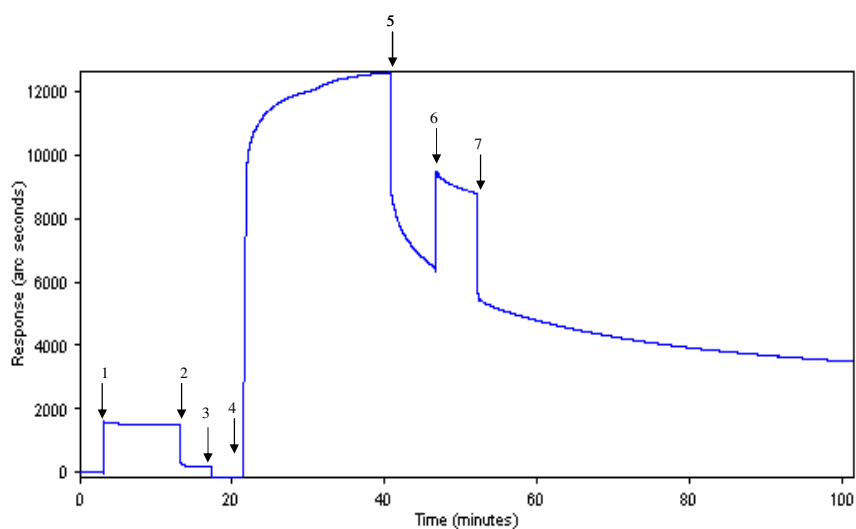


**Fig. 3.2.24 Immobilisation of vIL-6 to CMD using EDC/NHS:**

1- Experiment time: 3.0: activation with EDC/NHS (3x200 $\mu$ l)

2- Experiment time: 13.9: PBS-T wash (3x200 $\mu$ l)

3- Experiment time: 18.3: change to 10mm acetate pH=5.0 (3x200 $\mu$ l)

4- Experiment time: 22.2: added 40 $\mu$ g vIL-6 in 10mm acetate pH=5.0

5- Experiment time: 31.3: PBS-T wash (3x200 $\mu$ l)

6- Experiment time: 42.2: block with 1M ethanolamine pH=8.5 (3x200 $\mu$ l)

7- Experiment time: 47.0: PBS-T wash (3x200 $\mu$ l)

**CMD**- carboxymethyl dextran; **EDC**- 1-ethyl-3-(3-dimethylaminopropyl) carbodiimide;

**NHS**- N-hydroxysuccinimide

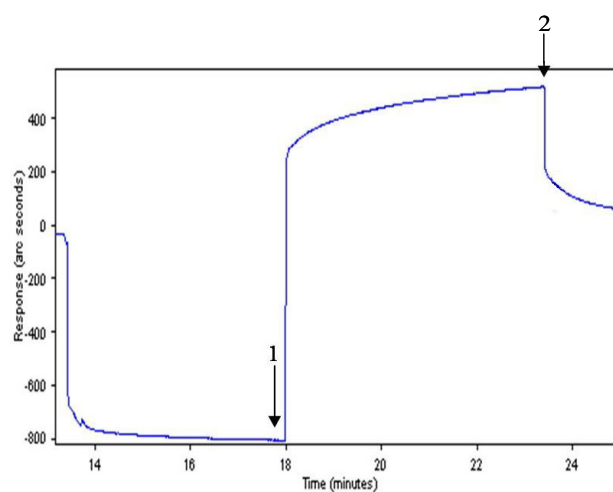


**Fig. 3.2.25 Association-dissociation curve of MAV binding to immobilised vIL-6:**

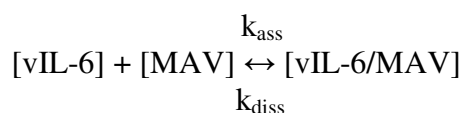
1- Experiment time: 18: adding of MAV (association curve)

2- Experiment time: 23.5: PBS-T wash (dissociation curve)



CMD immobilised with vIL-6 was then used to measure the binding kinetics of MAV to vIL-6. Binding of MAV led to an increasing protein mass on the biosensor surface and to changes of the refractive index. This was detected and expressed as association curves. By replacing MAV with buffer, dissociation of MAV could be detected (Fig. 3.2.25).

The theoretical model of interaction of a single molecule of ligand (vIL-6) with one molecule of ligates (MAV) can be described as:



The rate of complex formation is described by the second order association rate constant  $k_{\text{ass}}$  which has units of  $\text{M}^{-1}\text{s}^{-1}$ . The rate of complex dissociation is described by  $k_{\text{diss}}$ , the first order dissociation constant which has units of  $\text{s}^{-1}$ .

The amount of [vIL-6/MAV] complex formed in time  $t$  is given by:

$$[\text{vIL-6/MAV}]_t = [\text{vIL-6/MAV}]_{\text{eq}}[1 - \exp(-K_{\text{on}}t)]$$

In this equation  $[\text{vIL-6/MAV}]_{\text{eq}}$  is the concentration of complex at equilibrium.  $K_{\text{on}}$  is the pseudo-first order rate for the interaction where:

$$K_{\text{on}} = k_{\text{ass}} [\text{MAV}] + k_{\text{diss}}$$

Hence,  $K_{\text{on}}$  varies with ligand concentration.

The instrument response  $R$  (measured in arc seconds) is proportional to the mass of bound MAV, resulting in:

$$R_t = (R_{\text{eq}} - R_0)[1 - \exp(-K_{\text{on}}t)] + R_0,$$

where  $R_t$  is the response at time  $t$ ,  $R_0$  is the initial response, and  $R_{\text{eq}}$  the maximal response. Multiple determinations of  $K_{\text{on}}$  were obtained by repeating associations at various concentrations of MAV (Fig. 3.2.26). Hence, a plot of multiple  $K_{\text{on}}$  values, derived from a full interaction experiment, allowed determining  $k_{\text{ass}}$  (gradient) and  $k_{\text{diss}}$  (intercept) (Fig. 3.2.26 B), which was  $14500.5 \text{ M}^{-1}\text{s}^{-1}$  and  $0.005012 \text{ s}^{-1}$ , respectively. In this way, the affinity of MAV to vIL-6 was defined as dissociation equilibrium constant  $K_{\text{D}} = k_{\text{diss}}/k_{\text{ass}} = 340\text{nM}$ .

The affinity of MAV to vIL-6 was also determined by ELISA. MAV was added to immobilised vIL-6 in a range from 0 to 10  $\mu\text{g/ml}$ . Bound MAV was detected by an anti-myc antibody and an anti-mouse-AP as secondary antibody. The extinction curve of the AP

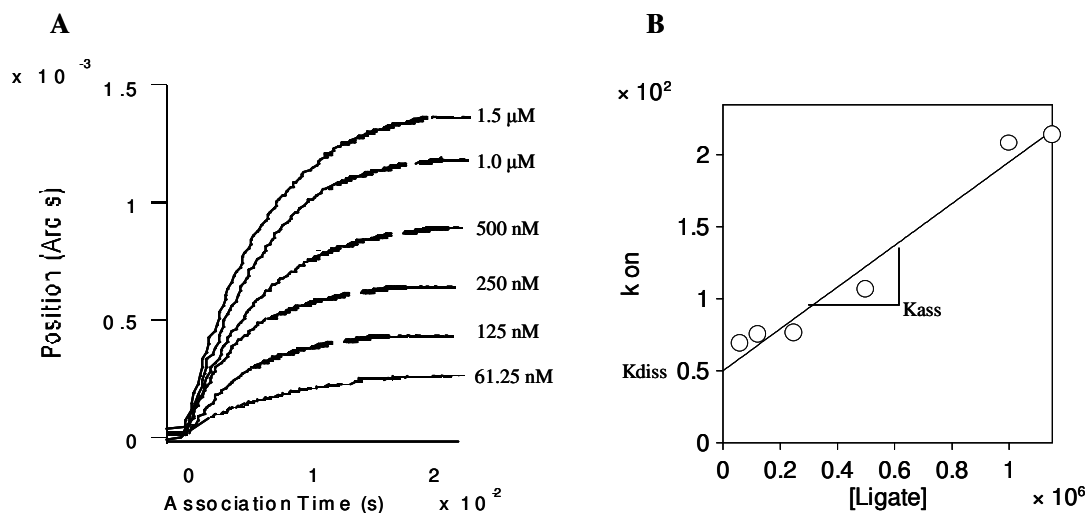


**Fig. 3.2.26 Kinetics of binding of MAV to vIL-6 bound to a solid phase:** **A** Association of MAV to immobilised vIL-6 led to the increase of the resonance angle  $\alpha$  as a function of time. The association phase was recorded for different nanomolar MAV concentrations as indicated. **B** Calculation of the data from A allows the determination of the dissociation rate constant  $k_{\text{diss}}$  from the ordinate intercept and the association rate constant  $k_{\text{ass}}$  from the slope of the graph.

reaction with substrate pNPP can be seen in figure 3.2.27. In the Scatchard analysis [152] the dissociation equilibrium constant ( $K_D$ ) is defined as the ligate concentration at which half the number of binding sites of the ligand ( $B_{\text{max}}/2$ ) is bound. The MAV concentration at which  $B_{\text{max}}/2$  of vIL-6 is at extinction 0.8, can be graphically determined as 0.5  $\mu\text{g}/\text{ml}$  (Fig. 3.2.27). It was calculated to 17 nM ( $M_{\text{rMAV}} = 30118\text{Da}$ ). The 20-fold difference between the  $K_D$  measured by plasmon resonance and the one determined by ELISA could be explained by the different

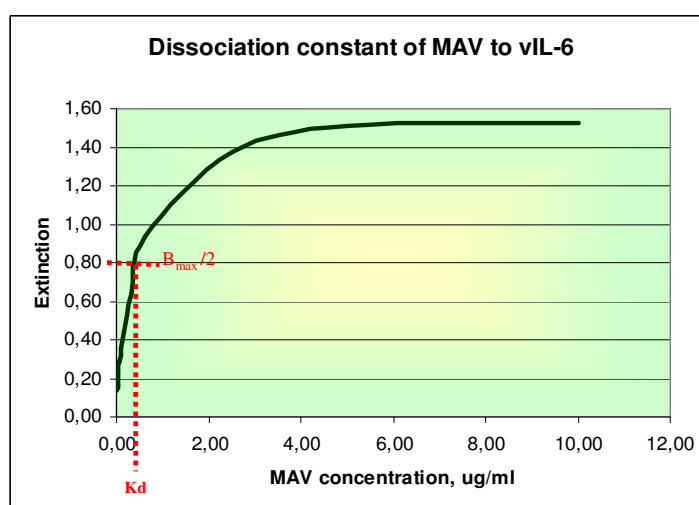


**Fig. 3.2.27 Scatchard analysis:** vIL-6 (1  $\mu\text{g}/\text{ml}$ ) was coated on the plate and ELISA with different concentrations of MAV was done.  $B_{\text{max}/2} = 0.8$  that correlated with  $C_{(\text{MAV})} \sim 0.5 \mu\text{g}/\text{ml} = 17 \text{nM}$ .  $K_{\text{D}(\text{MAV})} = 17\text{nM}$ .

methods and experimental conditions used. Similar differences were consistently observed for other proteins, too, e.g. for huIL-6 and the sIL-6R [153].

### **3.2.5 Model system for the intracellular retention of vIL-6**

Secreted vIL-6 exhibits its effect extracellularly via binding to the receptor homodimer of gp130 leading to signal induction [72]. Such an effect of vIL-6 can be neutralised by a suppression of its secretion. This can be realised by transfection of cells expressing vIL-6 with the cDNA coding for an antibody carrying the endoplasmic retention sequence KDEL (lys-asp-glu-leu) at the COOH-terminus. Proteins carrying the KDEL are recognised by the KDEL receptor in early Golgi compartments and are returned to the endoplasmic reticulum [154, 155]. To test for the intercellular retention of vIL-6, the MAV antibody fragment was fused with a COOH-terminal KDEL sequence, and COS-7 cells were used as a cell model system for intracellular retention of vIL-6 by ER anchored MAV-KDEL.

#### **3.2.5.1 Cloning and expression of the recombinant antibody carrying the retention sequence KDEL**

In eukaryotic cells, proteins destined for export from the cell are usually synthesised with an amino-terminal signal peptide. To clone a construct for eukaryotic expression of MAV-KDEL, the signal peptide of human IL-6 was added to the N-terminus and KDEL to the C-terminus of MAV (Fig. 3.2.28). The signal peptide was amplified by PCR using the primers MK104 and MK704. The MAV sequence was amplified from pIT1-MAV employing the forward primer MK304 and the reverse primer MK404 that included 12 nucleotides encoding the KDEL. The complete sequence of MAV with its signal peptide was obtained employing Splicing by Overlap Extension (SOE)-PCR [156-159] using the terminal primers MK104 and MK404 (Fig. 3.2.28 A and description in 2.2.2). Subsequently, the SP-MAV was cut with *PmeI* (which generates blunt ends) and cloned into the cloning vector pESL (Gibco; modified in our lab) opened by *EcoRV* (which also generates blunt ends). The gene of interest was then moved from the cloning vector into the expression vector by the LR-clonase reaction. In the LR-clonase reaction, DNA segments are transferred between a cloning vector and an expression vector using phage lambda-based site specific

recombination (Gateway cloning technology, Gibco) [160, 161]. As expression vector the p409B plasmid was used (Fig. 3.2.28 B).

A

MK104 5'- CA CGT TTA AAC GCC ACC ATG AAC TCC TTC TCC ACA -3'  
 MK704 5'- CAA CAG CTG CAC CTC GGC CAT CAC GTG TAC TGG GGC AGG GAA GGC -3'  
 MK304 5'- ATG GCC GAG GTG CAG CTG -3'  
 MK404 5'- GT GGT TTA AAC CTA GAG TTC GTC TTT CCG CGG ATT CAG ATC CTC TTC TGA -3'

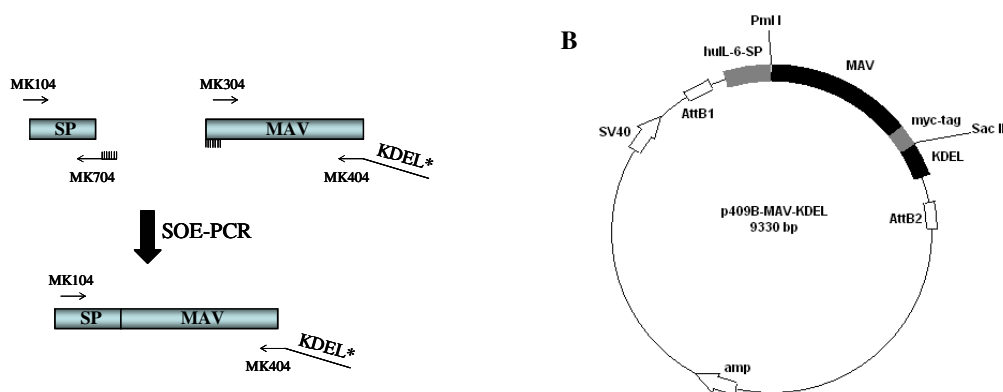


**Fig. 3.2.28 MAV-KDEL-expression construct:** MAV and the signal peptide of huIL-6 were amplified by SOE-PCR, cloned into an entry vector and recloned into the expression destination vector p409B via LR-clonase reaction (Gateway cloning technology). **A** Primer sequences and schematic illustration of SP-MAV amplification, SP- signal peptide of huIL-6, MAV- recombinant antibody fragment against vIL-6, KDEL- retention sequence, \*- stop-codon, SOE-PCR- splicing by overlap extension polymerase chain reaction; **B** Vector map of p409B-MAV-KDEL, SV40- SV40 promoter; AttB1/2- DNA recombinant sequences; huIL-6-SP- signal peptide of human IL-6; KDEL- KDEL sequence.

p409B-MAV-KDEL was transfected into COS-7 cells and MAV-KDEL expression was analysed by Western blotting of the cell lysate and the cell medium (supernatant). The anti-myc 9E10 antibody was used for MAV detection. As expected, the MAV-KDEL was detected in the cell lysate and was not detectable in the cell supernatant (Fig. 3.2.29). The expression of MAV and its localisation within the cell was additionally monitored by immunostaining of transfected COS-7 cells. MAV was stained by an anti-myc antibody followed by the anti-mouse Alexa Fluor 594 antibody, which can be detected by red fluorescence. As expected, the red fluorescence corresponding to MAV-KDEL was seen in the region of the endoplasmic reticulum and no plasmamembrane staining was detected (Fig. 3.2.30 c-d).

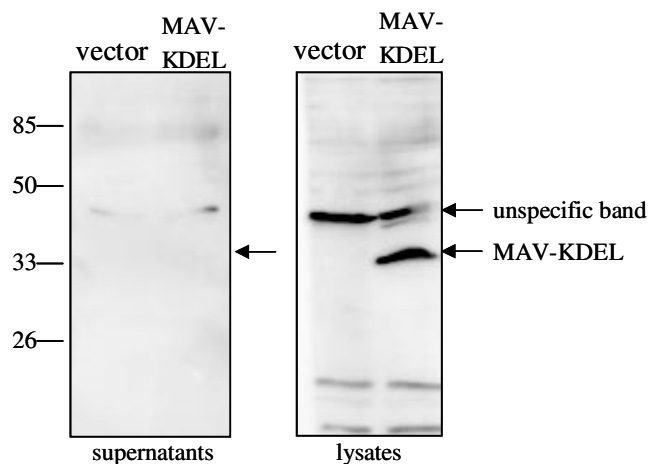


**Fig. 3.2.29 Western blot analysis of the MAV-KDEL expression in COS-7 cells:** Supernatants of the cells transfected with p409B-MAV-KDEL and cell lysates were prepared on the second day after transfection. MAV-KDEL was detected by Western blotting using an anti-myc antibody.

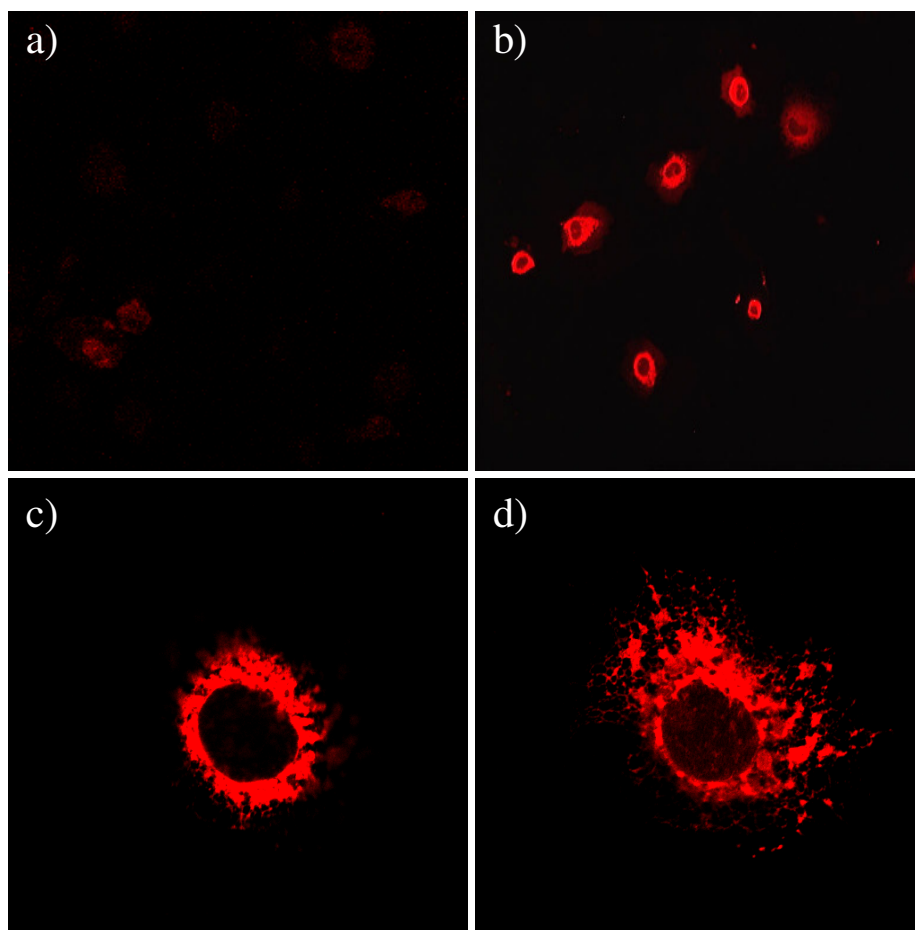


**Fig. 3.2.30 Immunofluorescence of COS-7 cells transfected with p409B-MAV-KDEL:** Cells on the 3rd day after transfection were stained with an anti-myc antibody (1:100) and the Alexa Fluor 594 anti-mouse antibody (1:1500) (b-d). Control staining (a) was prepared without an anti-myc antibody.

### 3.2.5.2 Cloning and expression of vIL-6 fused to GFP

To show if retention of vIL-6 occurs in the ER due to its binding to MAV-KDEL and if both proteins co-localise in transfected COS-7 cells, vIL-6 was fused to the Green Fluorescent Protein (GFP). The green fluorescence of GFP can be observed microscopically after excitation at 488 nm using a fluorescein isothiocyanate (FITC)-filter. The expression level of the protein can be estimated by the intensity of the green light. Additionally, the intracellular localisation of the protein can nicely be visualised. Plasmid pcDNA3.1-GFP was opened by *NheI* and *XhoI*. vIL-6 amplified with the primers MK504 and MK604 was cut with the same restriction endonucleases and inserted into the vector (Fig.3.2.31). The expression of this

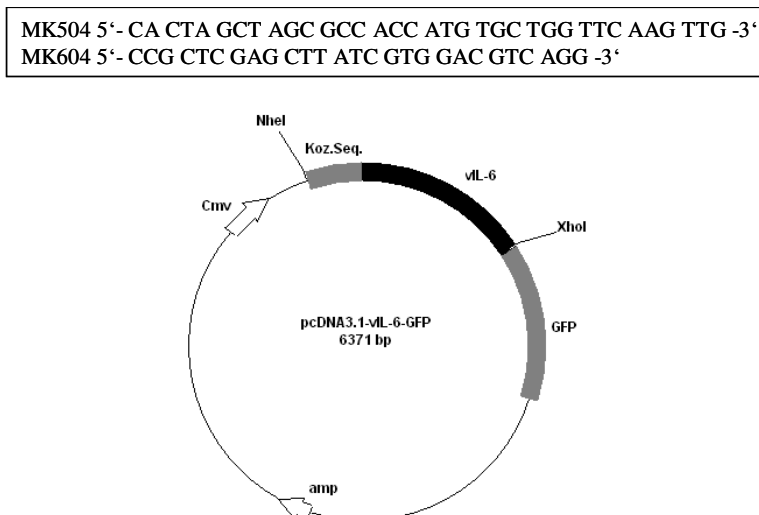


**Fig. 3.2.31 Primer sequences for vIL-6 amplification and plasmid map of the vIL-6-GFP-expression vector:** vIL-6 was amplified and cloned into the vector pcDNA3.1-GFP via *NheI* and *XhoI*. Amp- ampicillin resistance gene; Cmv- cytomegalovirus promoter; GFP- green fluorescent protein.

construct was checked via transient transfection of COS-7 cells. The green fluorescence of the cells expressing vIL-6-GFP was observed microscopically (Fig. 3.2.32). Strong fluorescence of the ER suggested a high expression level of vIL-6-GFP. The secretion of vIL-6-GFP was identified in Golgi vesicles seen as green dots (Fig. 3.2.32, white arrows) and observed as green fluorescence in the region of the plasmamembrane. Using an anti-vIL-6 serum for Western blot analysis, vIL-6-GFP was detected in the supernatant as well as in

the cell lysate of transfected COS-7 cells (Fig.3.2.33). The double band corresponding to vIL-6-GFP in the supernatant most likely reflects differentially glycosylated forms of vIL-6-GFP.

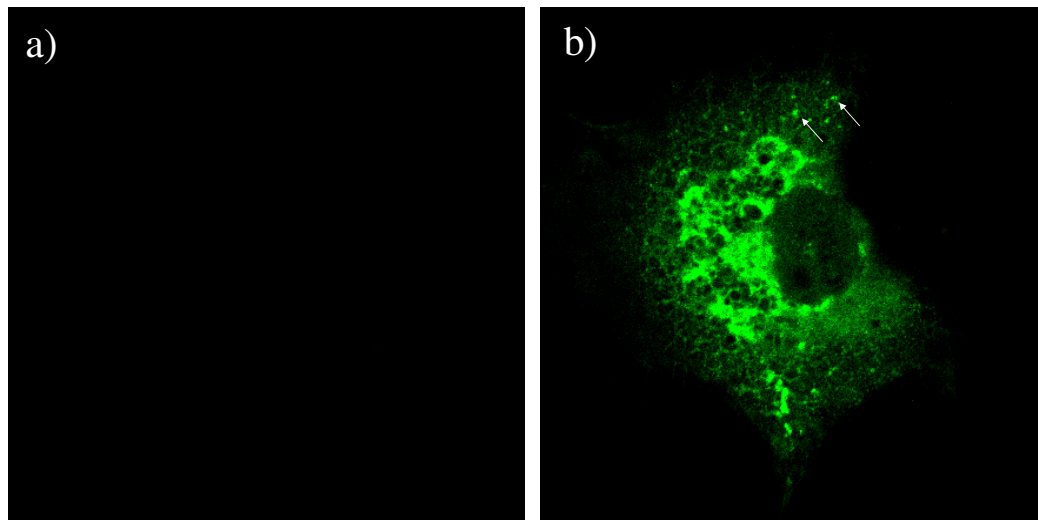


**Fig. 3.2.32** Fluorescence microscopy of untransfected (a) and with pcDNA3.1-vIL-6-GFP(b) transfected COS-7 cells.

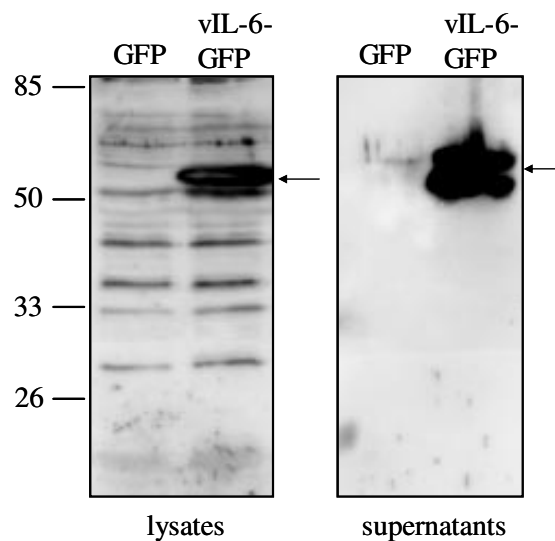


**Fig. 3.2.33** Western blot analysis of vIL-6-GFP expression in COS-7 cells: Supernatants of cells transfected with pcDNA3.1-vIL-6-GFP and cell lysates were prepared on the second day after transfection. vIL-6-GFP was detected in the Western blot using an anti-vIL-6 serum [69].

### 3.2.5.3 Retention of vIL-6 in the ER due to binding to MAV-KDEL

As demonstrated, vIL-6-GFP is secreted from transfected COS-7 cells, whereas MAV-KDEL is retained in the endoplasmic reticulum. The co-transfection of vIL-6-GFP and MAV-KDEL into COS-7 cells should result in intracellular binding of vIL-6-GFP to MAV-KDEL and in the retention of MAV-KDEL/vIL-6-GFP in the endoplasmic reticulum. This was demonstrated by Western blot analysis of the lysates and supernatants of the co-transfected COS-7 cells. vIL-6-GFP was detected in the cell supernatant by an anti-vIL-6 serum when the cDNA was transfected into the cells alone, but was not found to be secreted from the cells when co-transfected with MAV-KDEL cDNA (Fig.3.2.34). Interestingly, the expression of vIL-6 was lower after co-transfection with MAV-KDEL. By

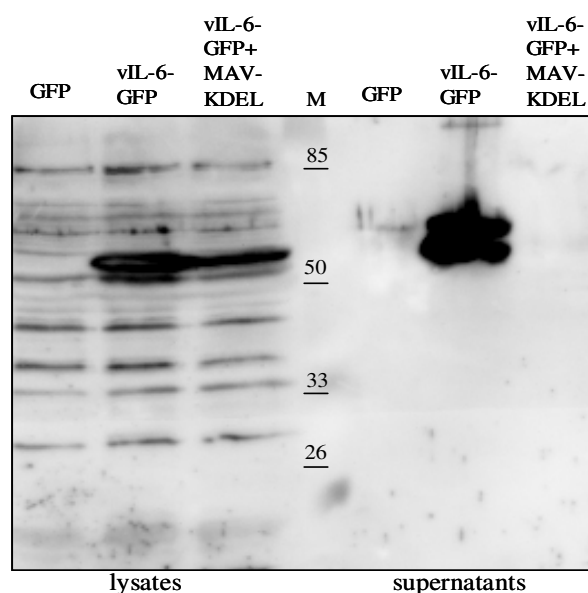


**Fig. 3.2.34 Co-transfection of MAV-KDEL and vIL-6-GFP cDNAs into COS-7 cells resulting in intercellular retention of vIL-6:** COS-7 cells were transfected with pcDNA3.1-vIL-6-GFP alone or co-transfected together with p409B-MAV-KDEL. Supernatants and lysates of the cells were prepared on the second day after transfection, separated by SDS-PAGE and blotted onto a PVDF membrane. vIL-6-GFP was detected by Western blotting using an anti-vIL-6 serum.

fluorescence microscopy, intracellular binding and co-localisation of vIL-6 and MAV-KDEL could be observed as yellow staining caused by the fusion of green (vIL-6-GFP) and red (MAV-KDEL-Alexa Fluor 594) fluorescence. Fig. 3.2.35 shows a cell with stronger expression of MAV-KDEL (left) and a cell with stronger expression of vIL-6-GFP (right). Consequently, we observed in the overlap picture more red fluorescence of the cell over-expressing MAV-KDEL, and more green fluorescence of the cell over-expressing vIL-6-



GFP. Clearly, yellow staining caused by co-localisation of MAV-KDEL and vIL-6-GFP was detected.

Taken together, vIL-6 secretion seems to be successfully suppressed due to binding to MAV-KDEL and retention of the vIL-6/MAV-KDEL complex in the ER. This experiment at cell-line level gives good reason to hope that future *in vivo* experiments with a mouse model will also result in inhibition of vIL-6 secretion.

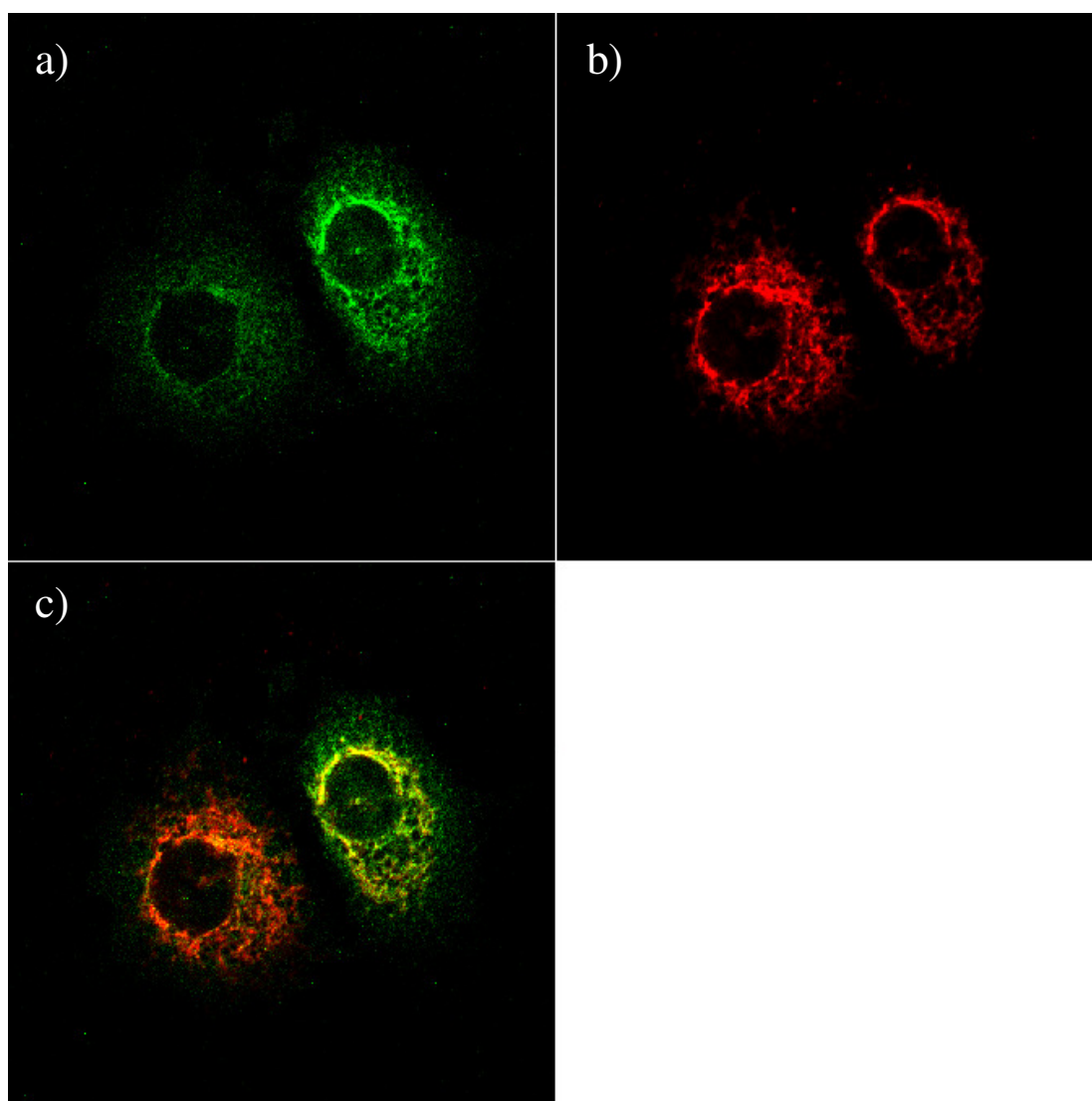


**Fig. 3.2.35 Immunofluorescence of COS-7 cells co-transfected with p409B-MAV-KDEL and pcDNA3.1-vIL-6-GFP:** Cells on the 3rd day after transfection were fixed and stained with an anti-myc antibody (1:100) and the Alexa Fluor 594 anti-mouse antibody (1:1500). Co-transfected cells were analysed microscopically. The expression of vIL-6-GFP is shown in green using a FITS-filter (a). The expressed MAV-KDEL was immunostained with the antibody fluorescing in red (b). The co-localisation of vIL-6-GFP and MAV-KDEL is seen in yellow (c). A 543-fold magnification was used to photograph the cells.

## 4 Discussion

In this study antibodies against viral interleukin-6 (vIL-6) were produced for neutralisation of the biological effect of vIL-6. Encoded by Human Hepesvirus-8 (HHV-8), viral IL-6 is believed to play an important role in the pathogenesis of Kaposi's sarcoma associated diseases. An antibody screened from a phage display human library is a promising candidate for the therapy of these diseases. To eliminate cells infected with HHV-8 different strategies were developed.

### 4.1 Expression, purification and biological activity of viral interleukin-6

In the first part of this study the production of recombinant vIL-6 was described. The biologically active pure protein was needed for the screening and selection of recombinant antibody fragments. Using a bacterial system for the expression of vIL-6 was not successful. Although it ensured a rapid production of vIL-6 in large amounts, the expressed protein was biologically inactive and was not able to induce proliferation of Baf/3-gp130 cells (Fig. 3.1.5). Changing to a eukaryotic expression system turned out to be worthwhile. vIL-6 isolated from the supernatant of EBNA-293-cells stably transfected with vIL-6 cDNA induced Baf/-gp130 cell proliferation at a concentration of 100 ng/ml. EBNA-293 cells were transfected with two constructs encoding vIL-6: vIL-6 with an N-terminal his-tag and vIL-6 with an N-terminal flag-tag and a C-terminal his-tag. The his-tag was critical for the protein purification by Ni-NTA agarose. The advantage of the secreted expression in mammalian cells over bacterial expression of vIL-6 in insoluble form is the native fold of the protein. The results of the CD-spectra shown in Fig. 3.1.10 supported the alpha-helical fold of EBNA-293 secreted vIL-6 proteins. The bacterial expressed vIL-6 was not completely folded, which could explain the lack of its biological activity and incapability to induce Baf/-

gp130 cell proliferation. The incomplete folding of recombinant proteins produced as insoluble inclusion bodies in a bacterial expression system is not an unusual observation [162]. Denaturation in a strong chaotropic agent followed by refolding in a redoxsystem-containing buffer does not always lead to the correct formation of the disulfide bridges. Moreover, bacterial proteins are usually unglycosylated, but vIL-6 N89-glycosylation could be important for the biological activity of the cytokine and for stimulating vIL-6-dependent cell proliferation [74].

About 7 mg of flag-vIL-6-his was expressed and purified from EBNA-293-supernatant and used for the production and characterisation of recombinant antibodies. His-vIL-6 from EBNA-293 cells was expressed in small amounts to be used as a control antigen to rule out any specificity of the produced antibodies for the flag-tag.

## **4.2 Phage display: human antibody library**

For the production of recombinant antibodies against vIL-6, which was subject of the second part of the study, the phage display technology was chosen.

The phage display of antibody fragments scFv [163] has its origins in experiments demonstrating that small proteins and peptides could be displayed on the surface of filamentous bacteriophage [143, 144]. Since the generation of the first human antibodies by phage display [5], the technology has developed to the point where large scFv repertoires have been created that yield antibodies with sub-nanomolar affinities [164, 165]. This is comparable with the best antibodies obtained using hybridoma technology. Phage display repertoires can also be used to isolate antibodies not easily obtained by hybridoma technology, such as those specific for toxic proteins and human anti-self antibodies [166, 167]. The using of monoclonal antibodies in the clinic has, until recently, been limited because they were originally derived by hybridoma technology and so were recognised by the human immune system as foreign. Attempts to humanise murine monoclonal antibodies and the development of chimeric antibodies has resulted in a number of these antibodies progressing through clinical trials [168]. However, both humanised and chimeric antibodies are still a combination of human and mouse sequences and the presence of any mouse protein is a disadvantage that could potentially result in a human anti-mouse antibody (HAMA) reaction. Therefore, phage display technology provides a means by which high

affinity, fully human monoclonal antibodies can be rapidly isolated and also provides a starting point from which a selected antibody can, if necessary, be affinity matured for improved neutralisation potency or binding kinetics. The use of naturally rearranged germline fragments in the construction of the library ensures that these fully human scFv fragments are unlikely to be immunogenic making them ideal therapeutic agents.

### 4.3 Properties of the selected scFv against vIL-6

As described, only one scFv antibody fragment specific for vIL-6 (MAV) was selected from the Tomlinson libraries A and B (Tomlinson, MRC, University of Cambridge, UK). The high specificity of MAV for vIL-6 was observed by ELISA. Because the recombinant flag-vIL-6-his was used for scFv screening and selection, it was necessary to prove that MAV is not specific for the flag- or his-tag. The binding of MAV to his-vIL-6 without flag-tag suggested that MAV did not recognise the flag-sequence. Besides, MAV did not react with his-tagged OSM, underlining that MAV is not specific for the his-tag either. Importantly, MAV was not cross-reactive with other antigens and did not bind to human IL-6.

The fact that MAV recognised vIL-6 in both the ELISA and the Western blot makes the antibody a suitable immunological reagent to detect vIL-6. However, an antibody which might be used for therapy has to recognise the antigen in solution. That MAV indeed is capable of doing so was demonstrated when vIL-6 secreted into the supernatant of transfected COS-7 cells bound to and was precipitated by MAV. The fact that MAV precipitated unglycosylated as well as glycosylated vIL-6 (Fig. 3.2.16) demonstrated that there was no reactivity of MAV for carbohydrate-residues.

The dissociation constant of MAV to vIL-6 was determined by plasmon resonance as 340 nM, which is about 10-fold lower than the dissociation constant of sgp130 to vIL-6, determined by the same method (2.5  $\mu$ M) [68]. Still, for an antibody screened from the Tomlinson human antibody library, this is surprisingly low [167]. In previous studies it was shown that the affinity of an antibody to an antigen that is immobilised on a solid phase is 10-100-fold lower than the one measured in solution (Tab. 4.1) [32, 119, 153, 169, 170, 171]. The difference might be a result of the different methods employed. Therefore, the binding kinetics of MAV to vIL-6 was measured and calculated by Scatchard analysis [152].

The calculated  $K_D$  was 17 nM, which is a reasonable value for an antibody obtained by phage display [167].

The MAV binding epitope of vIL-6 was identified on the D-helix of site III. As it is known, site III of vIL-6 is the binding site for the gp130 receptor [68]. Using the “sandwich” ELISA it was shown that vIL-6 bound to sgp130Fc could not bind to MAV any more.

**Tab. 4.1. Comparison of the affinity of a ligate to its ligand that is either immobilised on a solid phase or in solution**

Binding assay on the solid phase			
immobilised ligand	ligate	Kd, nM	Ref.
IL-6	sIL-6R	34	[153]
sgp130Fc	HIL-6	4.2	[32]
vIL-6	MAV	340	this study
Binding assay in solution			
ligand	ligate	Kd, nM	Ref.
IL-6	sIL-6R	0.5	[153]
sgp130Fc	HIL-6	0.06	[171]
vIL-6	MAV	17	this study

Possibly, site III of vIL-6 was first occupied with sgp130Fc leaving no free binding epitope for MAV. It would be interesting to find out whether vice versa sgp130Fc can bind to vIL-6 which has already bound to MAV. Moreover, it remains to be clarified what happens when MAV and sgp130Fc directly compete for vIL-6 binding when added together.

If MAV and gp130 interact with the same vIL-6 epitope, binding of MAV to vIL-6 *in vivo* should abrogate the signaling occurring upon vIL-6 binding to gp130 [68]. Stimulation of HepG2 cells with vIL-6 results in phosphorylation of STAT3 [77]. Adding of MAV led to reduced signaling and decreased STAT3 phosphorylation in a dose-dependent manner (Fig. 3.2.21). On the other hand, treatment of the cells with 15µg/ml of MAV did not completely eliminate the phosphorylation of STAT3. Moreover, MAV was not able to inhibit Baf/3-gp130 cell proliferation induced by vIL-6. A possible reason for this could be that MAV became instable during the 72h proliferation assay. In contrast, the stimulation of HepG2

cells in the presence of MAV lasted only 10 min and resulted in a decrease of vIL-6-induced STAT3 phosphorylation. Taken together, this suggests that MAV exhibits some neutralising activity which, however, is not sufficient to fully abrogate the vIL-6 effect. Strategies to increase MAV's neutralising properties, for example, by fusion with a cellular toxin, will be the objective of future experiments.

#### 4.4 Elimination of vIL-6 secretion

The synthesis of all proteins occurs at the ribosomes, where they are assigned to two different pathways: proteins with a signal peptide for the endoplasmic reticulum (ER) take the secretory pathway, while proteins without such a signal peptide take the cytoplasmic pathway. Secreted proteins are transported in vesicles from the ER to the Golgi-apparatus and then to the plasmamembrane. The proteins which are destined for the ER, are returned to the ER due to their COOH-terminal retention signal (Fig. 4.1).

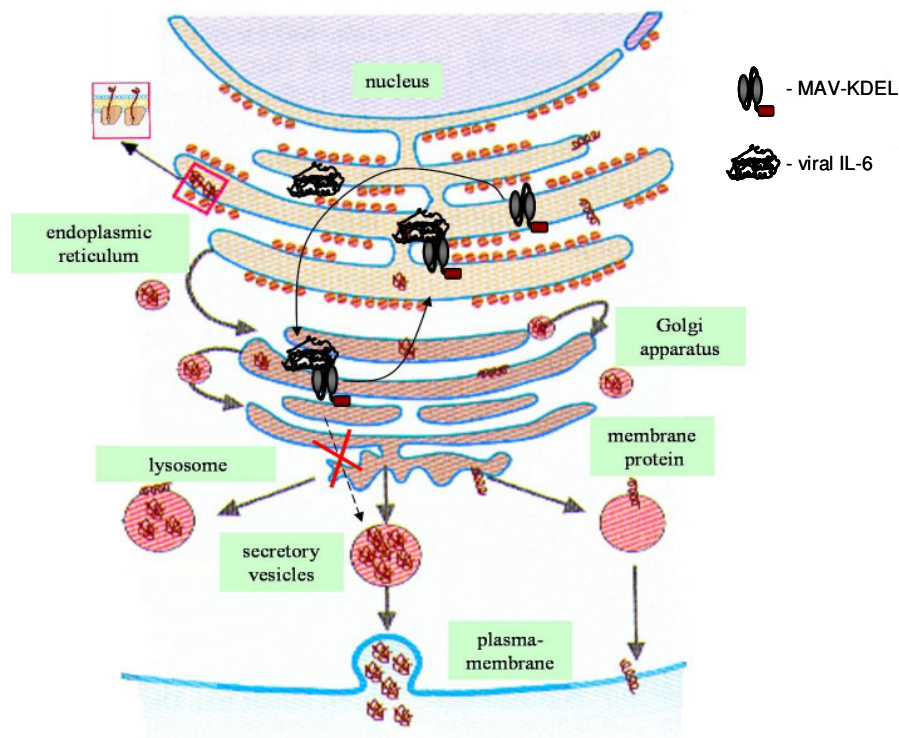


**Fig. 4.1. Protein synthesis and schematic illustration of vIL-6/MAV-KDEL retention.** All proteins are synthesised at the ribosomes of the endoplasmic reticulum (ER) and take the cytoplasmic or secretory pathway, dependent on their function. MAV containing the endoplasmic retention sequence returns to the ER and will not be secreted. vIL-6 bound to MAV-KDEL will not be secreted, either.

The synthetic fusion of a retention sequence to a protein which originally does not have such a sequence, leads to inhibition of its secretion and to its localisation in the ER. For example, recombinant human IL-6 carrying a retention signal accumulated intracellularly and therefore was able to inhibit the surface expression of IL-6R [120].

In this study, the construction of an anti-vIL-6 antibody (MAV) carrying the retention signal (KDEL) was described. Antibody retention in the ER was demonstrated by transfection of COS-7 cells with a plasmid encoding MAV-KDEL. Co-transfection with vIL-6 resulted in intracellular binding of vIL-6 to the antibody and in retention of vIL-6/MAV-KDEL in the ER. Using this cell model system, the secretion of vIL-6 was completely eliminated. Moreover, the expression of vIL-6 was lower after the co-transfection with MAV-KDEL (Fig. 3.2.35).

Very recently a paper about an intracellular signaling mechanism of vIL-6 was published [172]. It was speculated that only a small proportion of expressed vIL-6 is secreted and that intracellular signal activation via IL-6 is predominant. If this is the case, the MAV-KDEL antibody might have a beneficial effect by specifically blocking vIL-6 secretion and by neutralising vIL-6-induced signaling. In this study, the lack of vIL-6 secretion from cells co-transfected with MAV-KDEL cDNA was demonstrated. Additionally, it was shown that MAV is able to inhibit the signaling induced by stimulation of HepG2 cells with vIL-6 (Fig. 3.2.21). An important objective of future experiments will be the analysis of the neutralising property of the fusion antibody MAV-KDEL.

## **4.5 HHV-8 associated diseases and potential therapeutic application of anti-vIL-6 antibodies**

Human herpesvirus 8 (HHV-8), also called Kaposi's sarcoma associated herpesvirus, interferes with the body's immune response and causes Kaposi's sarcoma (KS). Kaposi's sarcoma is a cancer of blood vessel cells that often occurs in subepidermal tissues or the mucous membrane. Kaposi's sarcoma is one of the most common malignancies occurring among AIDS patients [60, 173]. HHV-8 encodes the cytokine vIL-6, which does not only inhibit immune function, but also causes cancerous cells to grow. vIL-6 protects virus-infected cells from undergoing growth arrest and apoptosis or cell death, which is one strategy the immune system applies to limit viral infection. vIL-6 inhibits the signaling of the

antiviral factor interferon which prevents virus-infected cells from growing [85]. In addition, in some cells, vIL-6 does not only stop the suppression of tumors, but also causes healthy cells that are not infected with HHV-8 to proliferate abnormally [174]. Therefore, vIL-6 is a promising target for novel therapies directed against HHV-8-associated tumors.

Although vIL-6 was initially isolated from Kaposi's sarcoma lesions, it was also found to be associated with lymphoproliferative diseases [175], such as primary effusion lymphoma (PEL) and multicentric Castleman's disease (MCD). Castleman's disease is a non-malignant atypical lymphoproliferative disorder, characterised by lymphadenopathy with angiofollicular hyperplasia and plasma cell infiltration. Virtually all HIV-positive patients with MCD and nearly 50% of HIV-negative patients are infected with HHV-8 [173, 176]. Furthermore, some patients have coexistent Kaposi's sarcoma (18-20%) [177]. Primary effusion lymphoma is a malignant effusion in the absence of a contiguous solid tumor mass that develops in the pleural, pericardial, or peritoneal cavity. Viral IL-6 is believed to play an important role in the pathogenesis of PEL and MCD, acting as an autocrine or paracrine factor in the lymphoproliferative processes common to both [178]. Variations in the level of vIL-6 expressions have been observed in Kaposi's sarcoma (~40 copies/cell), PEL (~648 copies/cell), and MCD (~1800 copies/cell), which may be due to tissue and cell-specific environment [178].

HHV-8 vIL-6 was found to be transcribed in the bone marrow dendritic cells of multiple myeloma patients [54]. Multiple myeloma is a fatal cancer characterised by the accumulation of malignant plasma cells in the bone marrow. The finding that viral IL-6, like human IL-6 [179, 180], induced DNA synthesis of human multiple myeloma cell lines in vitro [76], suggests a potential role of HHV-8 in tumor cell proliferation and survival.

HHV-8-associated tumors are highly aggressive and refractory to therapy. There are several approaches to treatment: surgical excisions, laser therapy (argon-laser, CO<sub>2</sub>-laser), photodynamic therapy, or systematic treatment with chemotherapy agents. AIDS-associated Kaposi's sarcoma can be successfully treated by Highly Active Anti-retroviral Therapy (HAART), although some HIV-infected patients suffer from herpesvirus-associated immune restoration disease after the beginning of HAART [181]. The study using protease inhibitors for KS treatment shows the improvement of the residual immune function of the patient and can lead to the elimination of KS [182]. Among other approaches for treatment, one can modulate the cytokines that cause KS to grow. Unlike other cancers, KS cells cannot grow



on their own. The inhibition of the virus's tat protein is essential to inhibit the growth of Kaposi's sarcoma cells. The neutralisation of vIL-6, the infectious agent of HHV-8 associated tumors, can be helpful to combat not only KS but also the other HHV-8-associated diseases. In this respect, recombinant soluble cytokine receptor gp130 (sgp130) has a high therapeutic potential. Viral IL-6 affects cells expressing gp130 on their surface. Recombinant sgp130 blocks the anti-apoptotic affect of vIL-6 mediated via membranebound gp130. On the other hand, sgp130 is an inhibitor of human IL-6 responses dependent on sIL-6R and therefore is a therapeutic tool to specifically block disease states in which sIL-6 transsignaling responses exist [32]. A highly specific inhibitor of vIL-6 can be a monoclonal antibody against the viral cytokine.

Phage display antibody technology opens a new spectrum of application of antibodies for tumor therapy. The ability to generate scFvs with novel binding capacities in a faster and easier way than monoclonal antibodies produced by hybridoma technology, coupled with the scFvs' lower immunogenicity given the lack of the Fc domain, makes them promising candidates. The first fully human therapeutic recombinant antibody isolated from a phage display library was for the treatment of rheumatoid arthritis and ocular scarring and is currently tested in phase II clinical trials [183]. In 1999 about 150 different clinical trials were under way employing recombinant antibodies, mostly for the treatment of cancer. Keeping in mind the delay between research and even first clinical trials and the approval as a drug, it can be expected that recombinant antibody based therapies will be a widespread and acknowledged tool in the hands of physicians by the year 2010.

We have selected the first recombinant antibody against vIL-6, which can be a promising candidate for the therapy of HHV-8-associated diseases. As described in this work, this antibody (MAV) specifically recognises and binds to native vIL-6. *In vivo*, MAV reduces the effect of viral IL-6 by inhibition of vIL-6 induced signaling.

Alternatively, a tumor-killing effect of MAV can be obtained from elimination of those cells affected by vIL-6. Along with other strategies the design of an antibody carrying a cytotoxic agent, for example *Pseudomonas exotoxin 38* (PE38), will be subject to future experiments. PE is one of the pathogenic proteins secreted by *Pseudomonas aeruginosa*. PE is a cellular toxin reaching the cytosol of cells by receptor-mediated endocytosis [121]. A variant PE38 which does not have a cell-binding domain, bound to an antibody, could be targeted via the antibody-part to the cells produced vIL-6. It was previously reported that the

fusion of huIL-6 with *Pseudomonas exotoxin* was able to lyse IL-6R expressing myeloma cells *in vitro* [184]. The first scFv-immunotoxin anti-Tac-PE38 is currently progressing through phase II clinical trials [121]. We expect that a fusion antibody consisting of MAV with the cellular *Pseudomonas exotoxin* 38 can recognise and selectively destroy the cell population affected by vIL-6, and therefore could be tested for therapeutic application.

Another strategy to target cytokine-secreting cells is based on the production of a bispecific antibody (diabody) recognising vIL-6 and the CD3 T cell receptor [185, 186]. Such a diabody would stimulate T cell mediated killing of cells that secrete vIL-6. Cells which do not express the viral cytokine remain unaffected. The elimination of the infected cells would be performed by cytotoxic T cells, which are recruited to the target cells by the vIL-6 part of the bispecific antibody. It was previously demonstrated that a diabody recognising human IL-6 and the CD3 T cell receptor induces specific lysis of HepG2 cells stably transfected with huIL-6 [119]. Interestingly, in contrast to cells secreting huIL-6, huIL-6 responder cells remained unaffected by the diabody. It should be noted that the anti-huIL-6 diabody has not reached therapeutic application so far. The anti-CD3 part of this diabody (mAb OKT3) is murine and would have to be humanised, or a recombinant human scFv with specificity for human CD3 from phage display library has to be selected.

For targeted gene therapy of the HHV-8-associated diseases, the anti-vIL-6 antibody MAV fused to the endoplasmic retention sequence KDEL (MAV-KDEL) might be useful [120]. As described, MAV-KDEL partly blocks the secretion of vIL-6 in COS-7 cells, thereby eliminating the autocrine and paracrine effects of the viral cytokine. This successful experiment on a cell-line level lets us hope that future *in vivo* experiments with a mouse model will also result in inhibition of vIL-6 secretion. One can also assume that MAV-KDEL will exhibit vIL-6-neutralising activity *in vivo*, which would be of particular importance if vIL-6 activity occurs intracellularly.

This study is an example for the production of recombinant proteins with the desired properties for *in vivo* application. We selected the first human anti-vIL-6 antibody, which could have a therapeutic future in the treatment of HHV-8-associated diseases. Based on this work, a large variety of other fusion proteins can be constructed and will hopefully demonstrate the potential of antibody engineering for generating new therapeutic agents. The antibody-based therapeutics has become a rising market that illustrates the substantial

change in the pharmaceutical development by utilising the body's own capabilities as a source for drug rather than chemical reagents.

## 5 Summary

The genome of Human herpesvirus 8 (HHV8), also called Kaposi's sarcoma associated herpesvirus, encodes several ORFs for putative oncogenes, which are homologues to cellular host genes known to function in cell-cycle regulation, control of apoptosis and cytokine signaling. One of these genes encodes viral interleukin-6 (vIL-6) that exhibits 24,7% homology to human interleukin-6 (huIL-6). vIL-6 mimics a number of huIL-6 activities, such as stimulating IL-6 dependent B-cell line growth and activating the JAK/STAT3 signaling pathway. Whereas human IL-6 first has to bind to IL-6R before it can interact with a homodimer of glycoprotein 130 (gp130) for signal activation, viral IL-6 directly binds to the signal transducer gp130 and thereby is able to induce the proliferation of cells that do not express IL-6R. vIL-6 was shown to induce angiogenesis and haematopoiesis. The viral cytokine is believed to play an important role in the pathogenesis of Kaposi's sarcoma as well as primary effusion lymphoma, multicentric Castelman's disease and perhaps multiple myeloma. Therefore, vIL-6 is a promising target for novel therapies directed against HHV-8-associated diseases.

In this study a recombinant antibody against vIL-6 was produced, consisting of a variable domain of the heavy chain (VH) and a variable domain of the light chain (VL) of human IgG connected to each other by a short linker sequence. This kind of antibody is termed “single chain variable fragment” (scFv) and, in this case, was screened from a phage display human antibody library. vIL-6, but not huIL-6 or other control antigens, was demonstrated to be specifically recognised by this antibody (called MAV). MAV binds to recombinant vIL-6 immobilised on a solid phase and to the native cytokine in solution. However, vIL-6 bound to its receptor gp130 can not be recognised by MAV, because the MAV binding epitop of vIL-6 localises on helix D, which is a part of the receptor binding site III of vIL-6. MAV was shown to inhibit vIL-6-induced signaling in human hepatoma cells but was not able to suppress the proliferation of Baf/3-gp130 cells stimulated with viral IL-6.

Based on the idea to block vIL-6 secretion, a strategy for the neutralisation of vIL-6 was developed and tested. The recombinant antibody MAV was fused with the endoplasmic

retention sequence KDEL (MAV-KDEL) to be retained in the endoplasmic reticulum. As a result, cells secreting vIL-6 ceased to secrete the cytokine after transfection with MAV-KDEL. The intracellular binding of vIL-6 to its antibody carrying the retention signal blocked the transport of expressed vIL-6 to the cell membrane and led to the retention of the vIL-6/MAV-KDEL complex in the endoplasmic reticulum.

The successful *in vivo* experiments with the MAV and MAV-KDEL antibodies for vIL-6 neutralisation and elimination of the HHV-8 infected cells make them promising candidates for the treatment of HHV-8 associated diseases. The development and modelling of new strategies for application of recombinant antibodies against vIL-6 will be the subject of future investigations.

## 6 Zusammenfassung

Das Genom des Humanen Herpesvirus 8 (HHV8), auch Kaposi Sarkom-assoziiertes Herpesvirus genannt, kodiert für mehrere mutmaßliche Oncogene, welche Homologe von zellulären Genen sind, die für die Regulation des Zell-Zyklus, für die Kontrolle der Apoptose sowie der Signalübertragung durch Zytokine von Bedeutung sind. Eines dieser Gene kodiert für virales Interleukin-6 (vIL-6), das 24,7 % Homologie zu humanem Interleukin-6 (huIL-6) aufweist. Einige Wirkungen des huIL-6 können von vIL-6 imitiert werden. Zum Beispiel ist es in der Lage, das Wachstum IL-6-abhängiger B-Zelllinien zu stimulieren und die JAK/STAT3 Signaltransduktion zu aktivieren. Während humanes IL-6 zunächst an den IL-6 Rezeptor (IL-6R) binden muss, bevor es mit einem Homodimer des Glykoprotein 130 (gp130) interagieren kann, um die Signaltransduktion zu aktivieren, bindet virales IL-6 direkt an gp130. Dadurch kann es auch die Proliferation von Zellen induzieren, die keinen IL-6R exprimieren. Es wurde bereits gezeigt, dass vIL-6 Angiogenese und Hämatopoese induziert. Vor diesem Hintergrund spielt das virale Zytokin eine wichtige Rolle in der Pathogenese des Kaposi Sarkoma, des Primären Effusions Lymphoms, der Castleman Krankheit sowie des Multiplen Myeloms.

In vorliegender Arbeit wurde ein rekombinanter Antikörper gegen vIL-6 generiert, der aus einer variablen Domäne der schweren Kette und einer variablen Domäne der leichten Kette des humanen IgG besteht, verbunden durch eine kurze Linker-Sequenz. Diese Art Antikörper wird „single chain variable fragment“ (scFv) genannt und wurde in dieser Arbeit mittels einer humanen Phagen-Oberflächenpräsentations-Bibliothek selektioniert. Es wurde gezeigt, dass vIL-6, aber nicht huIL-6 oder andere Kontroll-Antigene, spezifisch von diesem Antikörper, der „MAV“ genannt wurde, erkannt wird. MAV bindet sowohl an rekombinantes vIL-6, das auf einer festen Phase immobilisiert wurde, als auch an das native Zytokin in Lösung. Allerdings wird vIL-6, das an seinen Rezeptor gp130 gebunden ist, nicht von MAV erkannt, da das Bindungsepitop von vIL-6 für MAV auf der D-Helix liegt, welche einen Teil der Rezeptor-Bindungsstelle III für vIL-6 darstellt. Weiterhin wurde gezeigt, dass MAV die durch vIL-6 induzierte Signalaktivierung in menschlichen Hepatomzellen

inhibieren kann, aber nicht in der Lage ist, die Vermehrung von Baf/3-gp130-Zellen, die mit viralem IL-6 stimuliert wurden, zu verhindern.

Basierend auf der Idee, die Sekretion von vIL-6 aus infizierten Zellen zu blockieren, wurde eine Strategie zur intrazellulären Neutralisierung von vIL-6 entwickelt und getestet. Der rekombinante Antikörper MAV wurde mit der endoplasmatischen Retentionssequenz KDEL fusioniert (MAV-KDEL), um im Endoplasmatischen Reticulum zurückgehalten zu werden. Die Folge war, dass Zellen nach kurzer Zeit aufhörten vIL-6 zu sezernieren, nachdem sie mit MAV-KDEL transfiziert worden waren. Die intrazelluläre Bindung von vIL-6 an MAV-KDEL hatte zur Zurückhaltung von vIL-6/MAV-KDEL im Endoplasmatischen Reticulum geführt.

Die erfolgreichen *in vivo* Experimente mit MAV und MAV-KDEL zur vIL-6 Neutralisierung und Eliminierung vIL-6 sezernierender Zellen machen die beiden Antikörper zu aussichtsreichen Kandidaten für die Behandlung von HHV-8-assoziierten Krankheiten. Die Entwicklung neuer Strategien und Modelle zur Anwendung rekombinanter Antikörper gegen vIL-6 wird das Thema zukünftiger Arbeiten sein.

## 7 References

- [1] Iankov, L., Atanasova, G., Praskova, M., Kalenderova, S., Petrov, D., Mitev, V., Mitov, I. (2004) Bacterial lipopolysaccharide induces proliferation of IL-6-dependent plasmacytoma cells by MAPK pathway activation. *Immunobiology* **208**, 445-454
- [2] Dodd, D. A., Giddings, T. H. Jr, Kirkegaard, K. (2001) Poliovirus 3A protein limits interleukin-6 (IL-6), IL-8, and beta interferon secretion during viral infection. *J. Virol.* **75**, 8158-8165
- [3] Parsonage, G., Falciani, F., Burman, A., Filer, A., Ross, E., Bofill, M., Martin, S., Salmon, M., Buckley, C. D. (2003) Global gene expression profiles in fibroblasts from synovial, skin and lymphoid tissue reveals distinct cytokine and chemokine expression patterns. *Thromb. Haemost.* **90**, 688-697
- [4] Yamasaki, K., Taga, T., Hirata, Y., Yawata, H., Kawanishi, Y., Seed, B., Taniguchi, T., Hirano, T., and Kishimoto, T. (1988) Cloning and expression of the human interleukin-6 (BSF-2/IFN beta 2) receptor. *Science* **241**, 825-828
- [5] Taga, T., Hibi, M., Hirata, Y., Yamasaki, K., Mastuda, T., Hirano, T., and Kishimoto, T. (1989) Interleukin-6 triggers the association of its receptor with a possible signal transducer, gp130. *Cell* **58**, 537-581
- [6] Hibi, M., Murakami, M., Saito, M., Hirano, T., Taga, T., and Kishimoto, T. (1990) Molecular cloning and expression of an IL-6 signal transducer, gp130. *Cell* **63**, 1149-1157
- [7] Heinrich, P. C., Behrmann, I., Hann, S., Hermanns, H. M., Müller-Newen, G., Schaper, F. (2003) Principles of interleukin (IL)-6-type cytokine signalling and its regulation. *Biochem. J.* **374**, 1-20
- [8] Elson, G. C., Lelievre, E., Guillet, C., Chevalier, S., Plun-Favreau, H., Froger, J., Suard, I., de Coignac, A. B., Delneste, Y., Bonnefoy, J. Y., Gauchat, J. F., Gascan, H. (2000) CLF associates with CLC to form a functional heteromeric ligand for the CNTF receptor complex. *Nature Neuroscience* **3**, 867-872
- [9] Pflanz, S., Hibbert, L., Mattson, J., Rosales, R., Vaisberg, E., Bazan, J. F., Phillips, J. H., McClanahan, T. K., de Waal Malefyt, R., Kastelein, R. A. (2004) WSX-1 and glycoprotein 130 constitute a signal-transducing receptor for IL-27. *J. Immunol.* **172**, 2225-2231
- [10] Starr, R., Willson, T. A., Viney, E. M., Murray, L. J., Rayner, J. R., Jenkins, B. J., Gonda, T. J., Alexander, W. S., Metcalf, D., Nicola, N. A., Nilton, D. J. (1997) A family of cytokine-inducible inhibitors of signalling. *Nature* **387**, 917-921



- [11] Naka, T., Narazaki, M., Hirata, M., Matsimoto, T., Minamoto, S., Aono, A., Nishimoto, N., Kajita, T., Taga, T., Yoshizaki, T., Akira, S., Kashimoto, T. (1997) Structure and function of a new STAT-induced STAT inhibitor. *Nature* **387**, 924-929
- [12] Ernst, M., Inglese, M., Waring, P., Campbell, I. K., Bao, S., Clay, F. J., Alexander, W. S., Wicks, I.P., Tarlinton, D. M., Novak, U., Heath, J. K., Dunn, A. R. (2001) Defective gp130-mediated signal transducer and activator of transcription (STAT) signaling results in degenerative joint disease, gastrointestinal ulceration, and failure of uterine implantation. *J. Exp. Med.* **194**, 189-203
- [13] Horiuchi, S., Koyanagi, Y., Zhou, Y., Miyamoto, H., Tanaka, Y., Waki, M., Matsumoto, M., Yamamoto, M., Yamamoto, N. (1994) Soluble interleukin-6 receptors released from T cell or granulocyte/macrophage cell lines and human peripheral blood mononuclear cells are generated through an alternative splicing mechanism. *Eur. J. Immunol.* **24**, 1945-1948
- [14] Lust, J. A., Donovan, K. A., Kline, M. P., Greipp, P. R., Kyle, R. A., Maihle, N. J. (1992) Isolation of an mRNA encoding a soluble form of the human interleukin-6 receptor. *Cytokine* **4**, 96-100
- [15] Oh, J. W., Revel, M., Chebath, J. (1996) A soluble interleukin 6 receptor isolated from conditioned medium of human breast cancer cells is encoded by a differentially spliced mRNA. *Cytokine* **8**, 401-409
- [16] Horiuchi, S., Ampofo, W., Koyanagi, Y., Yamashita, A., Waki, M., Matsumoto, A., Yamamoto, M., Yamamoto, N. (1998) High-level production of alternatively spliced soluble interleukin-6 receptor in serum of patients with adult T-cell leukaemia/HTLV-I-associated myelopathy. *Immunology* **95**, 360-369
- [17] Müllberg, J., Schooltink, H., Stoyan, T., Gunther, M., Graeve, L., Buse, G., Mackiewicz, A., Heinrich, P. C., Rose-John, S. (1993) The soluble interleukin-6 receptor is generated by shedding. *Eur. J. Immunol.* **23**, 473-480
- [18] Müllberg, J., Oberthur, W., Lottspeich, F., Mehl, E., Dittrich, E., Graeve, L., Heinrich, P. C., Rose-John, S. (1994) The soluble human IL-6 receptor. Mutational characterization of the proteolytic cleavage site. *J. Immunol.* **152**, 4958-4968
- [19] Müllberg, J., Durie, F. H., Otten Evans, C., Alderson, M. R., Rose-John, S., Cosman, D., Black, R. A., Mohler, K. M. (1995) A metalloprotease inhibitor blocks shedding of the IL-6 receptor and the p60 TNF receptor. *J. Immunol.* **155**, 5198-5205
- [20] Mackiewicz, A., Schooltink, H., Heinrich, P. C., Rose-John, S. (1992) Complex of soluble human IL-6-receptor/IL-6 up-regulates expression of acute-phase proteins. *J. Immunol.* **149**, 2021-2027
- [21] Peters, M., Mueller, A., Rose-John, S. (1998) Interleukin-6 and soluble interleukin-6 receptor: direct stimulation of gp130 and hematopoiesis. *Blood* **92**, 3495-3504

- [22] Sui, X., Tsuji, K., Tanaka, R., Tajima, S., Muraoka, K., Ebihara, Y., Ikebuchi, K., Yasukawa, K., Taga, T., Kishimoto, T., Nakahata, T. (1995) gp130 and c-Kit signalings synergize for ex vivo expansion of human primitive hemopoietic progenitor cells. *Proc. Natl. Acad. Sci. U. S. A.* **92**, 2859-2863
- [23] Tamura, T., Udagawa, N., Takahashi, N., Miyaura, C., Tanaka, C., Tamada, Y., Koishihara, Y., Ohsugi, Y., Kumaki, K., Taga, T., Kishimoto, T., Suda, T. (1993) Soluble interleukin-6 receptor triggers osteoclast formation by interleukin 6. *Proc. Natl. Acad. Sci. U. S. A.* **90**, 11924-11928
- [24] März, P., Otten, U., Rose-John, S. (1999) Neural activities of IL-6-type cytokines often depend on soluble cytokine receptors. *Eur. J. Neurosci.* **11**, 2995-3004
- [25] Rose-John, S., Heinrich, P. C. (1994) Soluble receptors for cytokines and growth factors: generation and biological function. *Biochem. J.* **300**, 281-290
- [26] Jones, S. A., Rose-John, S. (2002) The role of soluble receptors in cytokine biology: the agonistic properties of the sIL-6R/IL-6 complex. *Biochimica et Biophysica Acta* **1592**, 251-263
- [27] Kallen, K.-J. (2002) The role of transsignalling via the agonistic soluble IL-6 receptor in human diseases. *Biochimica et Biophysica Acta* **1592**, 323-343
- [28] Romano, M., Sironi, M., Toniatti, S., Polentarutti, N., Fruscella, P., Ghezzi, P., Faggioni, R., Luini, W., van Hinsbergh, W., Sozzani, S., Bussolino, F., Poli, V., Ciliberto, G., Mantovani, A. (1997) Role of IL-6 and its soluble receptor in induction of chemokines and leukocyte recruitment. *Immunity* **6**, 315-325
- [29] Klouche, M., Bhakdi, S., Hemmes, M., Rose-John, S. (1999) Novel path to activation of vascular smooth muscle cells: up-regulation of gp130 creates an autocrine activation loop by IL-6 and its soluble receptor. *J. Immunol.* **163**, 4583-4589
- [30] März, P., Cheng, J.-C., Gadiant, R. A., Patterson, P., Stoyan, T., Otten, U., Rose-John, S. (1998) Sympathetic neurons can produce and respond to interleukin 6. *Proc. Natl. Acad. Sci. U. S. A.* **95**, 3251-3256
- [31] Müller-Newen, G., Kuester, A., Hemmann, U., Keul, R., Horsten, U., Martens, A., Graeve, L., Wijdenes, J., Heinrich, P. C. (1998) Soluble IL-6 receptor potentiates the antagonistic activity of soluble gp130 on IL-6 responses. *J. Immunol.* **161**, 6347-6355
- [32] Jostock, T., Müllberg, J., Özbek, S., Atreya, R., Blinn, G., Voltz, N., Fischer, M., Neurath, M. F., Rose-John, S. (2001) Soluble gp130 is the natural inhibitor of soluble interleukin-6 receptor transsignaling responses. *Eur. J. Biochem.* **268**, 160-167
- [33] Davis, S., Aldrich, T. H., Ip, N. Y., Stahl, N., Scherer, S., Farruggella, T., DiStefano, P. S., Curtis, R., Panayotatos, N., Gascan, H., Chevalier, S., Yancopoulos, G. D. (1993) Released form of CNTF receptor alpha component as a soluble mediator of CNTF responses. *Science* **259**, 1736-1739

- [34] Karow, J., Hudson, K. R., Hall, M. A., Vernallis, A. B., Taylor, J. A., Gossler, A., Heath, J. K. (1996) Mediation of interleukin-11-dependent biological responses by a soluble form of the interleukin-11 receptor. *Biochem. J.* **318**, 489-495
- [35] Hooper, W. C., Phillips, D. J., Evatt, B. L. (1997) Endothelial cell protein S synthesis is upregulated by the complex of IL-6 and soluble IL-6 receptor. *Haemost.* **77**, 1014-1019
- [36] Hurst, S. M., Wilkinson, T. S., McLoughlin, R. M., Jones, S., Horiuchi, S., Yamamoto, N., Rose-John, S., Fuller, G. M., Topley, N., Jones, S. A. (2001) IL-6 and its soluble receptor orchestrate a temporal switch in the pattern of leukocyte recruitment seen during acute inflammation. *Immunity* **14**, 705-714
- [37] Marin, V., Montero-Julian, F. A., Gres, S., Boulay, V., Bongrad, B., Farnarier, C., Kaplanski, G. (2001) The IL-6-soluble IL-6R $\alpha$  autocrine loop of endothelial activation as an Intermediate between acute and chronic inflammation: an experimental model involving thrombin. *J. Immunol.* **167**, 3435-3442
- [38] Modur, V., Li, Y., Zimmerman, G. A., Prescott, S. M., McIntyre, T. M. (1997) Retrograde inflammatory signaling from neutrophils to endothelial cells by soluble interleukin-6 receptor alpha. *J. Clin. Invest.* **100**, 2752-2756
- [39] Atreya, R., Mudter, J., Finotto, S., Müllberg, J., Jostock, T., Wirtz, S., Schutz, M., Bartsch, B., Holtmann, M., Becker, C., Strand, D., Czaja, J., Schlaak, J. F., Lehr, H. A., Autschbach, F., Schurmann, G., Nishimoto, N., Yoshizaki, K., Ito, H., Kishimoto, T., Galle, P. R., Rose-John, S., Neurath, M. F. (2000) Blockade of interleukin 6 trans signaling suppresses T-cell resistance against apoptosis in chronic intestinal inflammation: evidence in crohn disease and experimental colitis in vivo. *Nature Med.* **6**, 583-588
- [40] Oh, J.-W., van Wagoner, N., Rose-John, S., Benveniste, E. N. (1998) Role of IL-6 and the soluble IL-6 receptor in inhibition of VCAM-1 gene expression. *J. Immunol.* **161**, 4992-4999
- [41] Thier, M., März, P., Otten, U., Weis, J., Rose-John, S. (1999) Interleukin-6 (IL-6) and its soluble receptor support survival of sensory neurons. *J. Neurosci. Res.* **55**, 411-422
- [42] März, P., Heese, K., Dimitriades-Schmutz, B., Rose-John, S., Otten, U. (1999) Role of interleukin-6 and soluble IL-6 receptor in region-specific induction of astrocytic differentiation and neurotrophin expression. *Glia* **26**, 191-200
- [43] März, P., Herget, T., Lang, E., Otten, U., Rose-John, S. (1997) Activation of gp130 by IL-6/soluble IL-6 receptor induces neuronal differentiation. *Eur. J. Neurosci.* **9**, 2765-2773
- [44] Bataille, R., Harousseau, J.-L. (1997) Multiple myeloma. *N. Engl. J. Med.* **336**, 1657-1664
- [45] Singhal, S., Mehta, J., Desikan, R., Ayers, D., Roberson, P., Eddlemon, P., Munshi, N., Anaissie, E., Wilson, C., Dhodapkar, M., Zeddis, J., Barlogie, B. (1999) Antitumor activity of thalidomide in refractory multiple myeloma. *N. Engl. J. Med.* **341**, 1565-1571

- [46] Thabard, W., Barille, S., Collette, M., Harousseau, J.-L., Rapp, M. J., Bataille, R., Amiot, M. (1999) Myeloma cells release soluble interleukin-6/Ralpha in relation to disease progression by two distinct mechanisms: alternative splicing and proteolytic cleavage. *Clin. Cancer Res.* **5**, 2693-2697
- [47] Cohen, T., Nahari, D., Cerem, L.W., Neufeld, G., Levi, B. Z. (1996) Interleukin 6 induces the expression of vascular endothelial growth factor. *J. Biol. Chem.* **271**, 736-741
- [48] Kawasaki, K., Gao, Y. H., Yokose, S., Kaji, Y., Nakamura, T., Suda, T., Yoshida, K., Taga, T., Kishimoto, T., Kataoka, H., Yuasa, T., Norimatsu, H., Yamaguchi, A. (1997) Osteoclasts are present in gp130-deficient mice. *Endocrinology* **138**, 4959-4965
- [49] Van Valckenborgh, E., Croucher, P. I., De Raeve, H., Carron, C., De Leenheer, E., Blacher, S., Devy, L., Noel, A., De Bruyne, E., Asosingh, K., Van Riet, I., Van Camp, B., Vanderkerken, K. (2004) Multifunctional role of matrix metalloproteinases in multiple myeloma: a study in the 5T2MM mouse model. *Am. J. Pathol.* **165**, 869-878
- [50] Devenney, B., Erickson, C. (2004) Multiple myeloma: an overview. *Clin. J. Oncol. Nurs.* **8**, 401-405
- [51] Chatterjee, M., Stuehmer, T., Herrmann, P., Bommert, K., Dorken, B., Bargou, R. C. (2004) Combined disruption of both the MEK/ERK and the IL-6R/STAT3 pathways is required to induce apoptosis of multiple myeloma cells in the presence of bone marrow stromal cells. *Blood*, in press.
- [52] Chang, Y., Cesarman, E., Pessin, M. S., Lee, F., Culpepper, J., Knowles, D. M., Moore, P. S. (1994) Identification of herpesvirus-like DNA sequences in AIDS-associated Kaposi's sarcoma. *Science* **266**, 1865-1869
- [53] Cesarman, E., Chang, Y., Moore, P. S., Said, J. W., Knowles, D. M. (1995) Kaposi's sarcoma-associated herpesvirus-like DNA sequences in AIDS-related body-cavity-based lymphomas. *N. Engl. J. Med.* **332**, 1186-1191
- [54] Nador, R. G., Cesarman, E., Chadburn, A., Dawson, D. B., Ansari, M. Q., Said, J. W., Knowles, D. M. (1996) Primary effusion lymphoma: a distinct clinicopathologic entity associated with the Kaposi's sarcoma-associated herpes virus. *Blood.* **88**, 645-656
- [55] Soulier, J., Grollet, L., Oksenhendler, E., Cacoub, P., Cazals-Hatem, D., Babinet, P., d'Agay, M., Clauvel, J., Raphael, M., Degos, L., Sigaux, F. (1995) Kaposi's sarcoma-associated herpesvirus-like DNA sequences in multicentric Castlemans disease. *Blood* **86**, 1276- 1280
- [56] Rettig, M. B., Ma, H. J., Vescio, R. A., Pold, M., Schiller, G., Belson, D., Savage, A., Nishikubo, C., Wu, C., Fraser, J., Said, J. W., Berenson, J. R. (1997) Kaposi's sarcoma-associated herpesvirus infection of bone marrow dendritic cells from multiple myeloma patients. *Science* **276**, 1851-1854
- [57] Raje, N., Gong, J., Chauhan, D., Teoh, G., Avigan, D., Wu, Z., Chen, D., Treon, S. P., Webb, I., Kufe, D. W., Anderson, K. C. (1999) Bone marrow and peripheral blood

dendritic cells from patients with multiple myeloma are phenotypically and functionally normal despite the detection of Kaposi's sarcoma herpesvirus gene sequences. *Blood* **93**, 1487-1495

[58] Russo, J. J., Bohensky, R. A., Chen, M. C., Yan, M., Maddalena, D., Parry, J. P., Peruzzi, D., Edelman, I. S., Chang, Y., Moore, P. S. (1996) Nucleotide sequence of the Kaposi sarcoma-associated herpesvirus (HHV8). *Proc. Natl. Acad. Sci. U.S.A.* **93**, 14862-14867

[59] Neipel, F., Albrecht, J., Fleckenstein, B. (1997) Cell-homologous genes in the Kaposi's sarcoma-associated rhadinovirus human herpesvirus 8: determinants of its pathogenicity? *J. Virol.* **71**, 4187-419.

[60] Moore, P. S., Boshoff, C., Weiss, R. A., Chang, Y. (1996) Molecular mimicry of human cytokine and cytokine response pathway genes by KSHV. *Science* **274**, 1739-1744

[61] Neipel, F., Albrecht, J., Ensser, A., Huang, Y., Li, Y. Y., Friedman-Kien, A. E., Fleckenstein, B. (1997) Human herpesvirus 8 encodes a homolog of interleukin-6. *J. Virol.* **71**, 839-842

[62] Damania, B. (2004) Modulation of Cell Signaling Pathways by Kaposi's Sarcoma-Associated Herpesvirus (KSHV/HHV-8). *Cell Biochem. Biophys.* **40**, 305-322

[63] Klouche, M., Carruba, G., Castagnetta, L., Rose-John, S. (2004) Virokines in the pathogenesis of cancer – focus on human herpesvirus 8. *N. Y. Acad. Sci.*, in press

[64] Boulanger, M. J., Bankovich, A. J., Kortemme, T., Baker, D., Garcia, K. C. (2003) Convergent mechanisms for recognition of divergent cytokines by the shared signaling receptor gp130. *Moll. Cell* **12**, 577-589

[65] Grötzinger, J., Kernebeck, T., Kallen, K.-J., Rose-John, S. (1999) IL-6 type cytokine receptor complexes: hexamer, tetramer or both? *Biol. Chem.* **380**, 803-813

[66] Kalai, M., Montero-Julian, F. A., Grötzinger, J. (1997) Analysis of the human interleukin-6/human interleukin-6 receptor binding interface at the amino acid level: proposed mechanism of interaction. *Blood* **89**, 1319-1333

[67] Somers, W., Stahl, M., Seehra, J. S. (1997) 1.9 A crystal structure of interleukin 6: implications for a novel mode of receptor dimerization and signaling. *EMBO J.* **16**, 989-997

[68] Aoki, Y., Narazaki, M., Kishimoto, T., Tosato, G. (2001) Receptor engagement by viral interleukin-6 encoded by Kaposi sarcoma-associated herpesvirus. *Blood* **98**, 3042-3049

[69] Hoischen S. H., Vollmer, P., März, P., Özbek, S., Gotze, K. S., Peschel, C., Jostock, T., Geib, T., Müllberg, B., Mechttersheimer, S., Fischer, M., Grötzinger, J., Galle, P. R., Rose-John, S. (2000) Human herpes virus 8 interleukin-6 homologue triggers gp130 on neuronal and hematopoietic cells. *Eur. J. Biochem.* **267**, 3604-3612

- [70] Chow, D., He, X., Snow, A. L., Rose-John, S., Garcia, K. C. (2001) Structure of an extracellular gp130 cytokine receptor signaling complex. *Science* **291**, 2150-2155
- [71] Taga, T., Kishimoto, T. (1997) gp130 and the interleukin-6 family of cytokines. *Annu. Rev. Immunol.* **15**, 797-819
- [72] Müllberg, J., Geib, T., Jostock, T., Hoischen, S. H., Vollmer, P., Voltz, N., Heinz, D., Galle, P. R., Klouche, M., Rose-John, S. (2000) IL-6 receptor independent stimulation of human gp130 by viral IL-6. *J. Immunol.* **164**, 4672-4677
- [73] Wan, X., Wang, H., Nicholas, J. (1999) Human herpesvirus 8 interleukin-6 (vIL-6) signals through gp130 but has structural and receptor-binding properties distinct from those of human IL-6. *J. Virol.* **73**, 8268-8278
- [74] Dela Cruz, C. S., Lee, Y., Viswanathan, S. R., El-Guindy, A. S., Gerlach, J., Nikiforow, S., Shedd, D., Gradoville, L., Miller, G. (2004) N-linked glycosylation is required for optimal function of Kaposi's sarcoma herpesvirus-encoded, but not cellular, interleukin 6. *J. Exp. Med.* **199**, 503-514
- [75] Orita, T., Oh-eda, M., Hasegawa, M., Kuboniwa, H., Esaki, K., Ochi, N. (1994) Polypeptide and carbohydrate structure of recombinant human interleukin-6 produced in Chinese hamster ovary cells. *J. Biochem.* **115**, 345-350
- [76] Burger, R., Neioel, F., Fleckenstein, B., Savino, R., Giliberto, G., Kalden, J. R., Gramazki, M. (1998) Human herpesvirus type 8 interleukin-6 homologue is functionally active on human myeloma cells. *Blood* **91**, 1858-1863
- [77] Molden, J., Chang, Y., You, Y., Moore, P. S., Goldshmith, M. A. (1997) A Kaposi's sarcoma-associated herpesvirus-encoded cytokine homolog (vIL-6) activates signaling through the shared gp130 receptor subunit. *J. Biol. Chem.* **272**, 19625-19631
- [78] Hideshima, T., Chauhan, D., Teoh, G., Raje, N., Treon, S. P., Tai, Y.-T., Shima, Y., Anderson, K. C. (2000) Characterization of signaling cascades triggered by human interleukin-6 versus Kaposi's sarcoma-associated herpes virus-encoded viral interleukin 6. *Clinic. Cancer Res.* **6**, 1180-1189
- [79] Akira, S., Taga, T., Kishimoto, T. (1993) Interleukin-6 in biology and medicine. *Adv. Immunol.* **54**, 1-78
- [80] Kishimoto, T., Akira, S., Narazaki, M., Taga, T. (1995) Interleukin-6 family of cytokines and gp130. *Blood* **86**, 1243-1254
- [81] Jones, K. D., Aoki, Y., Chang, Y., Moore, P. S., Yarchoan, R., Tosato, G. (1999) Involvement of interleukin-10 (IL-10) and viral IL-6 in the spontaneous growth of Kaposi's sarcoma herpesvirus-associated infected primary effusion lymphoma cells. *Blood* **94**, 2871-2879

- [82] Aoki, Y., Tosato, G., Nambu, Y., Iwamoto, A., Yarchoan, R. (2000) Detection of vascular endothelial growth factor in AIDS-related primary effusion lymphomas. *Blood* **95**, 1109-1110
- [83] Stark, G. R., Kerr, I. M., Williams, B. R., Silverman, R. H., Schreiber, R. D. (1998) How cells respond to interferons. *Annu. Rev. Biochem.* **67**, 227-264
- [84] Taniguchi, T., Ogasavara, K., Takaoka, A., Tanaka, N. (2001) IRF family of transcription factors as regulators of host defense. *Annu. Rev. Biochem.* **19**, 623-655
- [85] Chatterjee, M., Osborne, J., Bestetti, G., Chang Y., Moore, P. S. (2002) Viral IL-6-induced cell proliferation and immune evasion of interferon activity. *Science* **298**, 1432-1435
- [86] Goodman, A. R., Gardozo, T., Abagyan, R., Altmeyer, A., Wisniewski, H. G., Vilcek J. (1996) Long pentraxins: an emerging group of proteins with diverse functions. *Cytokine Growth Factor Rev.* **7**, 191-202
- [87] Bottazzi, B., Vouret-Craviari, V., Bastone, A. (1997) Multimer formation and ligand recognition by the long pentraxin PTX3. Similarities and differences with the short pentraxins C-reactive protein and serum amyloid P component. *J. Biol. Chem.* **272**, 32817-32823
- [88] Klouche M., Brockmeyer, N., Knabbe, C., Rose-John, S. (2002) Human herpesvirus 8-derived viral IL-6 induces PTX3 expression in Kaposi's sarcoma cells. *AIDS* **16**, F9-F18
- [89] Dhingra, K., Sahin, A., Emami, K., Hortobagyi, G. N., Estrov, Z. (1998) Expression of leukemia inhibitory factor and its receptor in breast cancer: a potential autocrine and paracrine growth regulatory mechanism. *Breast Cancer Res. Treat.* **48**, 165-174
- [90] World, C. J., Rolfe, B. E., Campbell, J. H. (2001) Regulation of LIF receptor expression in vascular smooth muscle. *Ann. N. Y. Acad. Sci.* **947**, 323-328
- [91] Blanchard, F., Tracy, E., Smith, J., Chattopadhyay, S., Wang, Y., Held, W. A., Baumann, H. (2003) DNA methylation controls the responsiveness of hepatoma cells to leukemia inhibitory factor. *Hepatology* **38**, 1516-1528
- [92] Yoshino, J., Monkawa, T., Tsuji, M., Hayashi, M., Saruta, T. (2003) Leukemia inhibitory factor is involved in tubular regeneration after experimental acute renal failure. *J. Am. Soc. Nephrol.* **14**, 3090-3101
- [93] März, P., Özbek, S., Fisher, M., Voltz, M., Otten, U., Rose-John, S. (2002) Differential response of neuronal cells to a fusion protein of ciliary neurotrophic factor/soluble CNTF-receptor and leukemia inhibitory factor. *Eur. J. Biochem.* **269**, 3023-3031
- [94] Zvonic, S., Cornelius, P., Stewart, W. C., Mynat, P. L., Stephens J. M. (2003) The regulation and activation of ciliary neurotrophic factor signaling proteins in adipocytes. *J. Biol. Chem.* **278**, 2228-2235

- [95] Sleeman, M. W., Anderson, K. D., Lambert, P. D., Yancopoulos, G. D., Wiegand, S. J. (2000) The ciliary neurotrophic factor and its receptor, CNTFR alpha. *Pharm. Acta Helv.* **74**, 265-272
- [96] Fischer, M., Goldschmitt, J., Peschel, C., Brakenhoff P. G., Kallen, K.-J., Wollmer, A., Grötzing, J., Rose-John, S. (1997) A bioactive designer cytokine for human hematopoietic progenitor cell expansion. *Nature Biotech.* **15**, 142-145
- [97] Hecht, N., Pappo, O., Shouval. D., Rose- John, S., Galun, E., Alexrod, J. H. (2001) Hyper-IL-6 gene therapy reverses fulminant hepatic failure. *Mol. Ther.* **3**, 683-687
- [98] Galun, E., Alexrod, J. H. (2002) The role of cytokines in liver failure and regeneration: potential new molecular therapies. *Biochim. Biophys. Acta* **1592**, 345-358
- [99] Thier, M., März, P., Otten, U., Weis, J., Rose-John, S. (1999) Interleukin-6 (IL-6) and its soluble receptor support survival of sensory neurons. *J. Neurosci. Res.* **55**, 411-422
- [100] Bernhard, H., Lohmann, M., Batten, W., Metzger, J., Lohr, H. F., Peschel, C., Meyer zum Büschenfelde, K. H., Rose-John, S. (2000) The gp130-stimulating designer cytokine hyper-IL-6 promotes the expansion of human hematopoietic progenitor cells capable to differentiate into functional dendritic cells. *Exp. Hematol.* **28**, 365-372
- [101] Diamant, M., Rieneck, K., Mechti, N., Zhang, X. G., Svenson, M., Bendtzen, K., Klein, B. (1997) Cloning and expression of an alternatively spliced mRNA encoding a soluble form of the human interleukin-6 signal transducer gp130. *FEBS* **412**, 379-384
- [102] Hasegawa, M., Sato, S., Fujimoto, M., Ihn, H., Kikuchi, K., Takehara, K. (1998) Serum levels of interleukin 6 (IL-6), oncostatin M, soluble IL-6 receptor, and soluble gp130 in patients with systemic sclerosis. *J. Rheumatol.* **25**, 308-313
- [103] Radberg, F., Feneberg, W., Schmidt, S., Schwarz, M. J., Korschenhausen, D., Greenberg, B. D., Nolde, T., Muller, N., Trapmann, H., König, N., Moller, H. J., Hampel, H. (1999) CSF and serum levels of soluble interleukin-6 receptors (sIL-6R and sgp130), but not of interleukin-6 are altered in multiple sclerosis. *J. Neuroimmunol.* **99**, 218-223
- [104] Montero-Julian, F. A., Brailly, H., Sautes, C., Joyeux, I., Dorval, T., Mosseri, V., Yasukawa, K., Wijdenes, J., Adler, A., Gorin, I., Fridman, W. H., Tartour, E. (1997) Characterization of soluble gp130 released by melanoma cell lines: A polyvalent antagonist of cytokines from the interleukin 6 family. *Clin. Cancer Res.* **3**, 1443-1451
- [105] Nowell, M. A., Richards, P. J., Horiuchi, S., Yamamoto, N., Rose-John, S., Topley, N., Williams, A. S., Jones, S. A. (2003) Soluble IL-6 receptor governs IL-6 activity in experimental arthritis: blockade of arthritis severity by soluble glycoprotein 130. *J. Immunol.* **171**, 3202-3209
- [106] Becker, C., Fantini, M. C., Schramm, C., Lehr, H. A., Wirtz, S., Nikolaev, A., Burg, J., Strand, S., Kiesslich, R., Huber, S., Ito, H., Nishimoto, N., Yoshizaki, K., Kishimoto, T., Galle, P. R., Blessing, M., Rose-John, S., Neurath, M. F. (2004) TGF-beta suppresses tumor progression in colon cancer by inhibition of IL-6 transsignaling. *Immunity* **20**, 491-501



- [107] Zeissig, S., Bojarski, C., Buergel, N., Mankertz, J., Zeitz, M., Fromm, M., Schulzke, J. D. (2004) Downregulation of epithelial apoptosis and barrier repair in active Crohn's disease by tumour necrosis factor alpha antibody treatment. *Gut* **53**, 1295-1302
- [108] Kumar, R. K., Herbert, C., Webb, D. C., Li, L., Foster, P. S. (2004) Effects of anti-cytokine therapy in a mouse model of chronic asthma. *Am. J. Respir. Crit. Care Med.*, in press.
- [109] Van Gelder, T., Warle, M., Ter Meulen R. G. (2004) Anti-interleukin-2 receptor antibodies in transplantation: what is the basis for choice? *Drugs* **64**, 1737-1741
- [110] Zhen, Y. (2000) Advances in research on monoclonal antibody agents for cancer therapy. *Zhongguo Yi Xue Ke Xue Yuan Xue Bao* **22**, 9-13
- [111] Hasholzner, U., Stieber, P., Meier, W., Lamerz, R. (1997) Value of HAMA-determination in clinical practice - an overview. *Anticancer Res.* **17**, 3055-3058
- [112] Tan, P., Mitchell, D. A., Buss, T. N., Holmes, M. A., Anasetti, C., Foote, J. (2002) „Superhumanized” antibodies: reduction of immunogenic potential by complementarity-determining region grafting with human germline sequences: application to an anti-CD28. *J. Immunol.* **169**, 1119-1125
- [113] Xu, M. Y., Xu, X. H., Chen, G. Z., Deng, X. L., Li, J., Yu, X. J., Chen, M. Z. (2004) Production of a human single-chain variable fragment antibody against esophageal carcinoma. *World J. Gastroenterol.* **10**, 2619-2623
- [114] Broders, O., Breitling, F., Dubel, S. (2003) Hyperphage. Improving antibody presentation in phage display. *Methods Mol. Biol.* **205**, 295-302
- [115] Carmen, S., Jermutus, L. (2002) Concepts in antibody phage display. *Brief Funct. Genomic. Proteomic* **1**, 189-203
- [116] Hutchings, C., Carmen, S., Lennard, S. (2001) chapter **6**. In: *Antibody Engineering*, ed: Kontermann, R., Dubel, S., Springer Verlag, Heidelberg
- [117] Roehrig, J. T., Staudinger, L. A., Hunt, A. R., Mathews, J. H., Blair, C.D. (2001) Antibody prophylaxis and therapy for flavivirus encephalitis infections. *Ann. N. Y. Acad. Sci.* **951**, 286-297
- [118] Krebs, B., Griifin, H., Winter, G., Rose-John, S. (1998) Recombinant human single chain Fv antibodies recognizing human interleukin-6. Specific targeting of cytokine-secreting cells. *J. Biol. Chem.* **273**, 2858-2865
- [119] Krebs, B., Ackermann, B., Rose-John, S. (1998) Specific targeting of cytokine-secreting cells: a bispecific diabody recognizing human interleukin-6 and CD3 induces T cell-mediated killing. *J. Interferon Cytokine Res.* **18**, 783-791

- [120] Rose-John, S., Schooltink, H., Schmitz-Van de Leur, H., Müllberg, J., Heinrich, P. C., Graeve, L. (1993) Intracellular retention of interleukin-6 abrogates signaling. *J. Biol. Chem.* **268**, 22084-22091
- [121] Pastan, I. (2003) Immunotoxins containing *Pseudomonas* exotoxin A: a short history. *Cancer Immunol. Immunother.* **52**, 338-341
- [122] Andersson, Y., Juell, S., Fodstad, O. (2004) Downregulation of the antiapoptotic MCL-1 protein and apoptosis in MA-11 breast cancer cells induced by an anti-epidermal growth factor receptor-Pseudomonas exotoxin a immunotoxin. *Int J Cancer.* **112**, 475
- [123] FitzGerald, D.J., Kreitman, R., Wilson, W., Squires, D., Pastan, I. (2004) Recombinant immunotoxins for treating cancer. *Int J Med Microbiol.* **293**, 577-582
- [124] Engebraaten, O., Sivam, G., Juell, S., Fodstad, O. (2004) Systemic immunotoxin treatment inhibits formation of human breast cancer metastasis and tumor growth in nude rats. *Int J Cancer.* **88**, 970-976
- [125] Kreitman, R. J., Wang, Q. C., FitzGerald, D. J., Pastan, I. (1999) Complete regression of human B-cell lymphoma xenografts in mice treated with recombinant anti-CD22 immunotoxin RFB4(dsFv)-PE38 at doses tolerated by cynomolgus monkeys. *Int. J. Cancer* **81**, 148-155
- [126] Baluna, R., Coleman, E., Jones, C., Ghetie, V., Vitetta, E. S. (2000) The effect of a monoclonal antibody coupled to ricin A chain-derived peptides on endothelial cells in vitro: insights into toxin-mediated vascular damage. *Exp. Cell Res.* **258**, 417-424
- [127] Palacios, R., Steinmetz, M. (1985) IL-3 dependent mouse clones that express B-220 surface antigen, contain Ig genes in germ-line configuration, and generate B lymphocytes in vivo. *Cell* **41**, 727-734
- [128] Gearing, D. P., Ziegler, S. F., Comeau, M. R., Friend, D., Thoma, B., Cosman, D., Park, L., Mosley, B. (1994) Proliferative responses and binding properties of hematopoietic cells transfected with low affinity receptors for leukemia inhibitory factor, oncostatin M, and ciliary neurotrophic factor. *Proc. Natl. Acad. Sci. USA* **91**, 1119-1123
- [129] Laemmli, M.K. (1970) Cleavage of structural proteins during the assembly of the head of bacteriophage T4. *Nature* **227**, 680-685
- [130] Bellevik, S., Summerer, S., Meijer, J. (2002) Overexpression of *Arabidopsis thaliana* soluble epoxide hydrolase 1 in *Pichia pastoris* and characterisation of the recombinant enzyme. *Protein Expr. Purif.* **26**, 65-70
- [131] O’Shannessy, D. J., Brigham-Burke, M., Soneson, K. K., Hensley, P., Brooks, I. (1993) Determination of rate and equilibrium binding constants for macromolecular interactions using surface plasmon resonance: use of nonlinear least squares analysis methods. *Anal. Biochem.* **212**, 457-468

- [132] Mierendorf, R., Yeager, K., Novy, R. (1994) The pET system: your choice for expression. *In Novations (newsletter of Novagen)* **1**, 1-3
- [133] Ramos, C. R., Abreu, P. A., Nascimento, A. L., Ho, P. L. (2004) A high-copy T7 *Escherichia coli* expression vector for the production of recombinant proteins with a minimal N-terminal His-tagged fusion peptide. *Braz. J. Med. Biol. Res.* **37**, 1103-1109
- [134] Kallen, K.-J., Grötzinger, J., Lelievre, E., Vollmer, P., Aasland, D., Renne, C., Müllberg, J., Meyer zum Büschenfelde, K.-H., Gascan, H., Rose-John, S. (1999) Receptor recognition sites of cytokines are organized as exchangeable modules. Transfer of the leukemia inhibitory factor receptor-binding site from ciliary neurotrophic factor to interleukin-6. *J. Biol. Chem.* **274**, 11859-11867
- [135] Nalivaeva, N. N., Turner, A. J. (2001) Post-translational modifications of proteins: acetylcholinesterase as a model system. *Proteomics* **1**, 735-747
- [136] Brent, R., Kingston, R. E., Moore, D. D., Seidman, J. G., Smith, J. A., Struhl, K. (1999) chapter **16.12**. *In: Shortprotocols in molecular biology*, ed: Ausubel, F. M., WILEY, New York, Chichester, Weinheim, Brisbane, Singapore, Toronto
- [137] Lopata, M. A., Cleveland, D. W., Sollner-Webb, B. (1984) High level transient expression of a chloramphenicol acetyl transferase gene by DEAE-dextran mediated DNA transfection coupled with a dimethyl sulfoxide or glycerol shock treatment. *Nucleic Acids Res.* **12**, 5707-5717
- [138] Kohfeldt, E., Maurer, P., Vannahme, C., Timpl, R. (1997) Properties of the extracellular calcium binding module of the proteoglycan testical. *FEBS Lett.* **414**, 557-561
- [139] Young, J. M., Cheadle, C., Foulke, J. S., Drohan, W. N., Sarwer, N. (1988) Utilization of an Epstein-Barr virus replicon as a eukaryotic expression vector. *Gene* **62**, 171-85
- [140] Griffith, W. P., Kaltashov, I. A. (2003) Highly asymmetric interactions between globin chains during hemoglobin assembly revealed by electrospray ionization mass spectrometry. *Biochemistry* **42**, 10024-10033
- [141] Waxman, E., Rusinova, E., Hasselbacher, C. A., Schwartz, G. P., Laws, W. R., Ross, J. B. (1993) Determination of the tryptophan:tyrosine ratio in proteins. *Anal. Biochem.* **210**, 425-428
- [142] Smith, G. P., Petrenko, V. A. (1997) Phage Display *Chem. Rev.* **97**, 391-410
- [143] Smith G. P. (1985) Filamentous fusion phage: novel expression vectors that display cloned antigens on the virion surface. *Science* **228**, 1315-1317
- [144] Bass, S., Greene, R., Wells, J. A. (1990) Hormone phage: an enrichment method for variant proteins with altered binding properties. *Proteins* **8**, 309-314

- [145] De Bruin, R., Spelt, K., Mol, J., Koes, R., Quattrocchio, F. (1999) Selection of high-affinity phage antibodies from phage display libraries. *Nature Biotechnol.* **17**, 397-399
- [146] Eeckhout, D., Fiers, E., Sienaert, R., Snoeck, V., Depicker, A., De Jaeger, G. (2000) Isolation and characterization of recombinant antibody fragments against CDC2a from *Arabidopsis thaliana*. *Eur. J. Biochem.* **267**, 6775-6783
- [147] Rong, J., Xu, X., Ewen, C., Bleackly, R. C., Kane, K. P. (2004) Isolation and characterization of novel single-chain Fv specific for human granzyme B. *Hybrid Hybridomics* **23**, 219-231
- [148] Aasland, D., Schuster, B., Grötzinger, J., Rose-John, S., Kallen, K.-J. (2003) Analysis of the leukemia inhibitory factor receptor functional domains by chimeric receptors and cytokines. *Biochemistry* **42**, 5244-5252
- [149] Aasland, D., Oppmann, B., Grötzinger, J., Rose-John, S., Kallen, K.-J. (2002) The upper cytokine-binding module and the Ig-like domain of the leukaemia inhibitory factor (LIF) receptor are sufficient for a functional LIF receptor complex. *J. Mol. Biol.* **315**, 637-646
- [150] Turbadar, T. (1959) *Proc. Phys. Soc.* **73**, 40
- [151] Welford, K. (1991) *Opt. Quant. Elect.* **23**, 1
- [152] Wu, S.-C., Yeung, J. C., Duan, Y., Ye, R., Szarka, S. J., Habibi, H. R., Wong, S.-L. (2002) Functional production and characterization of a fibrin-specific single-chain antibody fragment from *Bacillus subtilis*: effects of molecular chaperones and a wall-bound protease on antibody fragment production. *Appl. Environ. Microbiol.* **68**, 3261-3269
- [153] Weiergraber, O., Hemmann, U., Kuster, A., Muller-Newen, G., Schneider, J., Rose-John, S., Kurschat, P., Brakenhoff, J. P., Hart, M. H., Stabel, S., Heinrich P. C. (1995) Soluble human interleukin-6 receptor. Expression in insect cells, purification and characterization. *Eur. J. Biochem.* **234**, 661-669
- [154] Murshid, A., Presley, J. F. (2004) ER-to-Golgi transport and cytoskeletal interactions in animal cells. *Cell. Mol. Life Sci.* **61**, 133-145
- [155] Cabrera, M., Muniz, M., Hidalgo, J., Vega, L., Martin, M. E., Velasco, A. (2003) The retrieval function of the KDEL receptor requires PKA phosphorylation of its C-terminus. *Mol. Biol. Cell* **14**, 4114-4125
- [156] Ho, S. N., Hunt, H. D., Horton, R. M., Pullen, J. K., Pease, L. R. (1989) Site-directed mutagenesis by overlap extension using the polymerase chain reaction. *Gene* **77**, 51-59
- [157] Horton, R. M., Hunt, H. D., Ho, S. N., Pullen, J. K., Pease, L. R. (1989) Engineering hybrid genes without the use of restriction enzymes: gene splicing by overlap extension. *Gene* **77**, 61-68

- [158] Villarreal, X. C., Long, G. L. (1991) A general method of polymerase-chain-reaction-enabled protein domain mutagenesis: construction of a human protein S-osteonectin gene. *Anal. Biochem.* **197**, 362-367
- [159] Zhong, D., Bajaj, S. P. (1993) A PCR-based method for site-specific domain replacement that does not require restriction recognition sequences. *BioTechniques* **15**, 874-878
- [160] Sasaki, Y., Sone, T., Yoshida, S., Yahata, K., Hotta, J., Chesnut, J. D., Honda, T., Imamoto, F. (2004) Evidence for high specificity and efficiency of multiple recombination signals in mixed DNA cloning by the Multisite Gateway system. *J. Biotechnol.* **107**, 233-243
- [161] Landy, A. (1989) Dynamic, structural, and regulatory aspects of lambda site-specific recombination. *Ann. Rev. Biochem.* **58**, 913-949
- [162] Mukhopadhyay, A. (1997) Inclusion bodies and purification of proteins in biologically active forms. *Adv. Biochem. Eng. Biotechnol.* **56**, 61-109
- [163] McCafferty, J., Griffiths, A. D., Winter, G., Chiswell, D. J. (1990) Phage antibodies: filamentous phage displaying antibody variable domains. *Nature* **348**, 552-554
- [164] Winter, G., Griffiths, A. D., Hawkins, R. E., Hoogenboom, H.R. (1994) Making antibodies by phage display technology. *Annu. Rev. Immunol* **12**, 433-455
- [165] Vaughan, T. J., Williams, T. J., Pritchard, K., Osbourn, J. K., Pope, A. R., Earnshaw, J. C., McCafferty, J., Hodits, R. A., Wilton, J., Johnson, K. S. (1996) Human antibodies with sub-nanomolar affinities isolated from a large non-immunized phage display library. *Nature Biotech.* **14**, 309-314
- [166] Xie, M.-H., Yuan, J., Adams, C., Gurney, A. (1997) Direct demonstration of MuSK involvement in acetylcholine receptor clustering through identification of agonist ScFv. *Nature Biotech.* **15**, 768-771
- [167] Griffiths, A. D., Malmqvist, M., Marks, J. D., Bye, J. M., Embleton, M. J., McCafferty, J. (1993) Human anti-self antibodies with high specificity from phage display libraries. *EMBO J.* **12**, 725-734
- [168] Johnson, K. S., Glover, D. R. (1998) Antibodies come in from the cold. *Innovations in Pharmaceutical Technology*, 82-85
- [169] Özbek, S., Grötzinger, J., Krebs, B., Fischer, M., Wollmer, A., Jostock, T., Müllberg, J., Rose-John, S. (1998) The membrane proximal cytokine receptor domain of the human interleukin-6-receptor is sufficient for ligand binding but not for gp130 association. *J. Biol. Chem.* **273**, 21374-21379
- [170] Toniatti, C., Cabibbo, A., Sporena, E., Salvati, A. L., Cerretani, M., Serafini, S., Lahm, A., Cortese, R., Ciliberto, G. (1996) Engineering human interleukin-6 to obtain variants with strongly enhanced bioactivity. *EMBO J.* **15**, 2726-2737

- [171] Kollet, O., Aviram, R., Chebath, J., ben-Hur, H., Nagler, A., Shultz, L., Revel, M., Lapidot, T. (1999) The soluble interleukin-6 (IL-6) receptor/IL-6 fusion protein enhances in vitro maintenance and proliferation of human CD34(+)CD38(-/low) cells capable of repopulating severe combined immunodeficiency mice. *Blood* **94**, 923-931
- [172] Meads, M. B., Medveczky, P. G. (2004) Kaposi's sarcoma-associated herpesvirus encoded viral interleukin-6 is secreted and modified differently than human interleukin-6: evidence for a unique autocrine signaling mechanism. *J. Biol. Chem.* in press
- [173] Oksenhendler, E., Boulanger, E., Galicier, L., Du, M. Q., Dupin, N., Diss, T. C., Hamoudi, R., Daniel, M. T., Agbalika, F., Boshoff, C., Clauvel, J. P., Isaacson, P. G., Meignin, V. (2002) High incidence of Kaposi sarcoma-associated herpesvirus-related non-Hodgkin lymphoma in patients with HIV infection and multicentric Castleman disease. *Blood* **99**, 2331-2336
- [174] Nishi, J., Maruyama, I. (2000) Increased expression of vascular endothelial growth factor (VEGF) in Castleman's disease: proposed pathomechanism of vascular proliferation in the affected lymph node. *Leuk. Lymphoma* **38**, 387-394
- [175] Luppi, M., Barozzi, P., Maiorana, A., Trovato, R., Marasca, R., Morselli, M., Cagossi, K., Torelli, G. (1999) Expression of cell-homologous genes of human herpesvirus-8 in human immunodeficiency virus-negative lymphoproliferative diseases. *Blood* **94**, 2931-2933
- [176] Parravinci, C., Corbellino, M., Paulli, M., Magrini, U., Lazzarino, M., Moore, P. S., Chang, Y. (1997) Expression of a virus-derived cytokine, KSHV vIL-6, in HIV-seronegative Castleman's disease. *Am. J. Pathol.* **151**, 1517-1522
- [177] O'Leary, J., Kennedy, M., Howells, D., Silva, I., Uhlmann, V., Luttich, K., Biddolph, S., Lucas, S., Russell, J., Birmingham, N., O'Donovan, M., Ring, M., Kenny, C., Sweeney, M., Sheils, O., Martin, C., Picton, S., Gatter, K. (2000) Cellular localisation of HHV-8 in Castleman's disease: is there a link with lymph node vascularity? *Mol. Pathol.* **53**, 69-76
- [178] Staskus, K. A., Sun, R., Miller, G., Racz, P., Jaslowski, A., Metroka, C., Brett-Smith, H., Haase, A. T. (1999) Cellular tropism and viral interleukin-6 expression distinguish human herpesvirus-8 involvement in Kaposi's sarcoma, primary effusion lymphoma, and multicentric Castleman's disease. *J. Virol.* **73**, 4181-4187
- [179] Ogata, A., Anderson, K. C. (1996) Therapeutic strategies for inhibition of interleukin-6 mediated multiple myeloma cell growth. *Leuk. Res.* **20**, 303-307
- [180] Ogata, A., Chauhan, D., Teoh, G., Treon, S. P., Urashima, M., Schlossman, R. L., Anderson, K. C. (1997) IL-6 triggers cell growth via the Ras-dependent mitogen-activated protein kinase cascade. *J. Immunol.* **159**, 2212-2221
- [181] Stone, S. F., Price, P., Brochier, J., French, M. A., (2001) Plasma bioavailable interleukin-6 is elevated in human immunodeficiency virus-infected patients who experience herpesvirus-associated immune restoration disease after start of highly active antiretroviral therapy. *J. Infect. Dis.* **184**, 1073-1077

- [182] Stebbing, J., Portsmouth, S., Nelson, M., Mandalia, S., Kandil, H., Alexander, N., Davies, L., Brock, C., Bower, M., Gazzard, B. (2004) The efficacy of ritonavir in the prevention of AIDS-related Kaposi's sarcoma. *Int. J. Cancer* **108**, 631-633
- [183] Glover, D. R. (1999) Fully human antibodies come to fruition. *SCRIP Magazine* (May), 16-19
- [184] Kreitman, R. J., Siegall, C. B., FitzGerald, D. J., Epstein, J., Barlogie, B., Pastan, I. (1992) Interleukin-6 fused to a mutant form of Pseudomonas exotoxin kills malignant cells from patients with multiple myeloma. *Blood* **79**, 1775-1780
- [185] Chau, L. A., Tso, J. Y., Madrenas, J. (2001) Generation of partial agonist ligands of the T-cell receptor by engineering of antibodies against CD3. *Transplant. Proc.* **33**, 528-529
- [186] Kjer-Nielsen, L., Dunstone, M. A., Kostenko, L., Ely, L. K., Beddoe, T., Mifsud, N. A., Purcell, A. W., Brooks, A. G., McCluskey, J., Rossjohn, J. (2004) Crystal structure of the human T cell receptor CD3 epsilon gamma heterodimer complexed to the therapeutic mAb OKT3. *Proc. Natl. Acad. Sci. USA* **101**, 7675-7680

## 8 Appendix

### 8.1 Abbreviations

Ab – antibody

Ag – antigen

AIDS – aquired immuno deficiency syndrome

Amp – ampicillin

AP – alkaline phosphates

APP – acute phase proteins

APS – ammonium persulfate

BSA – bovine serum albumine

CD – circular dichroism

CDR - complementarity determining regions

CLC - cardiotrophin-like cytokine

CMD - carboxymethyl dextran

CNTFR - ciliary neurotrophic facto receptor

CT-1 – cardiotrophin-1

DEAE - diethylaminoethyl

DMSO – dimethyl sulfoxide

dNTP – 2’-desoxyribonucleotide-5’-triphosphate

EDC - 1-ethyl-3-(3-dimethylaminopropyl) carbodiimide

EDTA – ethylendiamintetraacetic acid

ELISA – enzyme linked immunosorbent assay

ER – endoplasmic reticulum

FCS – fetal calf serum

FITC – fluorescein isothiocyanate

GFP – green fluorescent protein

gp – glycoprotein

Grb2 - growth-factor-receptor-bound protein



h - hour  
HAMA - highly active anti-retrovital therapy  
HHV-8 – human herpesvirus-8  
HIL-6 – Hyperinterleukin-6  
his – histidin  
huIL-6 – human interleukin-6  
IFN $\gamma$  – interferon  $\gamma$   
Ig – immunoglobulin  
IL - interleukin  
IPTG – isopropyl- $\beta$ -D-thiogalactoside  
JAK – janus-kinase  
kb – kilobase pairs  
kDa - kilodalton  
KS – Kaposi’s sarcoma  
KSHV - Kaposi’s sarcoma associated herpesvirus  
l - liter  
LIFR – leukemia inhibitory factor receptor  
MAPK - mitogen activated protein kinase  
MCD - multicentric Castleman’s disease  
mg – milligram  
 $\mu$ g - microgramm  
min - minute  
MM – multiple myeloma  
ml - milliliter  
Mr – molecular weight  
ng - nanogram  
NF – nuclear factor  
NHS - N-hydroxysuccinimide  
OD – optic density  
o/n – over night  
ORF – open reading frame  
OSMR – oncostatin M receptor  
PCR – polymerase chain reaction

PEL - primary effusion lymphoma  
pNPP – 4-nitrophenyl phosphate  
POD - peroxidase  
P-STAT3 - phospho-STAT3  
RT – room temperature  
scFv – single chain variable fragment  
SDS – sodium dodecyl sulfate  
SDS-PAGE - sodium dodecyl sulphate – polyacrylamide gel electrophoresis  
sgp130 – soluble glycoprotein 130  
SHP-2 - Src homology 2 domain containing tyrosine phosphatase-2  
sIL-6R - soluble interleukin-6 receptor  
SOCS – suppressor of cytokine signaling  
SOE-PCR – splicing by overlap extension by PCR  
SOS - son of sevenless  
ssDNA – single stranded DNA  
STAT - signal transducer and activator of transcription  
TEMED – N,N,N',N'-tetraethylenamine  
TNF $\alpha$  – tumor necrosis factor  $\alpha$   
TYK- tyrosine kinase  
VH – variable domain of heavy chain  
vIL-6 – viral interleukin-6  
VL - variable domain of light chain

## 8.2 Sequences

### A Nucleotide and amino acid sequence of vIL-6 (in p16b vector)

```

1 ggaattccatgatgTTGCCGACGCCCCCGAGTTTGAAAAGGATCTTCTCATTGAGACTCAATTGG ATG CTA TGG GTG ATC GAT GAA TGC 91
1 M L W V I D E C 8
92 TTC CGC GAC CTC TGT TAC CGT ACC GGC ATC TGC AAG GGT ATT CTA GAG CCC GCT GCT ATT TTT CAT CTG AAA CTA 166
9 F R D L C Y R T G I C K G I L E P A A I F H L K L 33
167 CCA GCC ATC AAC GAT ACT GAT CAC TGC GGG TTA ATA GGA TTT AAT GAG ACT AGC TGC CTT AAA AAG CTC GCC GAT 241
34 P A I N D T D H C G L I G F N E T S C L K K L A D 58
242 GGC TTT TTC GAG TTC GAG GTG TTG TTT AAG TTT TTA ACG ACG GAG TTT GGA AAA TCA GTG ATA AAC GTG GAC GTC 316
59 G F F E F E V L F K F L T T E F G K S V I N V D V 83
317 ATG GAG CTT CTG ACG AAG ACC TTA GGA TGG GAC ATA CAG GAA GAG CTC AAT AAG CTG ACT AAG ACG CAC TAC AGT 391
84 M E L L T K T L G W D I Q E E L N K L T K T H Y S 108
392 CCA CCC AAA TTT GAC CGC GGT CTA TTA GGG AGG CTT CAG GGA CTT AAG TAT TGG GTG AGA CAC TTT GCT TCG TTT 466
109 P P K F D R G L L G R L Q G L K Y W V R H F A S F 133
467 TAT GTT CTG AGT GCA ATG GAA AAG TTT GCA GGT CAA GCG GTG CGT GTT TTG AAC TCT ATC CCA GAC GTG ACT CCT 541
134 Y V L S A M E K F A G Q A V R V L N S I P D V T P 158
542 GAC GTC CAC GAT AAG TGA ggatccgcg 568
159 D V H D K * 164

```

### B Amino acid sequence of flag-vIL-6-his

APLV**YKDDDDKALA**KLPDAPEFEKDLLIQRLNWMLWVIDECFRDLCYTGICKGILEPA  
AIFHLKLPAINDTDHCGLIGFNETSCLKKLADGFFFEVLFKFLTTEFGKSVINVDVME  
LLTKTLGWDIQEELNKLTKTHYSPPKFDRGLLGRLLQGLKYWVRHFASFYVLSAMEKFAG  
QAVRVLNSIPDVTPDVHDKGS**HHHHHH**\*

blue – flag-tag

red – his-tag

### C Amino acid sequence of his-vIL-6

APLV**HHHHHH**KLPDAPEFEKDLLIQRLNWMLWVIDECFRDLCYRTGICKGILEPAAIFH  
LKLPAINDTDHCGLIGFNETSCLKKLADGFFFEVLFKFLTTEFGKSVINVDVMELLTK  
TLGWDIQEELNKLTKTHYSPPKFDRGLLGRLLQGLKYWVRHFASFYVLSAMEKFAGQAVR  
VLNSIPDVTPDVHDK\*

red – his-tag

### D Nucleotide and amino acid sequence of vIL-6-GFP

```

1 CACTAGCTAGCGCCACC ATG TGC TGG TTC AAG TTG TGG TCT ATC TTG CTG GTA GGT TCA CTG CTG GTA TCT GGA ACG 77
1 M C W F K L W S I L L V G S L L V S G T 20
78 CGG GGC AAG TTG CCG GAC GCC CCC GAG TTT GAA AAG GAT CTT CTC ATT CAG AGA CTC AAT TGG ATG CTA TGG GTG 152
21 R G K L P D A P E F E K D L L I Q R L N W M L W V 45
153 ATC GAT GAA TGC TTC CGC GAC CTC TGT TAC CGT ACC GGC ATC TGC AAG GGT ATT CTA GAG CCC GCT GCT ATT TTT 227
46 I D E C F R D L C Y R T G I C K G I L E P A A I F 70
228 CAT CTG AAA CTA CCA GCC ATC AAC GAT ACT GAT CAC TGC GGG TTA ATA GGA TTT AAT GAG ACT AGC TGC CTT AAA 302
71 H L K L P A I N D T D H C G L I G F N E T S C L K 95

```

```

303 AAG CTC GCC GAT GGC TTT TTC GAA TTC GAG GTG TTG TTT AAG TTT TTA ACG ACG GAG TTT GGA AAA TCA GTG ATA 377
96 K L A D G F F E F E V L F K F L T T E F G K S V I 120

378 AAC GTG GAC GTC ATG GAG CTT CTG ACG AAG ACC TTA GGA TGG GAC ATA CAG GAA GAG CTC AAT AAG CTG ACT AAG 452
121 N V D V M E L L T K T L G W D I Q E E L N K L T K 145

453 ACG CAC TAC AGT CCA CCC AAA TTT GAC CGC GGT CTA TTA GGG AGG CTT CAG GGA CTT AAG TAT TGG GTG AGA CAC 527
146 T H Y S P P K F D R G L L G R L Q G L K Y W V R H 170

528 TTT GCT TCG TTT TAT GTT CTG AGT GCA ATG GAA AAG TTT GCA GGT CAA GCG GTG CGT GTT TTG AAC TCT ATC CCA 602
171 F A S F Y V L S A M E K F A G Q A V R V L N S I P 195

603 GAC GTG ACT CCT GAC GTC CAC GAT AAG TCT CGA GCG GCC GCC ACC ATG AGC AAG GGC GAG GAA CTG TTC ACT 677
196 D V T P D V H D K S R A A A A T M S K G E E L F T 220

678 GGC GTG GTC CCA ATT CTC GTG GAA CTG GAT GGC GAT GTG AAT GGG CAC AAA TTT TCT GTC AGC GGA GAG GGT GAA 752
221 G V V P I L V E L D G D V N G H K F S V S G E G E 245

753 GGT GAT GCC ACA TAC GGA AAG CTC ACC CTG AAA TTC ATC TGC ACC ACT GGA AAG CTC CCT GTG CCA TGG CCA ACA 827
246 G D A T Y G K L T L K F I C T T G K L P V P W P T 270

828 CTG GTC ACT ACC TTC ACC TAT GGC GTG CAG TGC TTT TCC AGA TAC CCA GAC CAT ATG AAG CAG CAT GAC TTT TTC 902
271 L V T T F T Y G V Q C F S R Y P D H M K Q H D F F 295

903 AAG AGC GCC ATG CCC GAG GGC TAT GTG CAG GAG AGA ACC ATC TTT TTC AAA GAT GAC GGG AAC TAC AAG ACC CGC 977
296 K S A M P E G Y V Q E R T I F F K D D G N Y K T R 320

978 GCT GAA GTC AAG TTC GAA GGT GAC ACC CTG GTG AAT AGA ATC GAG CTG AAG GGC ATT GAC TTT AAG GAG GAT GGA 1052
321 A E V K F E G D T L V N R I E L K G I D F K E D G 345

1053 AAC ATT CTC GGC CAC AAG CTG GAA TAC AAC TAT AAC TCC CAC AAT GTG TAC ATC ATG GCC GAC AAG CAA AAG AAT 1127
346 N I L G H K L E Y N Y N S H N V Y I M A D K Q K N 370

1128 GGC ATC AAG GTC AAC TTC AAG ATC AGA CAC AAC ATT GAG GAT GGA TCC GTG CAG CTG GCC GAC CAT TAT CAA CAG 1202
371 G I K V N F K I R H N I E D G S V Q L A D H Y Q Q 395

1203 AAC ACT CCA ATC GGC GAC GGC CCT GTG CTC CTC CCA GAC AAC CAT TAC CTG TCC ACC CAG TCT GCC CTG TCT AAA 1277
396 N T P I G D G P V L L P D N H Y L S T Q S A L S K 420

1278 GAT CCC AAC GAA AAG AGA GAC CAC ATG GTC CTG CTG GAG TTT GTG ACC GCT GCT GGG ATC ACA CAT GGC ATG GAC 1352
421 D P N E K R D H M V L L E F V T A A G I T H G M D 445

1353 GAG CTG TAC AAG TGA GC 1369
446 E L Y K * 450

```

green – GFP

## E Nucleotide and amino acid sequence of MAV (in pIT1 vector)

```

1 ATG GCC GAG GTG CAG CTG TTG GAG TCT GGG GGA GGC TTG GTA CAG CCT GGG GGG TCC CTG AGA CTC TCC TGT GCA 75
1 M A E V Q L L E S G G G L V Q P G G S L R L S C A 25

76 GCC TCT GGA TTC ACC TTT AGC AGC TAT GCC ATG AGC TGG GTC CGC CAG GCT CCA GGG AAG GGG CTG GAG TGG GTC 150
26 A S G F T F S S Y A M S W V R Q A P G K G L E W V 50

151 TCA GAT ATT CGG GGG CGG GGT CCT CCG ACA GGT TAC GCA GAC TCC GTG AAG GGC CGG TTC ACC ATC TCC AGA GAC 225
51 S D I R G R G P P T G Y A D S V K G R F T I S R D 75

226 AAT TCC AAG AAC ACG CTG TAT CTG CAA ATG AAC AGC CTG A*A GCC *AG GAC ACG GCC GTA TAT TAC TGT GCG AAA 300
76 N S K N T L Y L Q M N S L X A X D T A V Y Y C A K 100

301 AGG ATG TGG GGT TTT GAC TAC TGG GGC CAG GGA ACC CTG GTC ACC GTC TCG AGC GGT GGA GGC GGT TCA GGC GGA 375
101 R M W G F D Y W G Q G T L V T V S S G G G S G G 125

376 GGT GGC AGC GGC GGT GGC GGG TCG ACG GAC ATC CAG ATG ACC CAG TCT CCA TCC TCC CTG TCT GCA TCT GTA GGA 450
126 G G S G G G G S T D I Q M T Q S P S S L S A S V G 150

451 GAC AGA GTC ACC ATC ACT TGC CGG GCA AGT CAG AGC ATT AGC AGC TAT TTA AAT TGG TAT CAG CAG AAA CCA GGC 525
151 D R V T I T C R A S Q S I S S Y L N W Y Q Q K P G 175

526 AAA GCC CCT AAG CTC CTG ATC TAT GGG GCA TCC CGC TTG CAA AGT GGG GTC CCA TCA AGG TTC AGT GGC AGT GGA 600
176 K A P K L L I Y G A S R L Q S G V P S R F S G S G 200

601 TCT GGG ACA GAT TTC ACT CTC ACC ATC AGC AGT CTG CAA CCT GAA GAT TTT GCA ACT TAC TAC TGT CAA CAG GCT 675
201 S G T D F T L T I S S L Q P E D F A T Y Y C Q Q A 225

676 TGG CAT CTT CCT TTG ACG TTC GGC CAA GGG ACC AAG GTG GAA ATC AAA CGG GCG GCC GCA GAA CAA AAA CTC ATC 750
226 W H L P L T F G Q G T K V E I K R A A A E Q K L I 250

751 TCA GAA GAG GAT CTG AAT GGG GCC GCA TAG 780
251 S E E D L N G A A * 260

```

blue – myc-tag

## F Nucleotide and amino acid sequence of MAV-KDEL

```

1 CACGTTTAAACGCCACC ATG AAC TCC TTC TCC ACA AGC GCC TTC GGT CCA GTT GCC TTC TCC CTG GGG CTG CTC CTG 77
1 M N S F S T S A F G P V A F S L G L L L 20
78 GTG TTG CCT GCT GCC TTC CCT GCC CCA GTA CAC GTG ATG GCC GAG GTG CAG CTG TTG GAG TCT GGG GGA GGC TTG 152
21 V L P A A F P A P V H V M A E V Q L L E S G G G L 45
153 GTA CAG CCT GGG GGG TCC CTG AGA CTC TCC TGT GCA GCC TCT GGA TTC ACC TTT AGC AGC TAT GCC ATG AGC TGG 227
46 V Q P G G S L R L S C A A S G F T F S S Y A M S W 70
228 GTC CGC CAG GCT CCA GGG AAG GGG CTG GAG TGG GTC TCA GAT ATT CGG GGG CGG GGT CCT CCG ACA GGT TAC GCA 302
71 V R Q A P G K G L E W V S D I R G R G P P T G Y A 95
303 GAC TCC GTG AAG GGC CGG TTC ACC ATC TCC AGA GAC AAT TCC AAG AAC ACG CTG TAT CTG CAA ATG AAC AGC CTG 377
96 D S V K G R F T I S R D N S K N T L Y L Q M N S L 120
378 A*A GCC *AG GAC ACG GCC GTA TAT TAC TGT GCG AAA AGG ATG TGG GGT TTT GAC TAC TGG GGC CAG GGA ACC CTG 452
121 X A X D T A V Y Y C A K R M W G F D Y W G Q G T L 145
453 GTC ACC GTC TCG AGC GGT GGA GGC GGT TCA GGC GGA GGT GGC AGC GGC GGT GGC GGG TCG ACG GAC ATC CAG ATG 527
146 V T V S S G G G S G G G G G S G G G G G S G G G G G S T D I Q M 170
528 ACC CAG TCT CCA TCC TCC CTG TCT GCA TCT GTA GGA GAC AGA GTC ACC ATC ACT TGC CGG GCA AGT CAG AGC ATT 602
171 T Q S P S S L S A S V G D R V T I T C R A S Q S I 195
603 AGC AGC TAT TTA AAT TGG TAT CAG CAG AAA CCA GGG AAA GCC CCT AAG CTC CTG ATC TAT GGG GCA TCC CGC TTG 677
196 S S Y L N W Y Q Q K P G K A P K L L I Y G A S R L 220
678 CAA AGT GGG GTC CCA TCA AGG TTC AGT GGC AGT GGA TCT GGG ACA GAT TTC ACT CTC ACC ATC AGC AGT CTG CAA 752
221 Q S G V P S R F S G S G S G T D F T L T I S S L Q 245
753 CCT GAA GAT TTT GCA ACT TAC TAC TGT CAA CAG GCT TGG CAT CTT CCT TTG ACG TTC GGC CAA GGG ACC AAG GTG 827
246 P E D F A T Y Y C Q Q A W H L P L T F G Q G T K V 270
828 GAA ATC AAA CGG GCG GCC GCA GAA CAA AAA CTC ATC TCA GAA GAG GAT CTG AAT CCG CGG AAA GAC GAA CTC TAG 902
271 E I K R A A A E Q K L I S E E D L N P R K D E L * 295
903 GTTTAAACCAC 913

```

blue – myc-tag

red – retention sequence

## 8.3 Curriculum Vitae

- Name:** Marina Kovaleva
- Place of birth:** Zelenodolsk, Russia
- Date of birth:** 28 Oct 1977
- Nationality:** Russian
- 
- Nov 2000-present: PhD student at the Faculty of Medicine, Department of Biochemistry, Christian-Albrechts University, Kiel, Germany. Supervisor: Prof. Dr. S. Rose-John
- Nov 1999-Oct 2000: PhD student at the Laboratory of Neuroreceptors and Neuroregulators, Shemyakin-Ovchinnikov Institute of Bioorganic Chemistry, Russian Academy of Science. Supervisor: Prof. E.V. Grishin
- June 1999: graduated with distinction with the diploma “Veterinary doctor-biochemist”. Completion and defence of graduate thesis “*Structure-Functional Analysis of the Ankirin Repeats Fragment of  $\alpha$ -latrotoxin from Black Widow Spider*” Supervisors: Prof. E.V. Grishin, Dr. A.V. Lipkin, Dr. A.V. Vasilyev
- Sept 1994-June 1999: student at the Faculty of Biology, K.I. Scryabin Moscow State Academy of Veterinary Medicine and Biotechnology. Address: 109472 Moscow, Scryabin street 23, Russia
- June 1994: graduation: A-levels, with distinction
- Sept 1984-June 1994: student at Kireewsk primary and highschool (Tula, Russia)

## 8.4 Publications

[1] Schuster, B., **Kovaleva, M.**, Sun, Y., Regenhard, P., Matthews, V., Grötzinger, J., Rose-John, S., Kallen, K.-J. (2003) Signalling of human ciliary neurotrophic factor (CNTF) revisited: the interleukin-6 (IL-6) receptor can serve as an alpha-receptor for CNTF. *J. Biol. Chem.* **278** (11), 9528-9537

[2] Scheller, J., **Kovaleva, M.**, Rabe, B., Eichler, J., Kallen, K.-J., Rose-John, S. (2004) Development of a monoclonal antibody-based enzyme-linked immunoabsorbent assay for the binding of gp130 to the IL-6/IL-6R complex and its competitive inhibition. *J. Immun. Meth.* **291** (1-2), 93-100

[3] **Kovaleva, M.**, Conrad, U., Rabe, B., Grötzinger, J., Rose-John, S., Scheller, J. Recombinant human single chain Fv antibody recognising viral interleukin-6 (in preparation)

## 9 Acknowledgements

I would like to express my special thanks to Prof. Dr. Stefan Rose-John for providing the project, for supervision of my work, and for supporting my scientific development. I am very grateful to him being always prepared to discuss problems and to encourage me by giving useful advice.

I also thank Prof. Dr. Matthias Leippe for reviewing my thesis.

Dr. Dr. Karl-Josef Kallen deserves my special thank not only for showing great interest in my work and helping me with his profound knowledge, but also for his warm support when I came to Germany.

I would like to thank Dr. Joachim Grötzinger for introducing me into the technique of protein purification, Dr. Oliver Hecht for recording the CD-spectra, Björn Rabe for generating the cytokine chimeras, and Dr. Marie-Luise Kruse for help with the LASER-microscopy.

For introducing me in the phage display technology I want to thank Dr. Udo Conrad and Ingrid Pfort from the IPK in Gatersleben.

I also thank Dr. Jutta Eichler from the GBF in Braunschweig for the successful collaboration concerning the EBNA cell transfection.

I warmly thank all members of the Department of Biochemistry, especially Dr. Jürgen Scheller, Dr. Björn Schuster, Dr. Petra Regenhard, Ingo Bußmeyer, Werner Meinert, Dr. Krzysztof Paliga, and Dr. Vance Matthews from lab 137, for the nice atmosphere and the good time we spent together.

For proof-reading my thesis and standing by my side in good as well as difficult times, I want to thank Christian Hundhausen.

Finally, I would like to thank Jurgita, Sergej and Tanja and in particular my Mum Galina, my best friend, who always thinks of me and who cares about my feelings.